A Comparison of Corneal Wound Healing after UVB and Nitrogen Mustard Exposure

By

Iris P. Po

A thesis submitted to the

Graduate School-New Brunswick

Rutgers, The State University of New Jersey

and

The Graduate School of Biomedical Sciences

University of Medicine and Dentistry of New Jersey

In partial fulfillment of requirements

For the degree of

Master of Science

Graduate Program in Toxicology

Written under the direction of

Dr. Marion Gordon

and approved by

_____

_____

_____

_____

New Brunswick, New Jersey

January, 2012

ABSTRACT OF THE THESIS

A Comparison of Corneal Wound Healing after UVB and Nitrogen Mustard Exposure

By Iris P. Po

Thesis director:

Marion K. Gordon

Vesicants such as nitrogen mustard (NM) cause blistering of skin, similar to that caused by ultraviolet B (UVB) exposure from the sun. In the cornea, such injury occurs as microbullae at the basal surface of the basal epithelial cells, where the cells sit on their basement membrane. We hypothesize that the steps in healing are not identical after exposure to these two blistering agents, since UV injury heals well, but mustards often cause injuries that can induce chronic complications. Twenty five years after a mustard exposure recurrent erosions can still develop (Javadi et al., 2005). In an effort to understand the pathogenesis of mustard exposure we investigated whether a NM injury heals more slowly than an equivalent UVB injury. To accomplish this, corneal organ cultures were exposed to different levels of UVB to determine conditions that would produce a 24 hour post-UVB phenotype equivalent to the 24 hour post-exposure phenotype of a 60 minute exposure to 100 nmol NM. Corneal organ cultures were irradiated for various times to produce different UVB exposures: 5 minutes exposure

resulted in 100 mJ/cm^2; 20 minutes, 400 mJ/cm^2; 40 minutes, 800 mJ/cm^2; 60 minutes, 1200 mJ/cm^2; 80 minutes, 1600 mJ/cm^2; and 100 minutes, 2000 mJ/cm^2. Corneas were embedded in O.C.T compound, frozen, and then sectioned for H&E staining. Micrographs of sections were overlapped to make composites covering the entire diameter of the cornea. From the composites, the degree of epithelial-stromal separation was calculated as a percentage of the entire width of the cornea. Our results demonstrated that, at 24 hour after a 60 minutes exposure to 100 nmol NM, the epithelial-stromal separation was 58 ± 13 % of the corneal diameter. Of the UVB exposures, a nearly equivalent phenotype, 60 ± 11 % separation between the cell layers, was produced by the 2000 mJ/cm^2 UVB exposure. The time needed for healing (i.e., a return to epithelial-stromal structural integrity) was found to be 7 days for NM exposure. In contrast, the equivalently damaged UVB-exposed corneas recovered in only 5 days. Immunofluorescence analysis showed that the provisional matrix components SPARC, hevin, tenascin-C, thrombospondin-1, and fibrillin-1 persisted at least 1 day longer in the NM-exposed corneas than in UVB-exposed corneas.

Dedication

All my school work and studies are dedicated to my loving parents, Chien-chi Po and Chia-yen Chu. Without their support and encouragement, I would not have been able to complete anything, especially my mother for being my best friend and forever supportive. Even though I am in the U.S.A alone, I can feel she is always with me.

Acknowledgements

I would like to thank my thesis advisor, Dr. Marion Gordon, who guided me along the path to becoming a good scientist. She always pushed me in the right direction and gave me useful advice when I needed it. I am really grateful for all the help and support she gave me. I would also like to thank Dr. Donald Gerecke, who along with Dr. Gordon made me feel like the time I spent in their lab was like a big warm family. I would also like to thank my other committee members, Dr. Jeffrey Laskin and Dr. Debra Laskin, who gave me useful comments and suggestions on my research.

I would also like to thank the other members of the Dr. Gordon and Dr. Gerecke Lab, Rita Hahn, John Beloni, Pei-Hong Zhou, Yokechen Chang, Hong-Mei Zhang, and Jei-Bo Liu for their countless support such as helping with eye dissections and other technical questions.

I also thank my friends and former lab mates, Ming-Wei Chao, Andrea DeSantis, Lakshmi Roman, and James Wang, who gave me support academically during my time at Rutgers. I would like to especially thank Ming-Wei Chao for his guidance and training in my labwork, who taught me many of the techniques I needed to be successful in my research.

I also would like to thank the other members of the Dr. Jeffrey Laskin and Dr. Debra Laskin labs, whose support and equipment were essential for the completion of my research.

Finally, I would like to thank my family and my sweet sons, bebe and didi. Who always kept me company during times of writing and practice.

Table of Contents

Abstract……..…ii

Dedication……..….....iv

Acknowledgements…….....v

Table of Contents…….……vi

List of Figures……..…x

List of Abbreviations……...…xii

Introduction…….……..1

1. Sulfur Mustard ……..…….…….1

1.1.Background on Sulfur Mustard and its Derivatives. ….……..……..1

1.2. Acute and Chronic Effects of SM Exposure…….3

1.3. Slower Wound Healing after SM Expsoure……..…5

2. Ultraviolet Irradiation……..…7

2.1. Acute and Chronic Effects of UVB Exposure..……9

3. Model System to Study Corneal Wound Healing….…….12

3.1. Anatomy and Physiology of Human Corneas…….……...12

3.2. Animal Studies……..…….……14

3.3. Corneal Organ Culture……15

4. Corneal Epithelial Wound Healing……...17

4.1. The Process of Corneal Epithelial Wound Healing…….…...17

4.2. Role of Provisional Matricellular Molecules…...……..…....19

4.2.1. SPARC (secreted protein, acidic and rich in cysteine a.k.a osteonectin or BM40)……20

4.2.2. Hevin (SPARCL1, SPARC like 1, SC1, MAST9) and ADAMTS4 (aggrecanase-1) ……...……...……...21

4.2.3. Tenascin-C……. ……22

4.2.4. Thrombospondin-1 (TSP-1)……...……..23

4.2.5. Fibrillin-1 (FBN-1)……...……...24

4.2.6. Fibronectin (FN)…….…….……24

5. Thesis Research Rationale..……...25

Statement of Hypothesis…….……..…….…..26

Specific Aims …………..…….26

Materials and Methods…….…….……..29

1. Models and Exposures…….……..29

1.1. List of Reagents..……...…….29

1.2.Rabbit Cornea Organ Culture Model…….…..30

1.3. Nitrogen Mustard Exposure……....31

1.4. UVB Irradiation…….……32

2. Histology……..…..32

3. Immunofluorescence…….…….…....34

3.1. Matricellular Proteins……...…...34

3.2. Co-localization of Hevin and ADAMTS4……..35

3.3. Ferritin Heavy Chain Detection……..36

4. Cell Lysates Preparation and Culture Medium Collection……36

5. Immunoblot……37

6. Evaluation of Corneal Wound Healing…….……38

6.1. Equivalent Injuries of NM and UVB …….……38

6.2. Corneal Wound Healing Evaluation by H&E Staining……..38

6.3 Expression of Provisional Matrix Components……..……39

Results……..……40

Dose-response of NM on the Degree of Corneal Injury …….…..40

Dose-response Relationship of UVB Irradiation……...44

Corneal Wound Healing of Equivalent NM and UVB Injuries……..……..48

Expression of Provisional Wound Matrix Components……53

SPARC…….……..……54

Hevin…….……57

Tenascin-C……60

Thrombospondin-1 (TSP-1).…….……..……..60

Fibrillin-1 (FBN-1).…….……..63

Expression of Fibronectin (FN)…….……65

Co-localization of Hevin and ADAMTS4…….....68

ADAMTS4 Western Analysis……...……....68

Nuclear Ferritin in the UVB Irradiated Corneas……69

Discussion……75

Summary and Future work……83

References……86

List of Figures

Fig.1. Structures of sulfur mustard, half mustard, and nitrogen mustard ……..2

Fig.2-1. Blisters on sulfur mustard exposed skin……6

Fig.2-2. Sunburn of skin…….....6

Fig.3. UVA, UVB, and UVC pass through different layers of eyes..……....10

Fig.4. Structure of the Human cornea…….……...13

Fig.5. A diagram of the rabbit cornea organ culture model that was used in this study… …..…….……..……..18

Fig.6. A diagram of the equipment that was used in UVB-irradiation ……....33

Fig.7-1. Determination of injury induced by NM exposures. ……...41

Fig.7-2. Calculation of the percentage of epithelial-stromal separation at 24 hours post NM exposure. ……..…….….42

Fig.7-3. Higher magnification of typical regions of H&E stained sections from three different corneas 24 hours post NM exposure (20 x) to show details of the epithelial-stromal separations…….……43

Fig.8-1. Determination of injuries induced by UVB-exposures..……..45

Fig.8-2. Calculation of the percentage of epithelial-stromal separation at 24 hr post UVB exposure…….....……46

Fig.8-3. Higher magnification of typical regions of H&E stained sections from three different corneas 24 hr post UVB exposure(20x) to show details of the epithelial-stromal separations ……...…..47

Fig. 9-1. Overlap composites of H&E stained corneal sections, spanning the entire corneal diameter. The following merged pictures show NM exposed corneas healing from 1 after exposure to 7 days after……..49

Fig.9-2. Higher magnification of selected areas 1of NM exposed corneas from figure 9-1……..…….…….50

Fig.10-1. Overlap composites of H&E stained corneal sections across the entire corneal diameter after a 100 minutes (2000 mJ/cm^2) UVB exposure. Healing was followed from 1 to 7 days post exposure……..……51

Fig. 10-2. Higher magnification of selected area OF UVB-exposed corneas from the figure 10-1……...……...52

Fig.11-1. Immunofluorescence of SPARC protein in NM and UVB exposed corneas.....55

Fig.11-2. Immunoblot analysis of SPARC expression…….……56

Fig.12-1. Immunofluorescence of hevin protein in NM and UVB exposed corneas…...58

Fig.12-2. Immunoblot analysis of hevin expression…….……59

Fig.13. Immunofluorescence of tenascin-C protein in NM and UVB exposed corneas…….……..61

Fig.14. Immunofluorescence of thrombospondin-1 (TSP-1) protein in NM and UVB exposed corneas…….62

Fig.15. Immunofluorescence of fibrillin-1 (FBN-1) protein in NM and UVB exposed corneas……...……64

Fig.16-1. Immunofluorescence of fibronectin (FN) protein in NM and UVB exposed corneas……...66

Fig.16-2. Immunoblot analysis of fibronectin (FN) expression……67

Fig.17. Hevin and ADAMTS4 co-localization in the immunofluorescence…….70

Fig.18. Immunoblot analysis of ADAMTS4 expression……...…71

Fig.19. Nuclear ferritin was detected post UVB irradiation with in short times……...73

List of Abbreviations

ADAMTS4	a disintergrin and metalloproteinase with thrombospondin motifs
BM	basement membrane
CEES	2 -chlorethylethyl sulfide
DNA	deoxyribonucleic acid
ECL	enhanced chemiluminescence
ECM	extracellular matrix
EGF	epidermal growth factor
EPA	environmental protection agency
FBN-1	fibrillin-1
FN	fibronectin
H&E	haematoxyline and eosin stain
HRP	horseradish peroxidase
NM	nitrogen mustard
O.C.T	optimal cutting temperature
PK	keratoplasty
SDS-PAGE	sodium dodecyl sulfate polyacrylamide gel elecrophoresis
SM	sulfur mustard
TSP-1	thrombospondin-1
UVB	ultraviolet B
UVI	UV index
UVR	Ultraviolet radiation

Introduction

1. Sulfur Mustard

1.1. Background on Sulfur Mustard and its Derivatives

Sulfur mustard (SM) is a potent warfare agent which has been used during two wars, World War I and the Iran Iraq War. Its use is still a military and civilian threat. Bis-2-chloroethyl sulfide is the chemical name of SM (Fig.1, top). SM exposure on skin results in delayed onset erythema, followed by characteristic edema with inflammatory cell infiltration, the appearance of large blisters. Healing is prolonged (Shakarjian et al., 2009). Two chemically related analogs are CEES (2-chloroethylethyl sulfide, or half mustard) which contains one chlorethyl functional group, and causes relatively mild vesicant activity (Fig.1, middle), and methylbis (2-chloroethyl) amine (HN_2), also called nitrogen mustard (NM), in which a sulfide is replaced with an amine (Fig.1, bottom). NM causes moderate to severe vesicant injury. It is also used in the treatment of leukemia (Hall et al., 1956). CEES and NM can be used as surrogates for SM exposure in laboratory experiments.

The two chloroethyl functional groups of SM alkylate molecules and form intra- and intermolecular cross-links in the extracellular matrix, the cell membranes and within the cells, including DNA, lipid, and protein. The initial reaction is formation of an ethylene sulfonium ion (SM and CEES) or an ethylene immonium ion (NM) intermediate, which releases one chloride and forms a positively charged intermediate. These intermediates are electrophilic, and attacks nucleophilic sites. Skin, lung and cornea are the major target sites affected by exposure.

Fig. 1. Structures of sulfur mustard, half mustard, and nitrogen mustard. The chloroethyl function group is labeled in a red frame. NM is different from SM with an amine instead of a sulfide, which is labeled in a green frame. Photo adapted and modified from Shakarjian et al., *Toxicol Sci.* 114(1):5-19.2010.

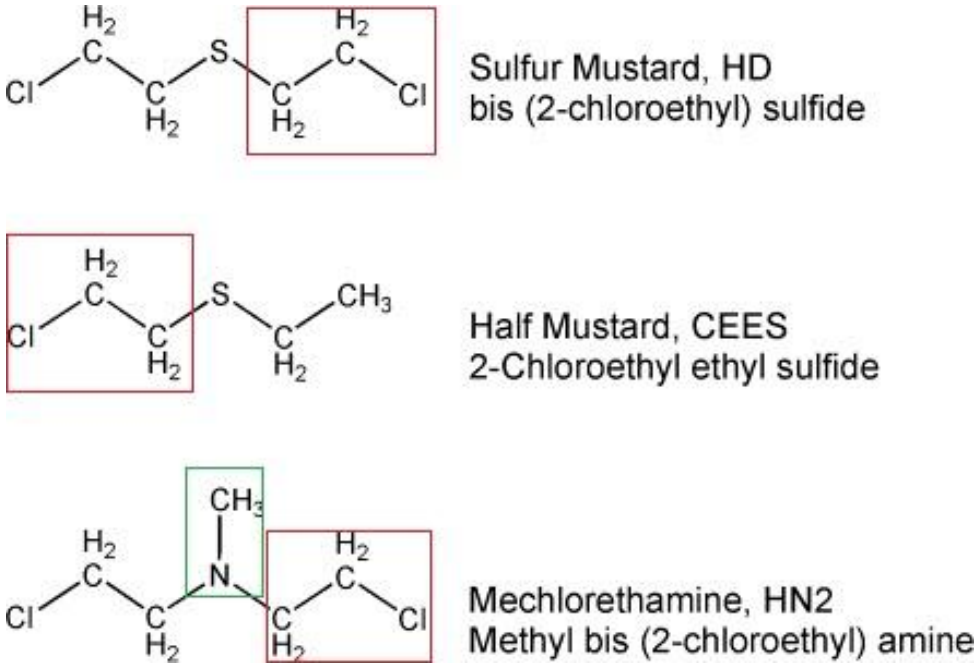

1.2. Acute and Chronic Effects of SM Exposure

SM exposure of the skin, eyes, and lungs is not felt immediately, but hours later. The eyes are the most sensitive organ and respond to SM faster than skin, probably because of the moist ocular surface and the lipid layer of the tear film. The threshold dose of eye exposure (12 µg x min/l) is also much lower than the threshold dose of skin exposure (200 µg x min/l) (Smith and Dunn, 1991; Solberg et al., 1997). SM-induced ocular injuries start with clinical symptoms at 2 - 6 hours post exposure (Kadar et al., 2001). The symptoms are dose dependent (Kadar et al., 2001). Early effects are photophobia, eyelid twisting, eye redness, irritation, blinking, eyelid swelling, conjunctival hyperemia, corneal erosion, and inflammation (Kadar et al., 2001; Solberg et al., 1997). Severe corneal injuries are characterized by loss of the epithelial layer and corneal stromal edema 24 - 48 hours post exposure (Kadar et al., 2001; Smith and Dunn, 1991; Solberg et al., 1997). Later effects can be temporary blindness and more severe corneal injury (Javadi et al., 2005; Kadar et al., 2001; Solberg et al., 1997). The corneal epithelium regenerates in about 72 hours (Javadi et al., 2005; Kadar et al., 2001; Solberg et al., 1997). The restoration of corneal integrity can occur as early as 1 - 2 weeks post exposure, depending on the SM dose (Kadar et al., 2001; Solberg et al., 1997). However, 25 - 40 % of exposed corneas undergo a chronic type of injury and continue on to a second phase of pathology, including periodic corneal edema, opacity, recurrent erosions, and neovascularization (Javadi et al., 2005; Kadar et al., 2001; Solberg et al., 1997). These reoccurring ocular injuries can be more severe than the initial injury (Javadi et al., 2005). The lung airway is the second most sensitive target site of SM exposure (Smith and Dunn, 1991). The main affected regions are the nasal, laryngeal, and tracheo-

bronchial mucosa (Smith and Dunn, 1991; Freitaq et al., 1991). Injuries can be mild to severe, ranging from mild irritation of laryngeal mucosa to bronchial edema and impairment of gas exchange from higher exposures (Freitaq et al., 1991). Skin responds more slowly to SM exposure than the eyes and the lung (Smith and Dunn, 1991). The effects are felt 4 - 24 hours after exposure (Zhang et al., 1995). The initial symptoms are intense inching and erythema often around 6 hours post exposure (Smith and Dunn, 1991). Thirteen to 48 hours after exposure large round blisters are filled with liquid (Smith and Dunn, 1991). The blisters are the result of separation of the epidermal and dermal layers with disruption of the basement membrane zone (Zhang et al., 1995; Monteiro-Riviere et al., 1999). Cornea does not blister like skin (Gordon et al., 2010). It is likely that, the dehydrating function of the corneal endothelial cells allow only the formation of microbullae (microblisters) by limiting fluid reaching the epithelial-stromal junction. These can, however, be spaced so close together that the epithelium eventually separates from the stroma.

Delayed mustard gas keratopathy was observed in Iranian survivors in the Iran-Iraq war in the 1980s (Javadi et al., 2005). Most victims experienced mild exposure and recovered completely. In some cases, victims exposed to high concentrations of SM experienced one of three different healing courses: (1) They completely healed with no further inflammation; (2) They showed chronic signs and symptoms; (3) or they experienced delayed onset keratitis with lesions that continue to reappear several years after the initial exposure. In more complicated situations, intrastromal exudation of plasma lipids and deposition of amyloid occur, with corneal scarring, opacity, neovascularization, and thinning. These severely injured eyes can suffer a permanent

reduction in visual acuity that ranges from mild impairment to total blindness (Javadi et al., 2005).

Despite 100 years of studying sulfur mustard injury, there is no curative therapy (Javadi et al., 2005; Shohrati et al., 2007). Treatments deal with symptoms only. For mild to moderate lesions, treatment is an anti-inflammatory drug (e.g. Dexamycin and Voltaten Ophtha) (Kadar et al., 2009). In rabbit eye exposures, inflammation was reduced by doxycycline (Kadar et al., 2009; Gordon et al., 2010). This drug also postponed neovascularization (Kadar et al., 2009), but did not prevent it. Applying doxycycline in a hydrogel, SM-exposed rabbit cornea at 28 days post exposure showed lower level of neovascularization than no drug treatment (Gordon et al., 2010). For humans, corneal transplant (penetrating keratoplasty) is the only effective treatment in dealing with long term corneal erosions if there is not a deficiency of the limbal stem cells (Javadi et al., 2005). However, transplants can be rejected, and often fail if neovascularization has occurred (Gebhardt and Shi, 2002; Shtein et al., 2008). Recently, limbal stem cell transplantation is being used as a method of ocular surface reconstruction (Javadi et al., 2011; Javadi and Baradaran-Rafii, 2009).

1.3. Slower Wound Healing after SM Exposure

SM's bifunctional chloroethyl groups cause severe blistering of skin, characterized by disruption of the epidermal-dermal junction of the basement membrane (Monteiro-Riviere et al., 1999). Physicians who treated the victims of exposure observed that SM-induced blisters healed more slowly than other similar blisters from a sunburn (Fig.2-2). Our work addresses potential causes of slower wound healing after mustard

Fig. 2-1. Blisters on sulfur mustard exposed skin. Sulfur mustard exposure can cause huge blisters on the skin, with fluid separating the epithelial and stromal layers. Photo adapted from Zachary R. "mustardgas-blister." Photo. *Moriches Daily July 3, 2010.* *<http://morichesdaily.com/2010/08/toxic-munitions-dumping-sites-shores/mustardgas-blister/>*

Fig. 2-2. Sunburn of skin. Excess exposure to UVB can cause huge blisters on skin as well. Photo adapted from Knoop, Kevin. "Sunburn." Photo. *McGraw-Hill's Access Medicine,* 2006. *<http://atlas-emergency-medicine.org.ua/ch.16.htm>*

exposure. One possible mechanism might be the loss of function of components in the basement membrane zone due to modification by SM. SM crosslinks basement membrane (BM) junctional proteins, altering cell adhesion (Zhang et al., 1995). Alternatively SM may cause prolonged expression of some proteases in the BM area, delaying healing (Calvet et al., 1999; Gordon et al., 2010; Shakarjian et al., 2006).

2. Ultraviolet Irradiation

The ozone layer in the earth's upper atmosphere is beneficial and protective, reducing the potential injuries of ultraviolet light reaching the Earth. It mainly filters UVB rays (wavelength 280 nm - 315 nm). Since the late 1970s, the Earth's ozone layer has declined about 5 percent per decade. The severity of the "ozone hole" varies year to year (Cowen, 1996). Ozone depletion leads to increased ultraviolet radiation reaching the Earth's surface and is implicated in skin cancer, eye injuries, immune system defect, and disruption of the entire ecosystem via generation of reactive oxygen species (superoxide, hydroxyl radicals, hydrogen peroxide, and singlet oxygen) (Cowen, 1996). The intensity of UV depends on the altitude above sea level, the degree of the sun from horizon (0 degree coordinates) to zenith (90 degree coordinates), and the location's thickness of the ozone layer of on the particular day (United States Environmental Protection Agency [U.S. EPA], 2010). The UV Index (UVI) value is predicted daily and is calculated at the solar noon hour daily from the National Weather Service forecast (U.S. EPA, 2010). The United States Environmental Protection Agency (U.S. EPA) developed a scale from 1 (low) to 11+ (extremely high) indicating the intensity of solar UV radiation (U.S. EPA, 2010). The UVI is determined as follows: The intensity of UV radiation is calculated

from the amount of UVB (280 nm -315 nm) and UVA (320 nm - 400 nm) that penetrate across the ozone layer. The ozone layer mainly filters most of the shorter wavelength radiation, UVC (100 nm-280 nm). The strength of ground-level UV radiation is calculated to a hypothetical value at a wavelength representing UV irradiance values ($mW/m^2/nm$). For example, 290 nm wavelength radiation gives an effective UV strength 4; 320 nm, 26; and 400 nm, 30. However, shorter wavelength radiation causes more skin injuries than longer wavelength radiation. Skin responses to certain wavelengths using the "McKinlay-Diffey Erythema action spectrum" weights factors for certain UV wavelengths. For example, 290 nm wavelength radiation has a weight factor of 15; 320 nm, 5; and 400 nm, 3. The strength values from different wavelengths multiplied by the appropriate weight factor gives a total UV effect when all the values are summed: (strength, 4 x weight factor,15 at 290 nm wavelength) + (strength, 26 x weight factor, 5 at 320 nm) + (strength, 30 x weight factor, 3 at 400 nm) = 280. The total UV effect multiplied by ground level elevation and percentage of cloud cover that day, divided by 25, generates a convenient index value. This number will be the UVI in units of hectoJoules/m^2 (U.S EPA, 1994). A scale value from 1 - 2 means low danger from the sun's UV rays; 3 – 5 is moderate; 6 – 7 is high; 8 – 10 is very high; and 11+ is extremely dangerous. The most intense UV exposure is mainly from 10 a.m. to 2 p.m. A very high skin exposure without protection will cause a sunburn in a short time. HectoJoules/m^2 equals to10 miliJoules/cm^2 (hecto = 10^5 milli). For instance, the UVI in New Jersey is 9 at the noon solar hour, meaning the intensity is 90 mJ/cm^2.

Safe levels (Threshold Limit Values [TLVs]) of UVB exposure for unprotected eye or skin range from 3.4 mJ/cm^2 (280 nm) to 500 mJ/cm^2 (313 nm) issued from the

American Conference of Governmental Industrial Hygienists (ACGIH) (Jo, 2005). The TLVs of a chemical is a safe range for occupational exposure after a working day (8 hour) without adverse health effects. This might indicate a safe exposure in the environment as well. In our experiments we used UVB intensities from 100 mJ/cm^2 to 2000 mJ/cm^2, equivalent to UVIs from 10 to 200. The lower doses used in our experiments were within the range of environmental UV exposures. Most were stronger, and were needed to achieve a UV injury similar to that of a mustard exposure.

The cornea is the outermost layer of eyes directly exposed to UV light. Corneas are exposed to both the ambient environment and the sun. Different UV wavelengths penetrate to different layers of the eyes. UVC is effectively filtered out by the ozone layer. UVB is partially absorbed by cornea, the first line defense at filtering the majority of the UVB rays (Fig.3). UVA can pass through the cornea and causes chronic lens damage, and cataract formation if there is long term low dose exposure. For the cornea, the most common acute effect of UV over-exposure is photokeratitis and snow blindness from welder's flash and snow reflection.

Although eyes are more sensitive to SM damage than skin is, they are less susceptible to UV injury than skin (Cullen, 2002). In chickens, ferritin in the corneal epithelium plays a role in protecting the DNA from oxidative damage due to UV (Cai et al., 2008). Nuclear ferritin in the corneal epithelial cells scavenges free radicals produced by the Fenton reaction, protecting the epithelia (Linsenmayer et al., 2005), whether this occurs in mammals has never been ascertained.

2.1. Acute and Chronic Effects of UVB Exposure

Fig. 3. UVA, UVB, and UVC pass through different layers of eyes. UVC has a shorter wavelength, and is filtered out by the ozone layer. UVB is partially absorbed by cornea. UVA has a longer wavelength, and can pass through the cornea to the lens causing cataract formation. Photo adapted from Jargon Buster."eyeuv1." Figure. *Steven Harris Opticians, 2003. < http://www.stevenharris-opticians.com/jargonbuster.html>*

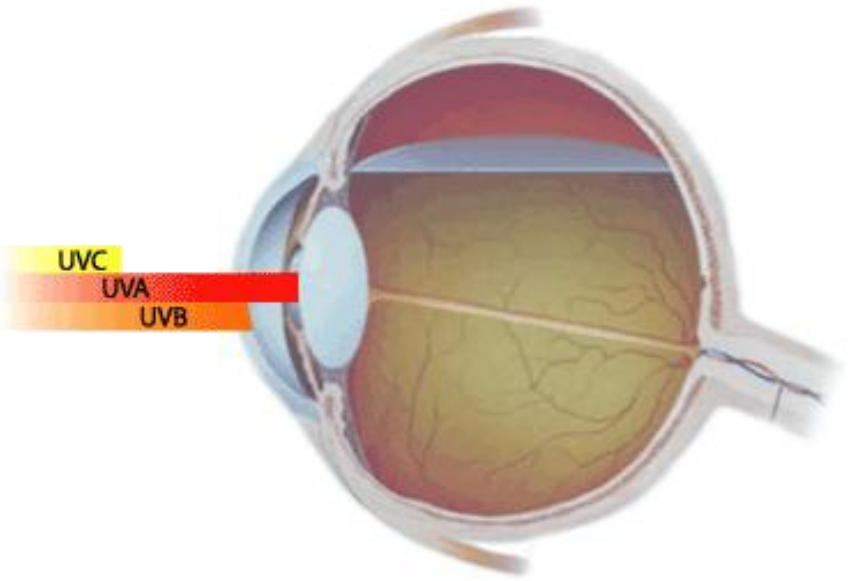

Acute photokeratitis can be caused by a single dose of UVB exposure. It may be characterized by inflammation, edema, and pain and possibly disruption of the attachment of the corneal epithelium to the stroma (Cullen, 2002; Young, 2006). Injury is dependent on dose and wavelength. In one study of acute ultraviolet radiation (UVR) exposure, 129 mice were examined for ultraviolet radiation-induced corneal degeneration. Mice were exposed to a single relatively high dose of 480 mJ/cm^2 that caused no significant changes of corneal edema, ulceration, or keratitis, but did show some apoptotic corneal stromal cells (Newkirk *et al*., 2007). In another study, a low dose exposure of rabbit corneas to UVB (10 mJ/cm^2 - 80 mJ/cm^2) resulted in a thicker epithelium and loss of the intercellular permeability barrier after 24 hours (Koliopoulos and Margaritis, 1979). A higher dose (500 mJ/cm^2) of UVB on rabbit corneas resulted in degeneration of the corneal endothelium four days after exposure (Koliopoulos and Margaritis, 1979). At a dose of 800 mJ/cm^2, mouse eyes developed cloudy corneas 4 days post exposure (Downes et al., 1994). Sprague-Dawley rat eyes developed corneal epithelial defects at 24 hours post a 1000 mJ/cm^2 UVB exposure (Fujihara et al., 2000). The highest UVB exposure (2000 mJ/cm^2) given daily for four days on rabbit corneas resulted in disorganization of collagen, swelling of the stroma, disappearance of the basement membrane, degeneration of the corneal endothelium, and reduction of epithelium thickness (Koliopoulos and Margaritis,1979).

Mice eyes chronically irradiated at lower doses everyday demonstrate many more adverse UVR effects such as cataract development and conjunctiva growth onto the cornea (pterygium) (Jose, 1986; Cullen, 2011). Albino mice receiving a high dose of UVR (greater than 4 J/cm^2 for 12 hours daily) developed cataracts as well as corneal

scars and vascularization after 1 - 2 months (Jose and Pitts, 1985). Even much lower doses (35 - 360 mJ/cm^2 for 12 hours per day) resulted in posterior cortical cataracts appearing after 5 - 6 months, but did not show a corneal effect (Jose, 1986). These data suggest overexposure of UVB causes corneal epithelial defects, but no evidences showed epithelial-stromal separation similar to SM exposure.

3. Model Systems to Study Wound Healing

3.1. Anatomy and Physiology of the Human Cornea:

The cornea is the outermost, transparent, disk-like, anterior portion of the eye which creates a barrier to the outside environment. As shown in Fig.4, the human cornea is composed of six regions: the corneal epithelium, the basement membrane, Bowman's layer, the stroma, Descemet's membrane, and the endothelium (DelMonte and Kim, 2011). The total thickness of the human epithelium is about 50 um and the whole cornea is about 0.5mm in the center (Farjo et al., 2009). The corneal epithelial cells are non-keratinized and are stacked about five to six layers high (Farjo et al., 2009).

The outermost cells are squamous epithelial cells, soon to be sloughed. These are separated from the basal epithelial cells by the wing cells. The basal cells sit on the basement membrane. The next region, the basement membrane, is mostly composed of type IV collagen, perlecan, and various laminins. In addition, transmembranous proteins, such as collagen XVII, and integrin α6β4 anchor the epithelium to the stromal layer (Gipson et al., 1987; Masunaga et al., 1996; Stepp et al., 1990). Basement membrane modifications determine when cell migration, cell adhesion, and cell differentiation

Fig. 4. Structure of the Human cornea. Three types of corneal epithelial cells, superficial, wing, and basal cells, are present in the 6-8 layers of the epithelium. The epithelium sits on a basement membrane (the second region). The third major region is Bowman's layer, and is an acellular collagenous matrix. The fourth region is the stroma, which is a matrix of collagens and proteoglycans with flattened fibroblasts called keratocytes. This region is architecturally arranged to permit transparency of the cornea. The region layer is Descemet's membrane, a modified basement membrane for the inner most region which is the corneal endothelial cells (the sixth region). These pump liquid from stroma, keeping it relatively dehydrated. Figure adapted from Oyster, C. The Human Eye: Structure and Function, 1999.

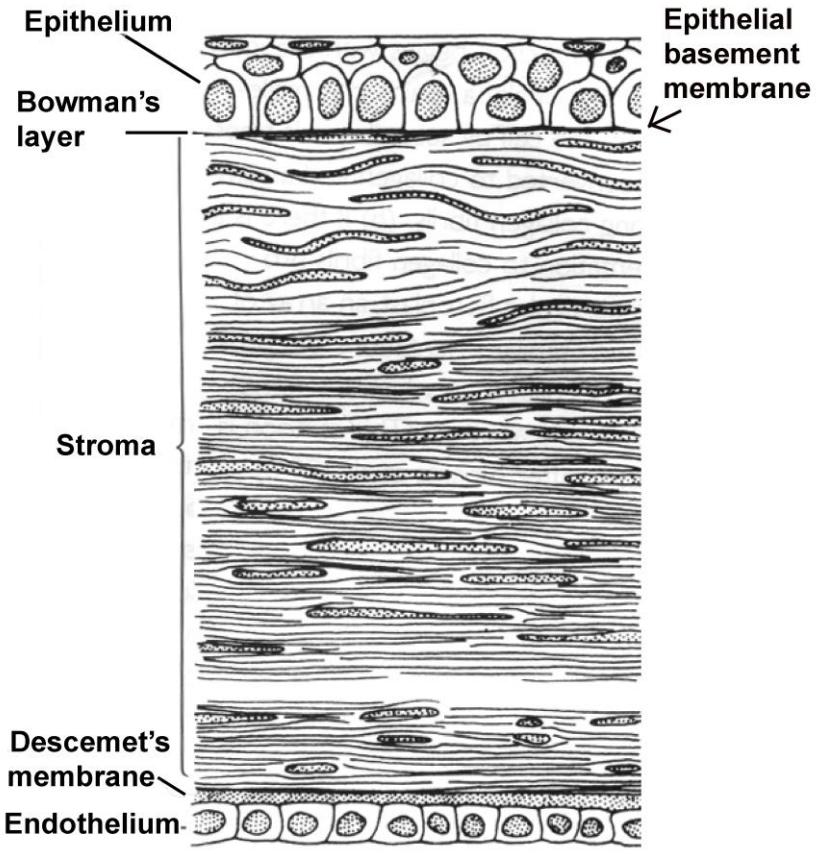

occur after wound healing occurs (Midwood et al., 2004). The basement membrane zone (i.e. the lower part of basal epithelial cells, the basement membrane and the upper part of the stroma) is the target region of interest in NM and UVB exposure.

The third region of the cornea is Bowman's layer and lies anterior to the stroma. This layer is not a membrane, but rather an acellular matrix zone. It is important for maintaining corneal shape (DelMonte and Kim, 2011). Some groups says that Bowman's membrane is only present in primates and birds (Merindano et al., 2002; Linsenmayer et al., 1998), but many groups disagree with this, postulating that it is present, but is much thinner in non-primates.

The fourth region is the corneal stroma. It is the largest portion of the cornea with about 60 - 70 layers of collagen fibrils, interspersed by stromal fibroblasts called keratocytes. The arrangement of stromal collagen fibrils affects the transparency of the cornea (Cox et al., 1970). The tight packing and parallel arrangement of corneal fibrils helps to maintain transparency.

The fifth region is the Descemet's membrane, synthesized produced by both the corneal endothelium and the keratocytes. It is about 8 to 10 um thick. The most posterior region of the cornea is the single layer of flat endothelial cells in a hexagonal pattern. These endothelial cells are linked together by desmosomal and occluding junctions and they pump water out of the corneal stroma to prevent excessive hydration of the extracellular matrix (Bonanno 2003).

3.2. Animal Studies

Rabbits

To study SM exposure, *in vivo* animal models have been used to mimic human exposure (Kadar et al., 2001; Kadar et al., 2009; Gordon et al., 2010). Rabbit eyes can be exposed to either SM vapor or SM liquid. The vapor method allows the agent to affect the entire external eye, including the conjunctiva and limbal region, exposures which might possibly contribute to long term injury. The liquid method affects these also, but not as severely. In animals, the dynamic processes of ocular injury and wound healing after exposure mimics human exposure (Kadar et al., 2001; Mann and Pullinger, 1941). Rabbit eyes and human eyes heal at the same rate after SM (Kadar et al., 2001).

Bovines and Rats

Enucleated Beef eyes also have been used to study the mustard and ultraviolet effects on the loosening of the corneal epithelium (Friedenwald et al., 1948(1); Friedenwald et al., 1948(2); Herrmann and Hickman, 1948) as well as the nuclear fragmentation in the corneal epithelium (Friedenwald et al., 1948(2)). However, beef corneas were less sensitive to develop nuclear fragments and loosening of the corneal epithelium caused by mustard and ultraviolet radiation than rats (Friedenwald et al., 1948(2)). Relatively high amounts of glutathione containing a sulphydryl side chain, a highly potent nucleophile, in the beef corneal epithelium might be a competition factor to other cellular components and cause mustard binding restrictions (Friedenwald et al., 1948(1)). This may affect the binding property and binding sites in the investigations of primary mustard reaction.

3.3. Corneal Organ Culture

In the past several years, the rabbit organ culture system has been developed to study corneal epithelial wound healing (Tanelian and Bisla, 1992; Kuwabara et al., 1976; Foreman et al., 1996). *In vitro* organ culture models were shown to mimic many features of *in vivo* wound healing (Tanelian and Bisla, 1992; Crosson et al., *1986;* Brazzell et al., *1991).* The *in vitro* studies demonstrated a wound closure rate for the corneal epithelium of 52 ± 14 µm/hr (Tanelian and Bisla, 1992). The rate closure *in vivo* is 64 ± 2 µm/hr and 89 ± 27 µm/hr, respectively (Crosson et al., *1986;* Brazzell et al., *1991).*

Corneal organ culture models are superior to cell cultures. The animal organ culture maintains the corneal architecture, preserving the cell layers as in *in vivo* eyes (Foreman et al., 1996). In our rabbit corneal organ culture model (Gordon et al., 2010) corneas with a 2 mm scleral rim were dissected from young adult New Zealand white rabbit eyes purchased from Pel-Freez. The endothelial side of the corneas was filled with 0.75 % agar. After hardening, the corneas were flipped over so the epithelial side of the corneas was facing up, and the corneas were placed in 60 mm pyrex tissue culture dishes and incubated at 37 ℃ in a 5 % CO_2 atmosphere. Serum-free Jester's medium (500 mL high glucose DMEM mixed with 5 mg ciprofloxacin, 5 mL of 100 x MEM-NEAA, 5 mL100 x diluted RPMI 1640 Vitamin solution, and daily fresh 0.25 mM L-ascorbic acid and 0.45 mM L-ascorbic acid 2- phosphate per 50 mL medium) was added only up to the corneal scleral rim to keep the epithelium air-lifted (Fig.5). The air/liquid interface in organ cultures helps retain epithelial differentiation. One study demonstrated that after three weeks in organ culture there was less intercellular epithelial edema than when corneas were submerged under the medium (Richard et al., 1991). Organ culture offers the advantage of following wound healing over a couple of weeks.

Fig. 5. A diagram of the rabbit cornea organ culture model that was used in this study (Gordon et al., 2010)**.** Rabbit corneas were air-lifted by filling with the endothelial concavity with 0.75% agar. The epithelial side of the corneas then were placed facing up. Serum-free medium was added up to corneal scleral rim. Fresh medium, nitrogen mustard, or therapies were all applied onto the central cornea via pipette.

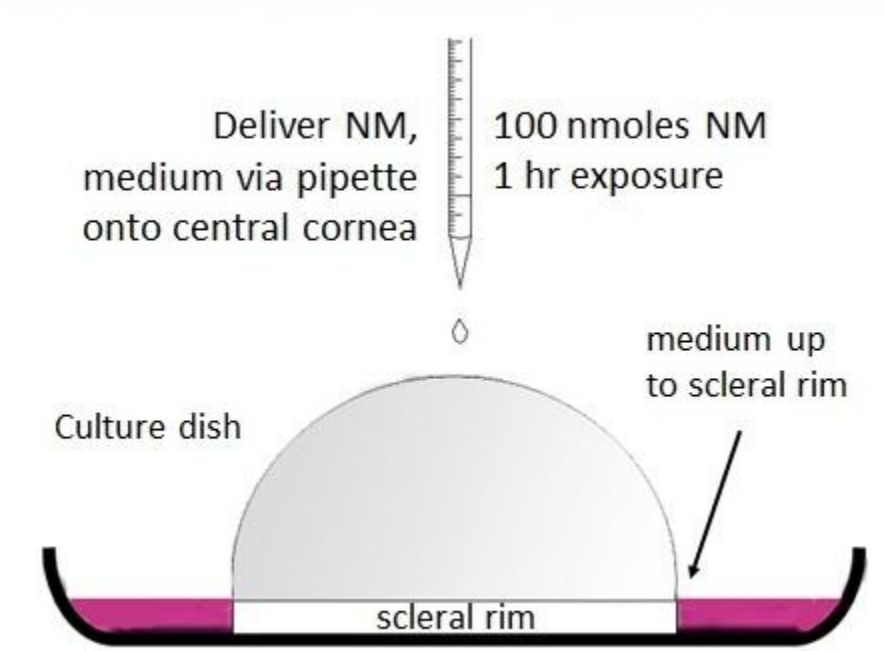

Focus can be placed on changes of the corneal basement membrane zone with NM and UVB exposure without variables that would need considering if the tear film or the conjunctiva were present. In both UVB irradiation and NM exposure, the integrity of the cornea can be easily followed with histology.

4. Corneal Epithelial Wound Healing

4.1. The Process of Corneal Epithelial Wound Healing

Corneal wound healing is a complex process involving in numerous chemical and biophysical activities to promote cell migration, proliferation, differentiation of new growing cells over the wound bed. The interactions between cell-cell and cell matrix communication is assisted by growth factors and extracellular matrix components (Bornstein and Sage, 2002; Nishida and Tanaka 1996). Some corneal injuries involve separation of the epithelial and stromal layers. Re-epithelialization, in which flatten cells send out pseudopodia at the wound edge and migrate as a sheet onto the basement membrane to cover the denuded area, repairs epithelial injury. The cells behind the wound edge proliferate and push the migrating edge until the new epithelium covers the injured area. For repairing epithelial damage to the cornea, the extracellular matrix must be degraded, rearranged, and reconstructed in the wound bed using a provisional matrix (Midwood et al., 2004). After cells migrate over the provisional matrix and close the wound, this matrix is degraded and replaced with a matrix similar to that of the pre-injury state (Midwood et al., 2004). In this way the cornea restores barrier function and transparency.

4.2. Role of Provisional Matricellular Molecules

Interactions between cells and the extracellular matrix (ECM) play important roles in cell signaling, promoting cell survival and cell differentiation during health and wound repair (Bornstein and Sage, 2002; Murphy-Ullrich, 2001). The ECM is an arrangement of several glycoproteins, collagens, proteoglycans, and growth factors. These components support the physical structure of the tissue (Bornstein and Sage, 2002; Murphy-Ullrich, 2001). Through cell surface receptors, ECM molecules also mediate intracellular signaling (Murphy-Ullrich, 2001; Bornstein and Sage, 2002). ECM glycoproteins such as vitronectin, laminin, entactin, collagen IV (in basement membranes), and fibronectin, the fibrillar collagens, such as collagen I, II, III, V, and XI (in stromal regions) can act as structural components or adhesion macromolecules for epithelial and mesenchymal cells. However, the secreted glycoproteins called matricellular proteins also act as modulators of cellular interaction with the extracellular matrix (Bornstein and Sage, 2002; Murphy-Ullrich, 2001). These matricellular proteins are also called provisional matrix components due to the fact that they are expressed in response to injury, but are replaced by mature matrix when the tissue is healed (Midwood et al., 2004). Provisional matrix components include SPARC (secreted protein, acidic and rich in cysteine; also known as osteonectin or BM40), hevin (SPARC like-1 or SPARCL1), thrombospondin-1 and 2, tenascin-C and X, fibronectin and osteopontin. SPARC, hevin, thrombospondin-1, and tenascin-C have de-adhesive properties allowing cells to partially detach from their substratum and migrate (Sage and Bornstein, 1991). Fibronectin has adhesive properties and aids migrating cells (Fujikawa et al., 1981; Nishida, 2010). Provisional matrix proteins are secreted locally at the wound bed

(Berryhill et al., 2003; Latvala et al., 1996). They regulate cell-matrix interaction during the wound healing process (Bornstein and Sage, 2002; Murphy-Ullrich, 2001). They do not usually remain in the healed corneal matrix (Berryhill et al., 2003; Latvala et al., 1996), unless they have a structural role in addition to a dynamic role in remodeling the injury.

4.2.1. SPARC (secreted protein, acidic and rich in cysteine a.k.a osteonectin or BM-40)

SPARC is a matricellular glycoprotein expressed by many different cell types. It plays an important role in development, tissue remodeling, and cell cycle regulation (Maillard et al., 1992; Latvala et al., 1996). SPARC/ osteonectin/ BM-40 was initially found in bone matrix, secreted by osteoblasts during bone formation and bone remodeling (Termine et al., 1981; Romberg et al., 1986). SPARC consists of an acidic N-terminal domain, a follistatin-like domain, and an extracellular Ca^{2+}-binding domain (Brekken and Sage, 2000). These distinct structural domains regulate different biological functions. The follistatin-like domain contains most of the disulfide-bonded cysteine residues of the protein and two Ca^{2+} -binding regions (Hohenester et al., 1997). The extracellular Ca^{2+}-binding (EC) domain also inhibits cells spreading and contributes to the interaction of cells with extracellular matrix (Lane and Sage, 1990; Tremble et al., 1993). This domain contains two EF-hand motifs (helix-loop-helix structure) to stabilize calcium ions within the loop (Hohenester et al., 1997).

SPARC is needed during development and during wound healing. While SPARC-null mice have inflexible tails and fragile bones (Muriel et al., 1991), the

molecule's importance to healing was apparent when it was observed that the lack of SPARC causes accelerated healing of dermal wounds (Bradshaw et al., 2002), along with collagen architecture abnormalities, i.e., scarring (Bradshaw et al., 2003). High levels of SPARC are present in the immature eye (Yan et al., 1998; Kantorow et al., 1998), and most developing organs (Alpers et al., 2002; Norose et al., 1998). The over-expression or under expression of SPARC disrupts eye integrity during development (Bassuk et al., 1999). SPARC is secreted during corneal wound healing by corneal epithelial cells (Latvala et al., 1996, Berryhill et al., 2003; Mishima et al., 1998).

4.2.2. Hevin (SPARCL1, SPARC like 1, SC1, MAST9) and ADAMTS4 (aggrecanase-1)

Hevin is a secreted glycoprotein that is related to SPARC. It is present in the brain, heart, and vasculature (Weaver et al., 2010). It is also expressed in many tissues during embryogenesis and tissue remodeling (Sullivan and Sage, 2004). In mouse, hevin exhibits 53 % identity at the amino acid level with SPARC. Both hevin and SPARC share a homologous C-terminal domain including the follistatin-like domain and the Ca^{2+}-binding domain (Sullivan and Sage, 2004). The follistatin-like domain of hevin shares 56 % identity and the Ca^{2+}-binding domain shares 61 % identity with SPARC (Sullivan and *Sage, 2004).* The three structural domains (follistatin-like, Ca^{2+}-binding and N-terminal domains) regulate cell adhesion, migration, and proliferation. Like SPARC, hevin also has shown a counter-adhesive activity in certain invasive tumors (Brekken et al., 2004). Hevin was first identified as a secreted synaptic junction glycoprotein in postnatal development of the brain, found as a cDNA in a rat brain

expression library (Johnston *et al., 1990).* Recently it was found that hevin is down-regulated in a number of cancers, and suggested a role in tumor-suppression and regulation of angiogenesis (Sullivan and *Sage, 2004),* rather than a role in cell migration (Sullivan et al., 2008). While the molecular weight of SPARC is 43 kDa, hevin is 75-80 kDa.

Hevin is distributed within many tissues including the adrenal gland, brain, eye, heart, pancreas, and lung. It is cleaved by ADAMTS4 (a disintegrin and metalloproteinase with thrombospondin motifs) at residues 358-364 (EA▲ERMHS), as shown in lung and brain tissue fragment (Weaver et al., 2010). Cleavage results in a SPARC-like fragment (Weaver et al., 2010). The generation of a SPARC-like fragment upon hevin digestion with ADAMTS4 suggests hevin may have multiple functions or opposing functions.

ADAMTS4 belongs to the matrix metalloproteinase family. One of its main biological functions is to cleave aggrecan and brevican in articular cartilage (Tang, 2001). This extracellular protease is also abundant in the lung, heart, and brain (Weaver et al., 2010). ADAMTS4 contains 837 residues with 7 main domains: (1) a prodomain (residues 1-207); (2) a furin cleavage site (residues 208-212); (3) a catalytic domain (residues 213-440); (4) a disintegrin-like motif (residues 441-462); (5) a TSP-1 like motif (residues 463-547); (6) a cysteine-rich domain (residues 548-694); and (7) a C-terminal spacer domain (residues 695-837) (Tortorella et al., 1999). Removal of the prodomain and the furin cleavage site (residues 1-212), as well as the C-terminal spacer domain (residues 695-837), are required to activate the enzyme (Gao et al., 2002).

4.2.3. Tenascin-C

In adult tissues tenascin-C, a secreted extracellular matrix glycoprotein, is located at regions where cells are continuously renewed (Maseruka et al., 1997). Tenascin-C is expressed at a low level in many tissues, including lung, skin, mammary gland, liver, prostate, ovary, intestine, and brain. It is highly expressed in human cancer cell lines as compared to normal tissues (Pas et al., 2006). In the amino half of this multi-domain glycoprotein is a heat shock protein 33 motif (HSP33) and epidermal growth factor-like repeats (EGF); in the carbonyl half are fibronectin type III-like repeats (FN III) and a fibrinogen-like region. The mature molecule is a hexamer of tenascin-C chains (Pas et al., 2006). Tenascin-C belongs to the family of counter-adhesive or anti-adhesive proteins, including TSP-1 and SPARC (Murphy-Ullrich, 2001). Like other matricellular proteins, tenascin-C expression is induced in regions of inflammation, fibrosis, neovascularization, and cutaneous or corneal wound healing (Maseruka et al., 1997; Matsuda et al., 1999; Sumioka et al., 2011). After healing, it is degraded and removed from the mature tissue (Maseruka et al., 1997; Matsuda et al., 1999). In bacterial keratitis, tenascin-C expression has been reported to be induced at the region of detachment of the epithelial from the substratum (Maseruka et al., 1997).

4.2.4. Thrombospondin-1 (TSP-1)

Thrombospondin-1(TSP-1) is another calcium-binding matricellular protein which has de-adhesive or counter-adhesive properties like SPARC and tenascin-C (Sullivan and Sage, 2004). TSP-1 also regulates angiogenesis, matrix metalloproteinase 9 (MMP9), and transforming growth factor β (TGF-β) levels during tissue remodeling

(Lawler and Detmar, 2004). TSP-1 was originally purified from human blood platelets (Lawler et al., 1978). It is rapidly deposited at sites of tissue injury (Uno et al., 2004). TSP-1 has been shown to bind to other extracellular matrix (ECM) components, such as proteoglycans, and membrane proteins (Tan and Lawler, 2009). TSP-1 is a trimeric glycoprotein. Each monomer is composed of a heparin binding domain in the N-terminus, a procollagen homology domain, three type I (properdin-like) repeat, three type II (EGF-like) repeat motifs, thirteen type III (calcium-binding) repeat motifs and a C-terminal domain (Lawler, 2000; Tan and Lawler, 2009; Bornstein, 1992).

TSP-1 is secreted by the basal cells of the corneal limbal epithelium to maintain corneal avascularization and integrity. It is increased in amount after injury (Sekiyama et al., 2006). The rate of re-epithelialization was found to increase when exogenous TSP-1 was added to wounded corneas in organ culture. TSP-1 antibody inhibited re-epithelization (Uno et al., 2004).

4.2.5. Fibrillin-1 (FBN-1)

Fibrillin-1 (FBN-1) is a large (~350kDa) acidic modular ECM component present as a structural component in elastic microfibril. It is also found in injured tissue as a provisional matrix component. Human corneas with bullous keratopathy (Ljubimov et al., 1998) contain FBN-1. In the normal cornea, FBN-1 is present in the limbal BM, limbal stroma, the corneal BM adjacent to limbal region, and around blood vessels, but not in the central cornea. In bullous keratopathy corneas, the FBN-1 was found as microfibrils deposited in the corneal stroma and injured epithelial BM.

4.2.6. Fibronectin (FN)

Fibronectin is an adhesive glycoprotein expressed during development as well as during injury (Fujikawa et al., 1981). In the normal healthy cornea, no FN is detected in the epithelial basement membrane. Small amounts are present, though, in Descemet's membrane and the stroma. Upon injury, FN is deposited in corneal basement membrane, and serves as provisional matrix for epithelial cell migration, allowing re-epithelization (Fujikawa et al., 1981; Watanabe et al., 1987). It is then removed from the basement membrane matrix upon healing (Fujikawa et al., 1981). Because it stimulates epithelial wound healing, it is currently being tested as eyedrops in *in vitro* and in animal models to treat persistent epithelial defects (Nishida, 2010).

5. Thesis Research Rationale

We chose UVB injury to compare the corneal healing time of this blistering agent with that of NM exposure injury. Both UVB and NM cause skin blistering several hours post exposure. In addition, UVB blistering normally heals perfectly but often NM injury does not. Our eyes can receive a UVB exposure from the sun at a dose of 110 mJ/cm^2 (UVI = 11). The UVB doses used in our experiments are 100 mJ/cm^2 to 2000 mJ/cm^2, which covers the high range of exposure as well as abnormally high ranges. People will never get a 2000 mJ/cm^2 exposure from the sun, but might get such an exposure from a welder's flash or snow reflection (Diffey, 1990). Our goal was to find the dose of UVB exposure that would induce the same percentage of separation at the epithelial-stromal junction as in corneas exposed to 100 nmol NM for 1 hour. Once this was determined, we used these exposures to follow healing by histology and by the expression of the

provisional matrix proteins. Prolonged expression of certain matricellular proteins such as SPARC, hevin, tenascin-C, TSP-1, and FBN-1 might explain the prolonged repair time observed in the healing of NM-exposed corneas. The removal of provisional matrix in UVB-exposed corneas reflects the normal rate of healing and may provide clues for improving the rate of healing of NM-induced corneal wounds.

Statement of Hypothesis

My hypothesis is that NM-induced corneal injury heals slower than injuries induced by blistering agents like UVB. This may result from the prolonged residence of provisional matrix in the wound bed after mustard exposure, delaying proper healing. To test this hypothesis, the injury to rabbit corneal organ cultures exposed to NM and UVB were set to be equivalent at 24 hours post exposure. They were then used to evaluate and compare corneal healing time after the exposures. Healing was evaluated by both histology and by the length of time the expression of provisional matrix components persisted. Molecules examined were SPARC, hevin, tenascin-C, thrombospondin-1, fibrillin-1, and fibronectin.

Specific Aims

<u>Specific Aim 1:</u> To determine whether corneal organ cultures heal more slowly when injured by nitrogen mustard exposure than by UVB exposure.

Sulfur mustard and its derivates are blistering agents that induce epithelial-stromal separations. Physicians who treated SM-exposed soldiers observed that the mustard-induced skin blisters healed more slowly than skin blisters caused by other agents, such

as sun exposure. This has never been proven experimentally, whether in skin or in the cornea. We will compare ultraviolet B (UVB) exposure of the cornea with NM exposure, to investigate whether the time of corneal healing after both injuries is the same or different.

To accomplish this, the conditions that generate equivalent epithelial-stromal separation at 24 hours post UVB and NM exposure will be determined in rabbit corneal organ cultures. Once determined, the time needed to restore epithelial-stromal reattachment after NM and UVB exposure will be evaluated for each injury. The time course of epithelial migration over the wound bed will be assessed by histology over the course of 10 days.

<u>Specific Aim2:</u> To determine whether provisional matrix components persist longer after nitrogen mustard (NM) injury than after an equivalent UVB injury.

After determining if UVB exposed corneas heal faster than those exposed to NM, whether the provisional matricellular proteins persist in the wound bed the same length of time will be tested. Several provisional matrix components, including SPARC, hevin, TSP-1, tenascin-C, FBN-1, and FN will be examined by immunofluorescence and western analysis to correlate whether the healing time for injury matches the expression pattern of the provisional matrix over the course of 10 days. This experiment could lead to identification of provisional matrix components in the wound bed that might persist after NM exposure and might be a target for developing countermeasures against mustard injury.

<u>Specific Aim 3:</u> To evaluate whether ferritin is present in the nuclei of rabbit corneal epithelial cell, as it is in those of the chick cornea.

Nuclear ferritin heavy chain has been shown to protect chicken corneal epithelial cells from UVB damage. This has not yet been examines in mammalian corneas. At a series of time points after UVB exposure, ferritin heavy chain will be followed by immunofluorescence analysis of rabbit corneal organ cultures.

Materials and Methods

1. Models and Exposures

1.1. List of Reagents

Young adult New Zealand white rabbit eyes were purchased from Pel-Freez (Rogers, AR). Bovine serum albumin (BSA), DAPI, high glucose Dulbecco's modified Eagle's medium (DMEM), 100 x MEM-NEAA, Alexa Fluor 488 conjugated goat anti-mouse, Alexa Fluor 488 conjugated goat anti-rat, Alexa Fluor 488 conjugated donkey anti-goat, Alexa Fluor 488 conjugated donkey anti-rat, Alexa Fluor 568 donkey anti-goat IgG antibodies, ProLong® Gold antifade reagent (P-36930) and with DAPI (P-36931) were from Invitrogen (Carlsbad, CA). Agar, ciprofloxacin, EDTA, HEPES buffer, L-ascorbic acid, L-ascorbic acid 2-phosphate, nitrogen mustard powder (cat# 122564), RPMI 1640 Vitamin solution, Trizma base were from Sigma-Aldrich (St. Louis, MO). Pen-Fix was from Richard Allen Scientific (Kalamazoo, MI). Optimal cutting temperature (O.C.T) was from Tissue Tek (Torrance, CA). Hematoxylin and Triton X-100 were from Fluka (St. Louis, MO). Sodium chloride was from JT Baker (Austin, TX). EDTA-free protease inhibitor cocktail tablets (cat#04 693 159 001) was from Roche (Indianapolis, IN). Normal goat serum and normal donkey serum were from Jackson ImmunoResearch (West Grove, PA). Mouse anti-human SPARC monoclonal antibody (cat# ab25764), mouse anti-human tenascin-C monoclonal antibody (cat# ab88280), mouse anti- human thrombospondin-1 (TSP-1) monoclonal antibody (cat# ab1823), and mouse anti-human fibronectin monoclonal antibody (cat# ab6328), goat anti-human ferritin heavy chain polyclonal antibody (cat# ab80587) were from Abcam (Cambridge,

MA). Rat anti- mouse hevin (SPARC-like 1/SPARCL1) monoclonal antibody (cat# LS-C39200) was from Lifespan Biosciences (Seattle, WA). Mouse anti- human fibrillin-1(FBN-1) monoclonal antibody (cat# MA1-21805) was from Thermo Fisher Scientific (Waltham, MA). Goat anti-human ADAMTS4 polyclonal antibody (cat#AF4307) and goat anti-human SPARC-like 1/SPARCL1 polyclonal antibody (cat#AF2728) was from R&D Systems (Minneapolis, MW). Horseradish peroxidase (HRP) conjugated secondary antibodies (goat anti-mouse, donkey anti-goat) were from BioRad (Hercules, CA). SuperSignal West Pico Chemiluminescent Substrate was from Thermo Scientific (Rockford, IL).

1.2. Rabbit Cornea Organ Culture Model

Whole eyes from young adult New Zealand white rabbit (mixed gender rabbits, approximately aged 8-12 weeks) were collected fresh and delivered next day for dissection. These eyes were shipped and stored within DMEM containing penicillin, streptomycin, amphotericin B, and gentamicin, and kept cold on ice. Regular serum-free Jester's medium contains 500 mL of high glucose DMEM with 5 mg ciprofloxacin, 5 mL of 100 x MEM-NEAA, 5 mL of 100 x RPMI 1640 Vitamin solution. And then daily, fresh 0.25 mM L-ascorbic acid and 0.45 mM L-ascorbic acid 2-phosphate was added to 50 mL Jester's medium. Bench buffer consisted of Jester's medium with 50 mM HEPES and was used during corneal eye dissection. A stock of 1.5 % Agar in water was autoclaved, and immediately set it a boiling water bath, to keep the agar liquid. A stock of 2 x DMEM (resuspend 13.5 g DMEM powder in 500 mL dH_2O; pH 7.4) was filter sterilized (0.22 um). In a 1.5 mL microfuge tube, a mixture of 0.5 µL of 1.5 % agar (set

in a 70 ℃) and 0.5 µL 2 x DMEM was vortexed and set in a 50 ℃ heat block until ready for future use.

Corneas with a 2 mm surrounding scleral rim were dissected from the eyes, the iris and the lens were removed, and the corneas were individually placed in a well of a 12-well culture plate (each well containing 2-3 mL of bench buffer). A few drops of Jester's medium was added to the wells of a sterile spot plate before the corneas were transferred, epithelial side down. The corneal endothelial concavity (facing upward) was filled with 200-500 µL of the warm agar/DMEM mixture. This mixture was allowed to solidify at RT for 4 minutes. Corneas (with their agar filling/base) were inverted and transferred into sterile 60 mm pyrex tissue culture dishes. Approximately 2 mL Jester's medium was added to reach the top of the scleral rim, and stored at 37 ℃ in a 5 % CO_2 humidified incubator. Every 6 hours, 500 µL of Jester's medium was wetted to the central corneal epithelium to help keep the epithelia moist.

1.3. Nitrogen Mustard Exposure

Young adult rabbit corneas in organ culture were initially exposed to different doses of nitrogen mustard. The goal was to attain greater than 50 % epithelial-stromal separation. Nitrogen mustard powder was dissolved in sterilized PBS to 50 mM and 100 mM. These were diluted to 5 mM and 10 mM respectively and were used immediately. Ten µL of these concentrations (50 nmol and 100 nmol, respectively) were applied to the center of the corneas (Fig.5), and then cultures were returned to the 37 ℃, humidified, 5 % CO_2 incubator. Nitrogen Mustard exposures ran for 30 minutes or 1 hour before washing the corneas with fresh medium. Corneas were returned to the 37 ℃, humidified,

5 % CO_2 incubator for 24 hours. Four corneas were used in each exposure group to evaluate the 24 hours post-exposure injuries. Additional dishes of corneal organ cultures were prepared as unexposed controls.

1.4. UVB Irradiation

Again the goal was to attain greater than 50 % epithelial-stromal separation, which was likely to require exposures higher than what humans would experience in nature. Organ cultured corneas were placed in a UVB box at a distance of 14 cm from the lamps. At this distance, the exposure per minute is 20 mJ/cm^2. Corneas were irradiated with 100 mJ/cm^2 (5 minutes), 400 mJ/cm^2 (20 minutes), 800 mJ/cm^2 (40 minutes), 1200 mJ/cm^2 (60 minutes), 1600 mJ/cm^2 (80 minutes), and 2000 mJ/cm^2 (100 minutes). Control organ cultures were placed in the box at the same time, but were covered with black vinyl to block the UVB irradiation (Fig.6). All corneas were wetted every 20 minutes with 20 µL of sterile PBS. The temperature in the box during the UVB irradiation was 27 ℃ to 30 ℃.

For nuclear ferritin experiments, corneas were exposed to UVB as described above. Two corneas were exposed for each of the following experimental time points: 2 minutes (40 mJ/cm^2); 15 minutes (300 mJ/cm^2); 30 minutes (600 mJ/cm^2); and 60 minutes (1200 mJ/cm^2). As controls, corneas was placed under the UVB box at the same time as the 60 minutes exposed corneas, but were covered with black vinyl. One cornea from each time point (plus one 60 minutes control) were collected immediately for nuclear ferritin histological analysis. The others were placed in the 37 ℃, 5 % CO_2 incubator for 3 hours before being collected for nuclear ferritin histological analysis.

Fig. 6. A diagram of the equipment that was used in UVB-irradiation. The set up of a UVB exposure box was used to irradiate to corneas. The rabbit cornea organ cultures placed under the UVB lamps were exposed to UVB light for the times indicated in the text (**UVB intensity of lamps: 20 mJ/cm^2 per minute)**. As controls, some corneas were covered with black vinyl (indicated by the umbrella in figure) to allow identical conditions, but without the UVB exposure. After UVB exposure, all corneas were incubated at 37 ^{o}C for a minimum of 24 hours, to allow for epithelial-stromal separation, after which analyses were performed.

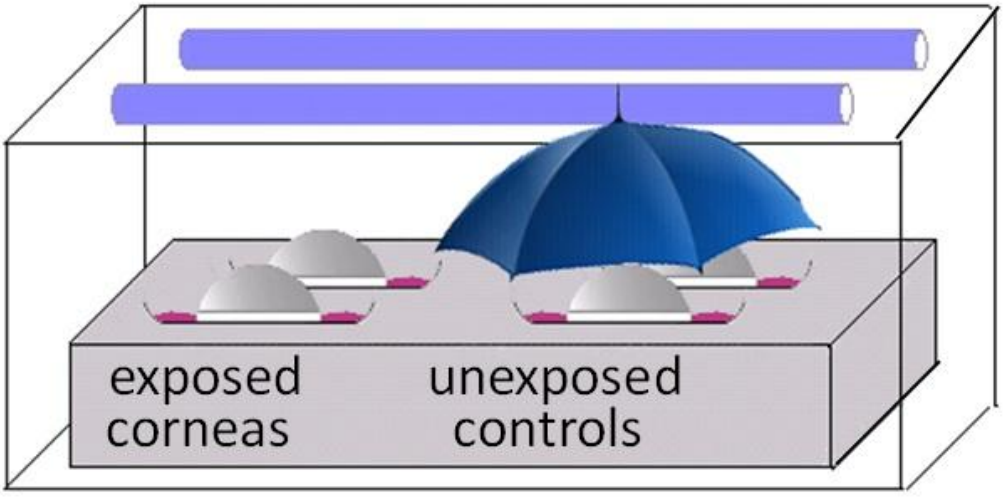

2. Histology

For histology, controls, NM-exposed, and UVB-exposed corneas were collected at times ranging from 24 hours to 10 days prior to embedding in O.C.T compound. Samples sat on wet ice for 15 minutes, then were immediately frozen in liquid nitrogen, and were stored at -80 ℃ until analysis. The central portions of corneas were cryostat sectioned at -20 ℃ at a thickness of 10um and were transferred to super frost plus glass slides (Fisher Scientific). A modified haematoxyline and eosin stain (H&E) was used on the sectioned corneas as follows: Sections were fixed with Pen-Fix for 1 minute and rinsed with distilled water for 8 minutes. Staining with Mayer's hematoxylin was done for 8 minutes, followed by rinsing with warm tap water for 16 minutes, then a quick stain with eosin for one second. Sections were dehydrated with 95 % alcohol, 100 % alcohol, and xylene, each twice for 2 minutes. The stained slides were cover slipped (Corning, No.1, 24 x 50mm) with Permount. Digital images were captured with a light microscope (Leica DMLB microscope with Jenoptik digital camera) at 40 x and 200 x magnification.

3. Immunofluorescence

3.1. Matricellular Proteins

For immunofluorescence analysis, the frozen sectioned corneas were fixed in cold methanol (-20℃) for 10 minutes and air dried. After rinsing with PBS for 5 minutes three times, slides were blocked for non-specific binding using 5 % normal goat serum or normal donkey serum by incubating in a humidity chamber for 60 minutes at room temperature. The blocking agent was removed and the slides were incubated with primary antibody diluted in 1.5 % normal goat serum or 1.5 % normal donkey serum for

1 hour at room temperature or at 4 ℃ overnight. For the detection of provisional extracellular matrix components, sections were incubated with 50 µL primary mouse anti-human SPARC monoclonal antibody (10 µg/mL, final concentration); 50 of primary rat anti- mouse hevin (SPARC-like 1/SPARCL1) monoclonal antibody (10 µg/mL, final concentration); 50 µL primary mouse anti-human tenascin-C monoclonal antibody (10 µg/mL, final concentration); 50 µL primary mouse anti- human thrombospondin-1 (TSP-1) monoclonal antibody (8 µg/mL, final concentration); 50 µL primary mouse anti-human fibrillin-1(FBN-1) monoclonal antibody (10 µg/mL, final concentration); and 50 µL primary mouse anti-human FN monoclonal antibody (10 µg/ml, final concentration). After primary antibody incubation, slides were washed 4 times (10 min each) with PBS containing 0.2 % Tween-20. Sections were then incubated in 100 µL of appropriate Alexa-Fluor 488 secondary antibody for 1 hour at RT. For SPARC, tenascin-C, TSP-1, FBN-1, FN, the conjugated goat-anti-mouse IgG secondary antibody was diluted 1:1,000 in 1.5% normal goat serum. For hevin, conjugated goat-anti-rat secondary antibody was diluted 1:1,000 in 1.5% normal donkey serum. After incubation, the slides were washed with PBS/Tween-20 for 5 minutes three times and mounted with ProLong® Gold antifade reagent with DAPI. The stained slides were cover slipped and were allowed to sit overnight at 4 ℃. Digital epiflorescent images of corneas were captured with a fluorescent microscope (Carl Zeiss Axio Observer Inverted Microscope) at 200 x and 400 x magnification. SPARC, hevin (SPARC-like -/SPARCL1), thrombospondin-1 (TSP-1), fibrillin-1(FBN-1), tenascin- C, and fibronectin (FN) were examined by immunofluorescence in NM- and UVB-exposed corneas. Their detection was at 517 nm emission (green) and the detection of DAPI (nuclei stain, blue) at 455 nm emission.

3.2. Co-localization of Hevin and ADAMTS4

For the simultaneous immunostaining of hevin and ADAMTS4, fixation of the sections was as above, cold methanol. Sections were blocked in 5 % normal donkey serum for 1 hour at room temperature. The sections were double-stained with a mixture of 50 µL of monoclonal rat anti-mouse hevin IgG (10 µg/ml) and 50 µL of polyclonal goat anti-human ADAMTS4 (15 µg/ml) diluted in 1.5% normal donkey serum, and incubated overnight in 4 ℃. Primary was washed off with PBS/Tween-20 three times for 10 minutes. A mixture of the secondary antibodies (Alexa Fluor 488 conjugated donkey anti-rat and Alexa Fluor 568 donkey anti-goat) were diluted 1:1,000 in 1.5 % normal donkey serum. This was applied to the sections for an hour incubation at room temperature in the dark. The slides were washed with PBS/Tween-20 three times for 5 minutes and incubated in DAPI (1 µg/ml in PBS) for 5 minutes. Following one wash for 5 minutes with PBS/Tween-20, the sections were mounted with ProLong® Gold antifade reagent.

3.3. Ferritin Heavy Chain Detection

The ferritin in the rabbit corneas was detected using 50 µL of primary polyclonal goat anti-human ferritin heavy chain (8 µg/ml, final concentration, in 1.5% normal donkey serum) and Alexa-Fluor 488 conjugated donkey anti-goat IgG secondary antibody (diluted 1:1000). The nuclear and cytoplasmic ferritin was detected at 517 nm emission and DAPI (nuclear stain, pseudo colored red) for nuclei at 455 nm emission.

4. Protein Extraction Preparation and Culture Medium Collection

Control, NM, and UVB exposed corneas, incubated for 1 - 10 days post exposure, were cut into halves. One half was embedded in O.C.T., while the other half for protein extraction was frozen in liquid nitrogen and stored in the -70 ℃ freezer. Frozen samples were crushed using a pulverizer gun, then ground in liquid nitrogen with a mortar and a pestle to a fine powder. To the ground material was added low salt extraction buffer (25 mM Trizma base, 200 mM NaCl, 10 mM EDTA, and 1 % Triton X-100; pH 7.4) containing a EDTA-Free protease inhibitor cocktail tablet. The ground tissue was homogenized with the Polytron homogenizer at 20,000 rpm for pulses of 30 seconds on, 30 seconds off. This was repeated 3 - 4 times on ice. The samples were centrifuged at 12,000 x g for 30 minutes at 4 ℃. The supernatant was collected and the protein concentration was measured using the bicinchoninic acid method (BCA Protein Assay, Pierce). For secreted proteins, serum-free medium from organ cultures were collected and clarified by centrifugation at 20,000 rpm for 15 minutes at 4 ℃. The supernatant was stored at -20 ℃ until used.

5. Immunoblot

Cell lysate protein and secreted proteins in cell culture medium were diluted in dH_2O and sample buffer, and 20 µg/well was loaded onto a 5 - 7.5 % sodium dodecyl sulfate polyacrylamide elecrophoresis gel (SDS-PAGE). Proteins were trans-blotted to a 0.2 µm nitrocellulose membrane (Bio-Rad) at 100 volts for 1 hour or at 25 volts at 4 ℃ overnight. Non-specific binding to the blot was blocked by incubation for 1 hour with 3% BSA diluted in 1x TBS/ 0.2 % Tween-20 buffer (TBST) containing 0.02 % NaN_3.

Membranes were incubated in primary antibodies against SPARC (1:1,000), hevin (1:100), tenascin-C (1:100), thrombospondin-1(1:250), fibronectin (1:400) and ADAMTS4 (1:125) diluted in 2 % BSA blocking buffer and incubated overnight at 4 ℃ on a shaker. Blots were washed 3 times for 5 minutes each in 1 x TBST and incubated in HRP conjugated secondary antibodies goat anti-mouse (SPARC, 1:10,000; thrombospondin-1, 1:5,000; tenascin-C, 1:5,000; fibronectin, 1:5,000), or donkey anti-goat (hevin, 1:5,000; ADAMTS4, 1:5,000). These were diluted in 5 % non-fat milk in 1x TBST for 1 hour at room temperature. Blots were treated with ECL reagent for detection of HRP. X-ray films were then exposed.

6. Evaluation of Corneal Wound Healing

6.1. Equivalent Injuries of NM and UVB

Corneas were embedded in O.C.T compound and frozen at -80 ℃ until sectioned. Sections were stained with H&E as described previously and visualized by light microscopy, then photographed across the full diameter of the cornea. Composites of overlapping micrographs across the entire cornea were analyzed to determine what conditions resulted in equivalent phenotypes of NM and UVB exposed corneas at 24 hours post exposure. The percentage of epithelial-stromal separation was determined across the entire length of the cornea for each exposure condition. The lengths of regions with epithelial-stromal separations, divided by the length of the entire corneal diameter, times 100, yield the percentage of separation. The separation of the epithelial and stromal layers in UVB exposed corneas was accompanied by regions where the basal epithelial cells remained attached to the stroma, but were clearly dead. These areas of

unclear separation were counted as the loss of the epithelial layer (Fig.8-3. panels R, S, and W).

6.2. Corneal Wound Healing Evaluation by H&E Staining

Epithelial-stromal separation was evaluated for UVB-exposed corneas. Using 100 nmol NM for 60 minutes gave 58 ± 13% epithelial-stromal separation at 24 hours post-exposure, which was close to the 60 ± 11% separation induced by 2000 mJ/cm^2 UVB. These conditions were used to induce equivalent 24 hours post-exposure injury, then the corneas were allowed to heal from 1-10 days. The corneal "healing time" was the time it took to achieve the presence of a thin layer of corneal epithelial cells to cover the entire cornea.

6.3 Expression of Provisional Matrix Components

In addition to H&E staining, sections were analyzed by immunofluorescence microscopy using antibodies against the provisional extracellular matrix components, SPARC, hevin, tenascin-C, TSP-1, FBN-1, and FN. As provisional matrix components, these proteins are deposited after injury and are removed when the tissue is healed. Thus, they provide an additional parameter to assess healing.

The persisting time of the provisional matrix components on the wounded bed post NM-exposed and UVB-exposed corneas, and the co-localization of hevin and ADAMTS4, were evaluated by immunofluorescence analysis. The quantity of these proteins was analyzed by western blotting.

Results

Dose-response of NM on the Degree of Corneal Injure

In order to compare corneal wound healing time after NM and UVB exposures, it was necessary to define parameters that give equivalent injuries at a specific time point. Our previous experiment with 100 nmol NM for 2 hours produced 82 % epithelial-stromal separation and the corneas were not healed even after 7 days (data not shown), therefore shorter NM exposure times (30 and 60 minutes) were chosen as well as lower exposure doses (50 nmol). These two amounts of NM were used on corneas for two different exposure times to optimize the chances of finding a condition that produced around 50 % separation of the epithelial-stromal junction at 24 hours post exposure. We found that, 50 nmol NM exposure for an hour resulted in 5 ± 2% separation 24 hours later (Fig.7-1, panel A); 100 nmol for 30 minutes, gave 31 ± 5% separation 24 hours later (Fig.7-1, panel B); and 100 nmol for 60 minutes yielded 58 ± 13% separation 24 hours post-exposure (Fig.7-1, panel C). The calculated results are presented in figure 7-2. The 100 nmol exposure for 1 hour produced somewhat more than 50 % epithelial-stromal separation, and was in the desired range of injury. Higher magnifications are shown in Fig. 7-3. In the low dose (50 nmol) of NM exposure for one hour, there was some downward hyperplasia of the epithelia in some regions with loose connections between epithelial cells and stroma (Fig.7-3. panels B - D). Larger regions of separation were shown in the high dose (100 nmol) of NM exposure for 30 minutes (Fig. 7-3. Panels F - H) and one hour (Fig. 7-3. Panels J - L). The cornea controls (Fig. 7-3. Panels A, E, and I) were patterned with four to five layers of epithelial cells.

Fig. 7-1. Determination of injury induced by NM exposures. The goal was to produce more than 50% separation of the epithelial-stromal junction at 24 hours post exposure. (A) 50 nmol NM exposure for 1 hour; (B) 100 nmol for 30 minutes; and (C) 100 nmol for 60 minutes.

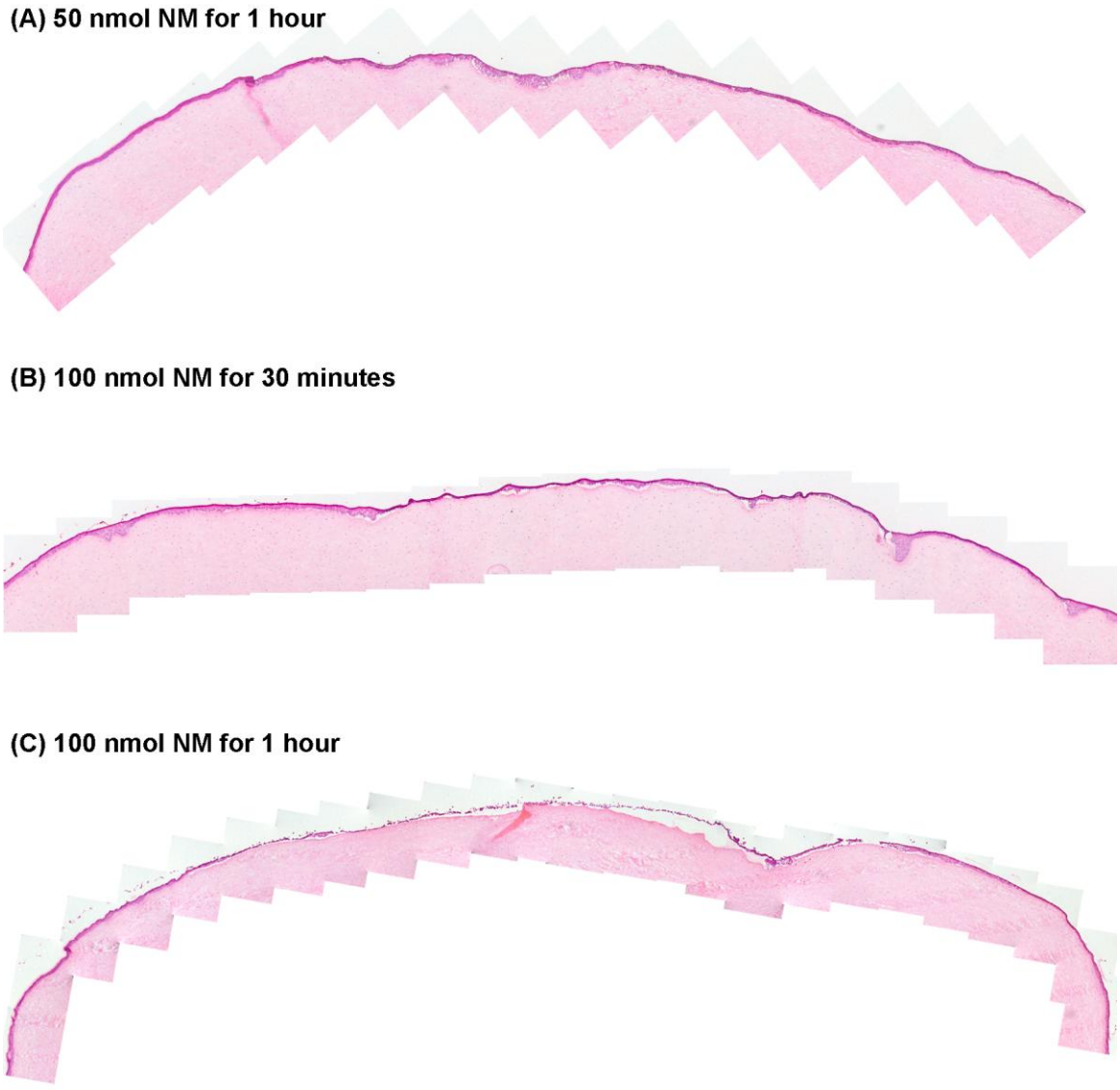

Fig. 7-2. Calculation of the percentage of epithelial-stromal separation at 24 hours post NM exposure. 50 nmol NM exposure for 1 hour resulted in 5 ± 2 % separation 24 hours post exposure; 100 nmol for 30 minutes, gave 31 ± 5 % separation 24 hours post NM; and 100 nmol for 60 minutes yielded 58 ± 13 % separation 24 hours post-exposure.

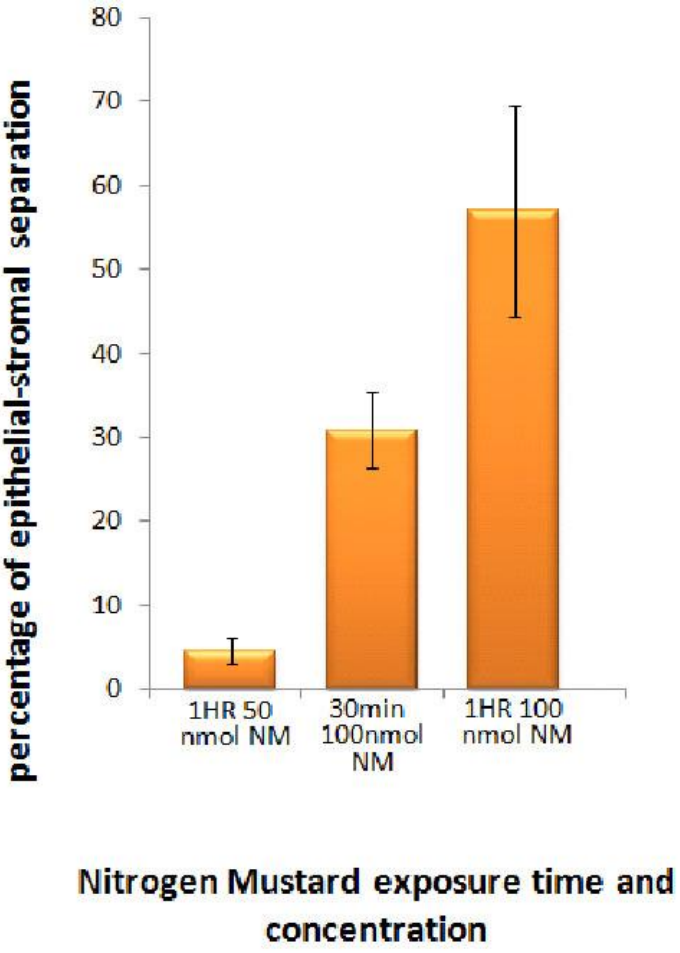

Fig. 7-3. Higher magnification of typical regions of H&E stained sections from three different corneas 24 hours post NM exposure (20 x) to show details of the epithelial-stromal separations; (B) - (D) 50 nmol NM for 1 hour; (F) - (H) 100 nmol NM for 30 minutes; and (J) - (L) 100 nmole NM for 1 hour. The controls of each intensity of UVB irradiation are shown in (A), (E), and (I).

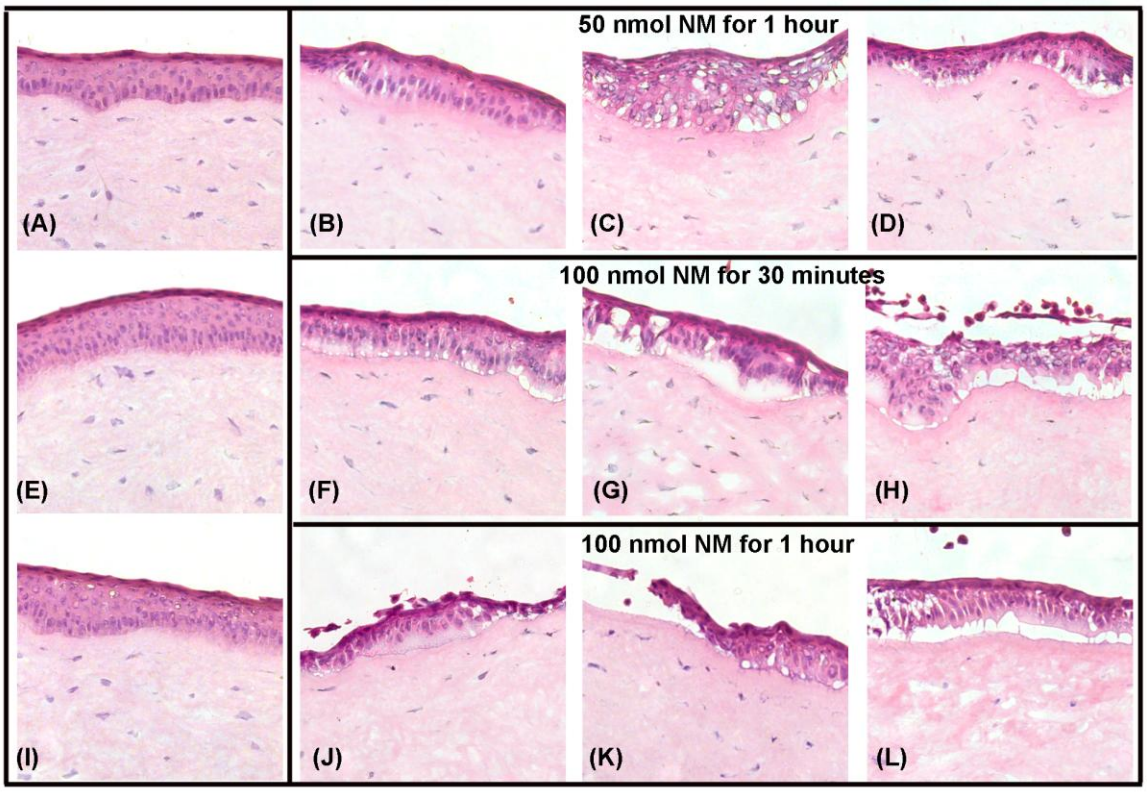

Dose-response Relationship of UVB Irradiation

To find the dose of UVB irradiation needed to produce more than 50 % epithelial-stromal separation, different intensities of UVB were used, and corneas were analyzed at 24 hours post exposure. As seen in Fig. 8-2, a 100 mJ/cm^2 (5 minutes) UVB exposure resulted in no epithelial-stromal separation (Fig.8-1, panel A); 400 mJ/cm^2 (20 minutes) resulted in 1 ± 1% (Fig. 8-1, panel B); 800 mJ/cm^2 (40 minutes) resulted in 5 ± 5% (Fig.8-1, panel C); 1200 mJ/cm^2 (60 minutes) resulted in 12 ± 1% (Fig.8-1, panel D); 1800 mJ/cm^2 (80 minutes) induced 25 ± 1% (Fig.8-1, panel E); and 2000 mJ/cm^2 (100 minutes) led to 60 ± 11% epithelial-stromal separation (Fig.8-1, panel F). A graph of the measured results is shown in Fig. 8-2. Higher magnifications are shown in Fig. 8-3. In the short time exposure (5 minuts; 100 mJ/cm^2), there was some downward hyperplasia of the epithelia in many regions (Fig.8-3. panels B - D). The 20 minutes UVB exposure (400 mJ/cm^2) showed minimal separation of the epithelium and stroma and more epithelium hyperplasia than the shorter exposure (Fig.8-3. panels F-H). However, larger regions of separation started to show after 40 minutes UVB exposure (800 mJ/cm^2) and resulted in loose connections between epithelial cells (Fig.8-3. panels J-L). Twenty four hours after 60 minutes (1200 mJ/cm^2) (Fig.8-3, panels N-P) and 80 minutes (1600 mJ/cm^2) (Fig.8-3, panels R-T) UVB, epithelial layers were thinner, and had more extensive regions of separation. Cells appeared unhealthy and were falling off individually and as layers. The 80 minutes (1600 mJ/cm^2) and 100 minutes (2000 mJ/cm^2) (Fig.8-3, panels V-X) irradiated corneas had many very clear separations of the epithelial and stromal layers. Occasionally some basal cells remained on the BM, but they looked unhealthy with many vacuoles. The controls for the different intensities of

Fig. 8-1. Determination of injuries induced by UVB-exposures. (A) 100 mJ/cm^2 UVB for 5 minutes exposure resulted in no epithelial-stromal separation; (B) 400 mJ/cm^2 for 20 minutes; (C) 800 mJ/cm^2 for 40 minutes; (D) 1200 mJ/cm^2 for 60 minutes; (E) 1800 mJ/cm^2 for 80 minutes; and (F) 2000 mJ/cm^2 for 100 minutes.

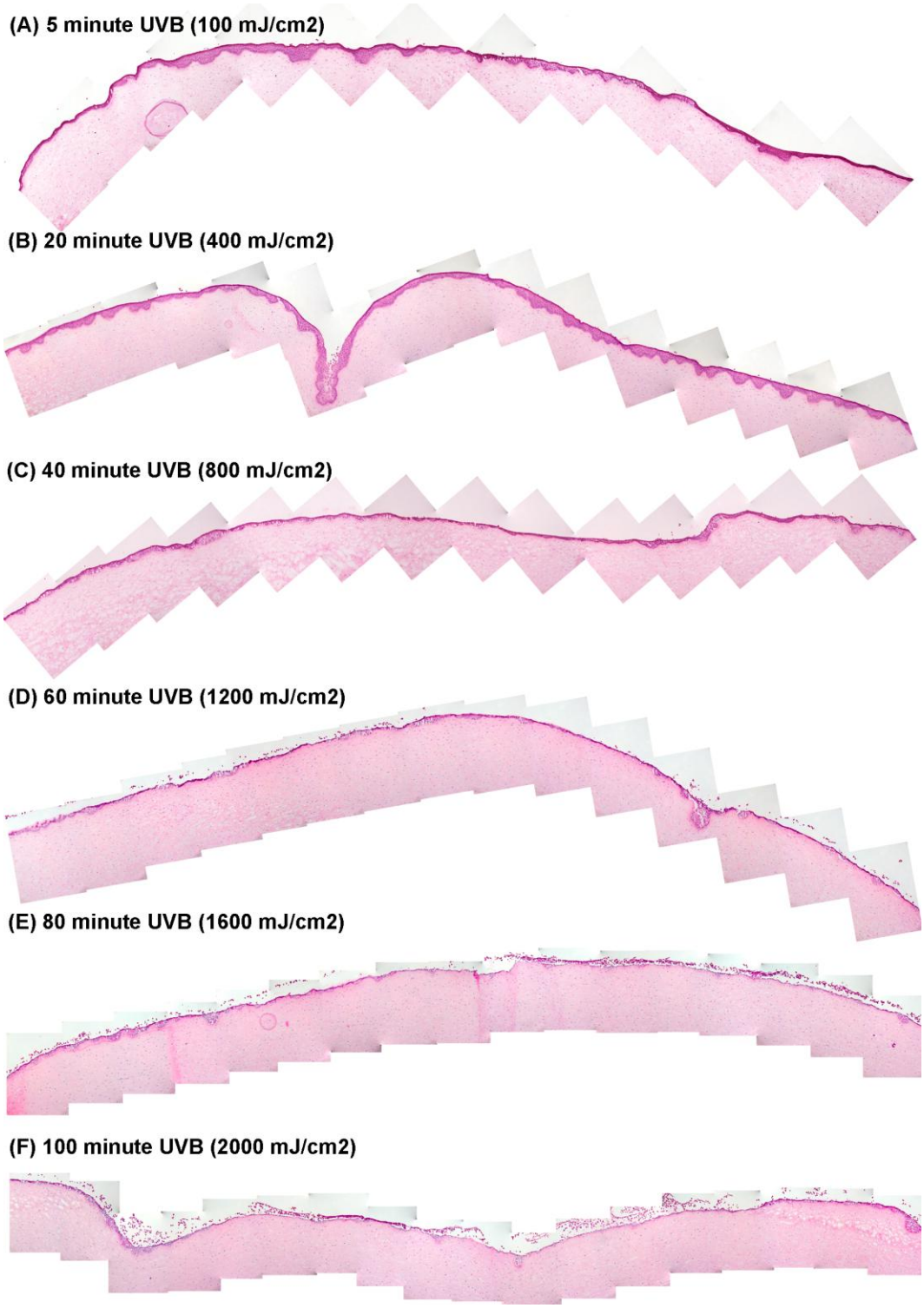

Fig. 8-2. Calculation of the percentage of epithelial-stromal separation at 24 hours post UVB exposure. 100 mJ/cm^2 UVB exposure resulted in no epithelial-stromal separation; 400 mJ/cm^2 resulted in 1 ± 1%; 800 mJ/cm^2 resulted in 5 ± 5%; 1200 mJ/cm^2 resulted in 12 ± 1%; 1800 mJ/cm^2 induced 25 ± 1%; and 2000 mJ/cm^2 led to 60 ± 11% epithelial-stromal separation.

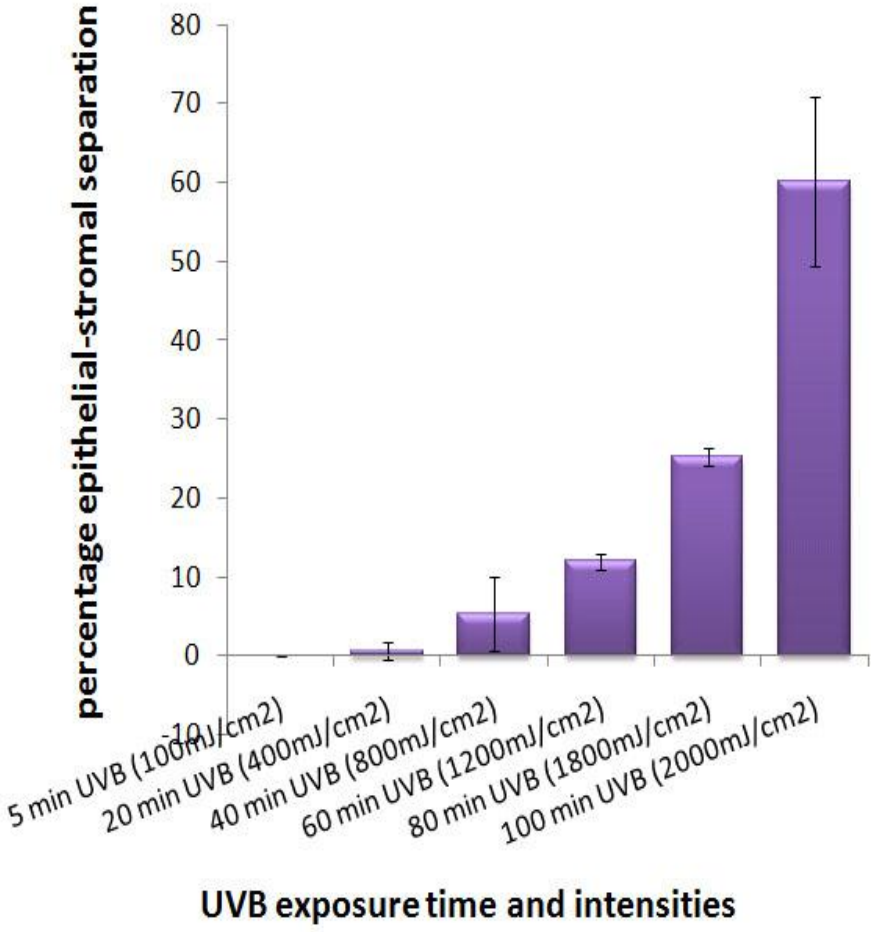

Fig. 8-3. Higher magnification of typical regions of H&E stained sections from three different corneas 24 hours post UVB exposure (20 x) to show details of the epithelial-stromal separations; (B) - (D) 5 minute UVB exposure (100 mJ/cm^2); (F) - (H) 20 minute UVB exposure (400 mJ/cm^2); (J) - (L) 40 minute UVB (800 mJ/cm^2); (N) - (P) 60 minute UVB (1200 mJ/cm^2); (R) - (T) 80 minute UVB (1600 mJ/cm^2); and (V)-(X) 100 minute UVB (2000 mJ/cm^2). The controls of each intensity of UVB irradiation are shown in (A), (E), (I), (M), (Q), and (U).

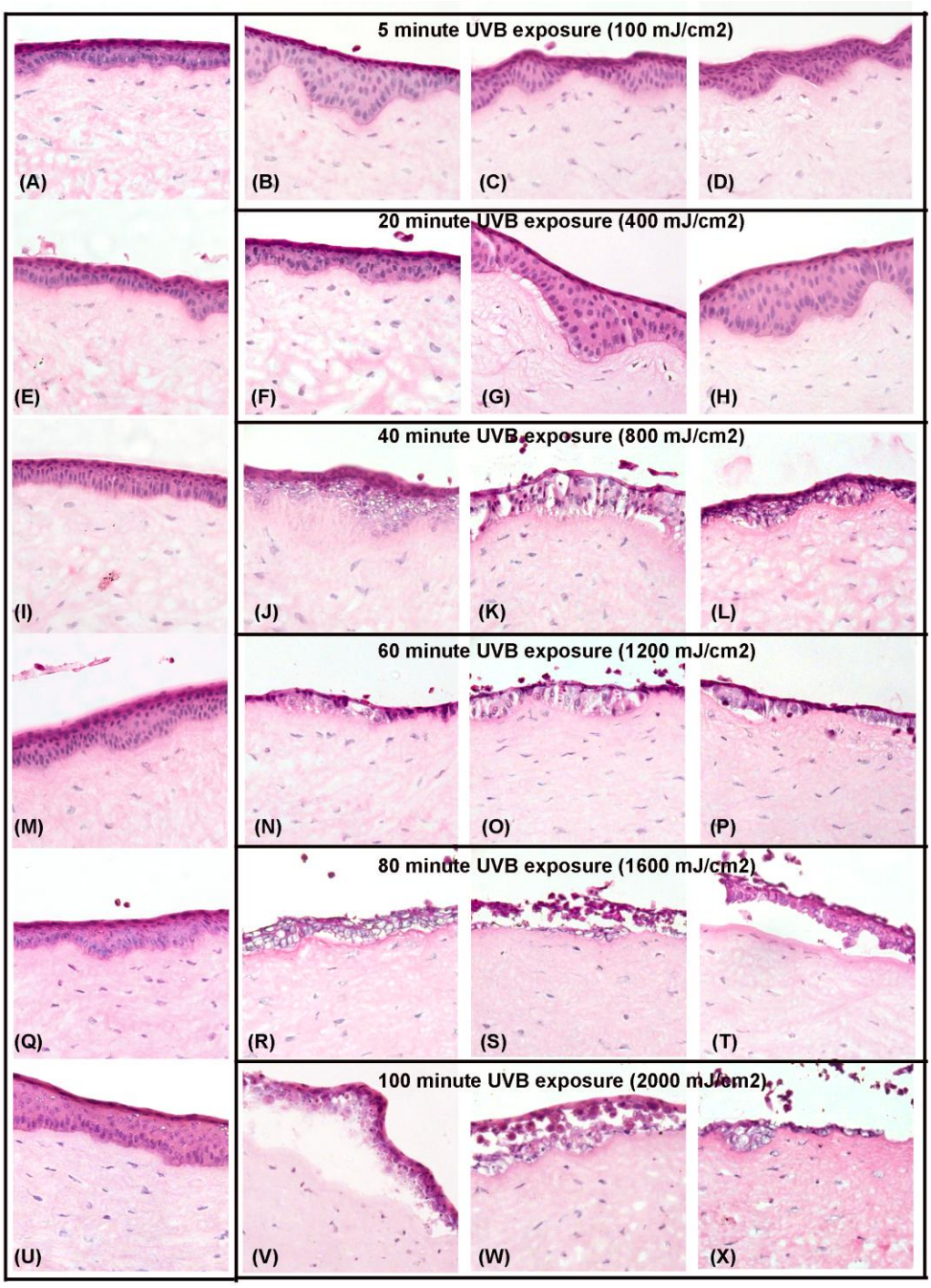

UVB irradiation are also shown at the left. These controls had been placed under the UVB lamp at the same time as the corneas to be exposed, but they were covered with black vinyl. Therefore they were treated exactly as the exposed samples in all other ways. (Fig.8-3. panels A, E, I, M, Q, and U). The controls had the appearance of normal corneas in culture for 24 hours.

Corneal Wound Healing of Equivalent NM and UVB Injuries

The time course of epithelial repair was evaluated histologically by first making composites of overlapping H&E stained sections across the entire diameter of the cornea as shown for the initial exposures. Normal unexposed corneas have 6-8 layers of epithelial cells (Fig.9-1, Fig.9-2, Fig. 10-1, and Fig. 10-2, panels A). Equivalent injury from NM and UVB was determined, with the percentage of epithelial-stromal separation at 24 hours post-NM exposure being 58 % (Fig.9-1and Fig.9-2, panels B), and post-UVB being 60 % (Fig.10-1and Fig.10-2, panels B). Using these exposure conditions, the time for wound healing to cover the entire stroma with an epithelial layer was evaluated over the course of 10 days by calculating the percentage of epithelial cells covering the whole length of the cornea diameter. Two days after exposure, the epithelium in NM- and UVB-exposed corneas had peeled off (data not shown). At 3 days post UVB exposure, the corneal epithelium had started to migrate and cover the wound (Fig.10-1. panel C). The reformed epithelial layer is about one cell thick, and the adhesion appears imperfect at higher magnification (Fig. 10-2, panel C). However, the NM-exposed corneas had not yet started to repair (Fig.9-1. panel C), and the BMZ looked disrupted (Fig.9-2. panel C).

Fig. 9-1. Overlap composites of H&E stained corneal sections, spanning the entire corneal diameter. The following merged pictures show NM-exposed corneas healing from 1 day after exposure to 7 days after. (A) Control cornea. (B) The epithelium is ~60% separated from the stroma in corneas from NM 24 hours post exposure. (C) The epithelium is still separated from the stroma 3 days after NM exposure. (D) After 5 days, the epithelium doesn't cover the whole diameter of the cornea. (An arrow points to the direction of cell migration.) (E) The healing of the NM-exposed cornea is nearly complete after 7 days, although superficial epithelia are still being shed.

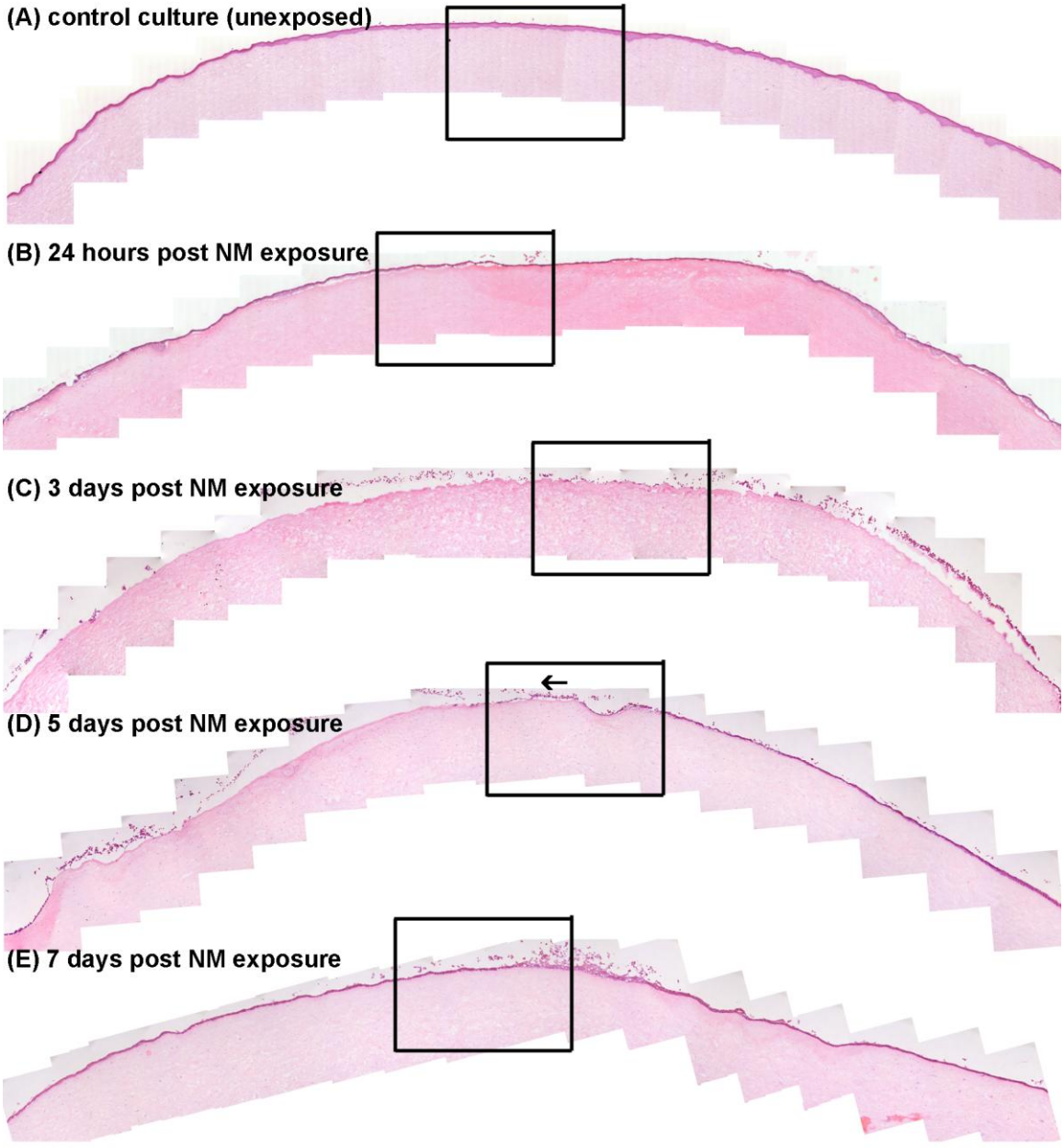

Fig. 9-2. Higher magnification of selected areas of NM-exposed corneas from figure 9-1. (A) Intact epithelial cells and stroma in the control, unexposed cornea. (B) Microbulle appeared in the cornea 24 hours after a 100 nmol NM exposure applied for 1 hour. (C) All epithelial cells have sloughed from the central portion of cornea 3 days after exposure. (D) A thin layer of epithelial cells are seen migrating toward the central portion of the cornea 5 days after exposure, but adhesion was not strong. (E) One or two cell layers cover the basement membrane across the entire diameter of the corneas at 7 days post exposure.

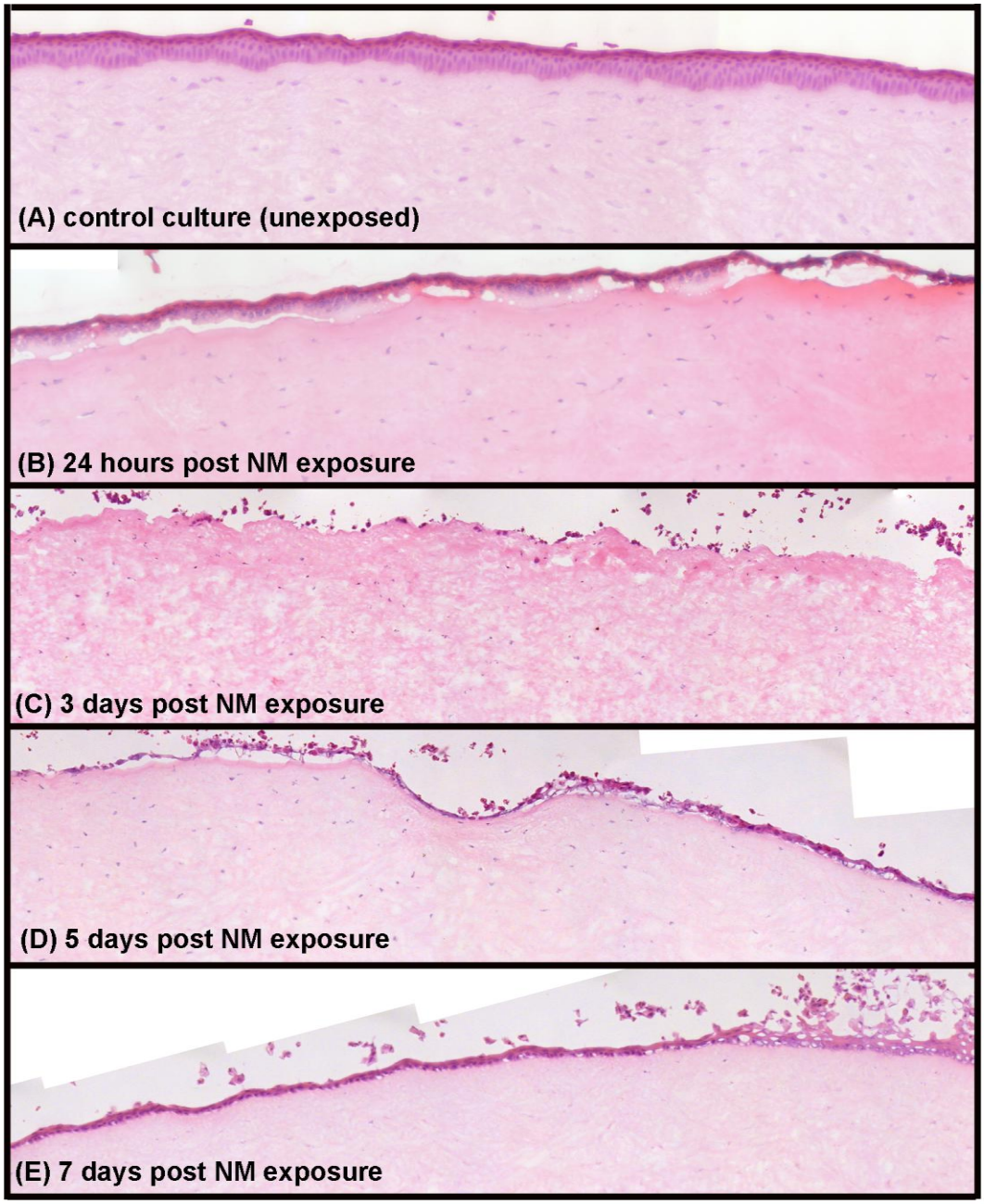

Fig. 10-1. Overlap composites of H&E stained corneal sections across the entire corneal diameter after a 100 minute (2000 mJ/cm^2) UVB exposure. Healing was followed from 1 to 7 days post exposure. (A) UVB controls were covered with black vinyl and placed under the UVB lamp for 100 minutes. (B) The epithelium is ~60% separated from the stroma in corneas. (C) Three days after exposure, the epithelium of the UVB exposed corneas had started to migrate across areas where the epithelium was lost. (D) The time to achieve complete epithelial-stromal integrity was 5 days post UVB injury, however the epithelium was at most 2 cell layers thick. (E) The epithelium is thicker after 7 days, in some places reaching the normal 7 cell layers of thickness.

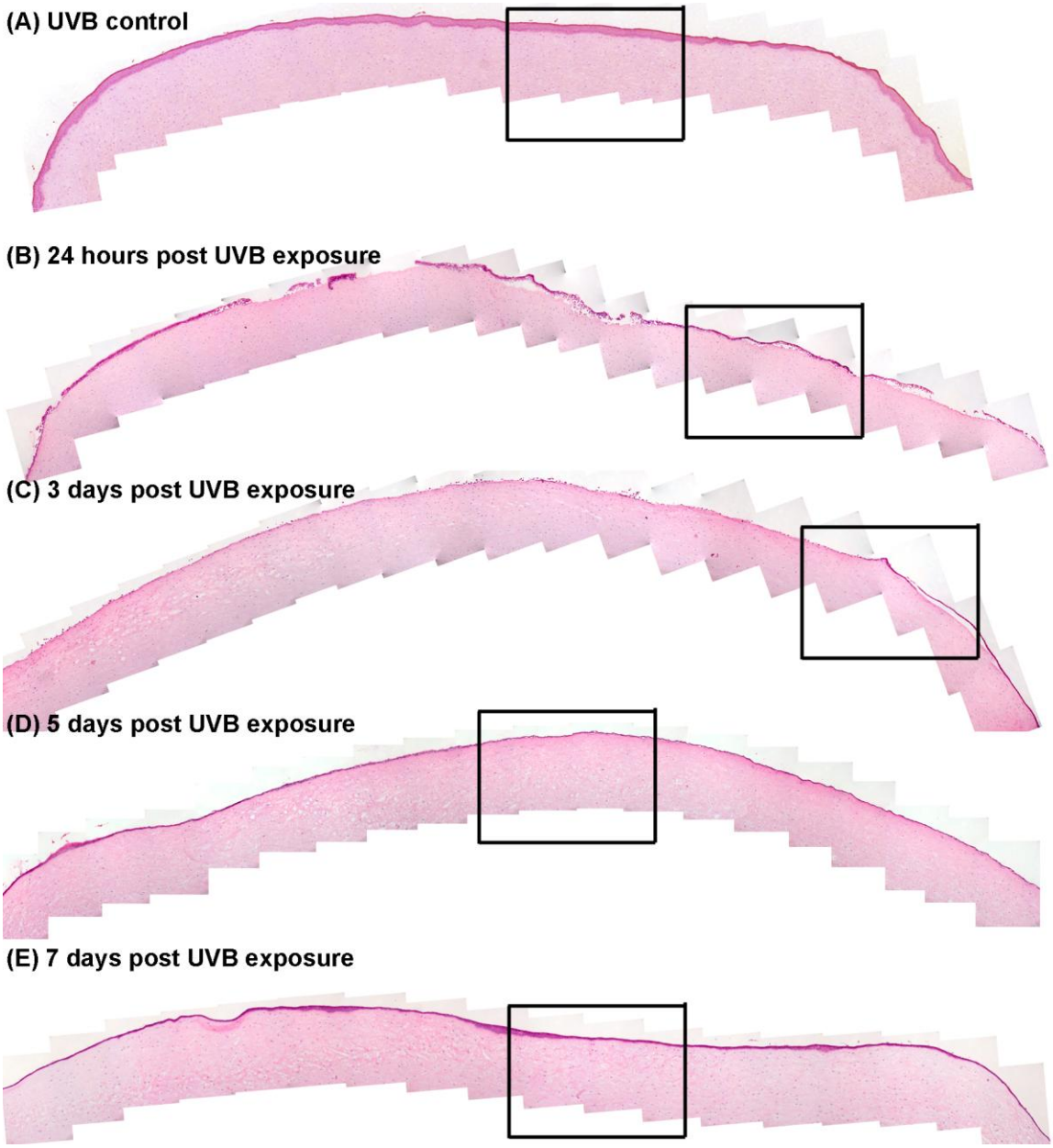

Fig. 10-2. Higher magnification of selected area OF UVB-exposed corneas from the figure 10-1. (A) Intact epithelial cells and stroma in the UVB control which was covered with black vinyl. Note the 6-8 cell layer thickness of the epithelium. (B) Microbulle appeared in the cornea 24 hours after a 2000 mJ/cm^2 UVB irradiation (100 minutes). (C) No epithelial cells remained on the stroma in the central cornea. A thin layer of epithelial cells are seen migrating toward center. (D) The epithelial cells covered the whole diameter of cornea within five days, but the cellular adhesion was weak and showed some microbullae in areas. (E) The normal thickness of epithelial cell layers is clearly visible at 7 days post exposure.

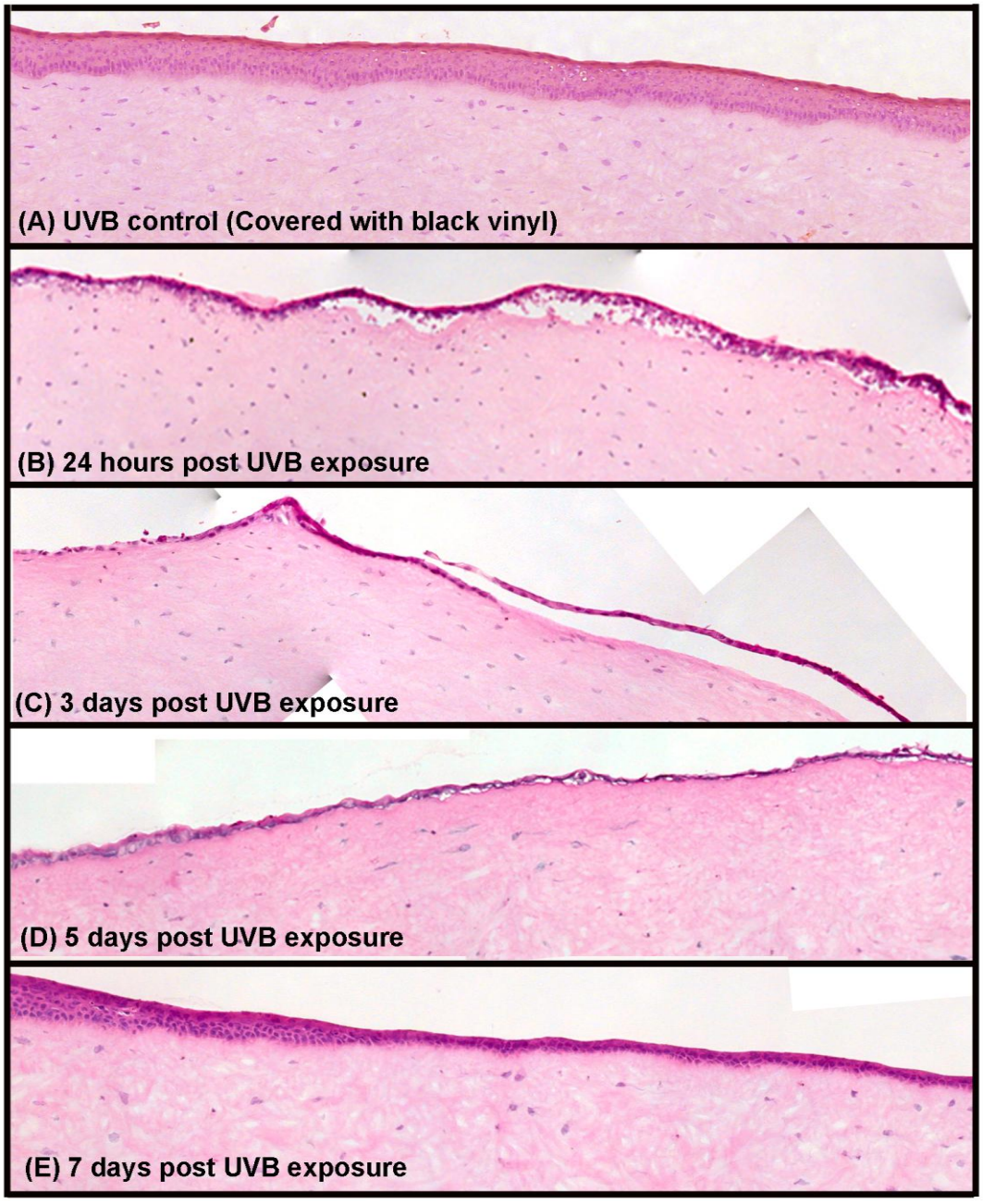

The time to achieve almost completely cover the wound with a monolayer of epithelium was 5 days for UVB injury (Fig.10-1 and Fig. 10-2, panels D) and more than 7 days for NM injury (Fig.9-1. panels D and E). Select areas in figure 9-1 and 10-1were looked at with higher magnification (Fig. 9-2 and 10-2). These demonstrate that the UVB-exposed corneas at 7 days post exposure were closer to the pre-exposure phenotype than the NM-exposed corneas at 7 days.

Expression of Provisional Wound Matrix Components

The distribution of provisional matricellular proteins participates in the regulation of wound healing in the normal process of repair. Because knocking out SPARC and hevin cause tissues to heal faster, but with scarring, we hypothesized that NM, with its presumed slower healing, might induce the provisional matrix to persist longer than it should, thereby providing a mechanism for why NM injuries may heal more slowly.

To test this idea we looked at the localization of the provisional matrix proteins during wound healing after NM and UVB. Immunofluorescence analysis demonstrated that the provisional wound matrix components, SPARC, hevin, tenascin-C, TSP-1, FBN-1, and FN, are deposited mainly at or nearby the BMZ, as well as in some basal epithelia and in the upper stroma in NM and UVB-exposed corneas while during repair. The delayed repair process may involve a combination of matricellular proteins activities. In normal corneas, little or no staining of these matricellular molecules was observed in the corneal epithelial BMZ (Maseruka et al., 1997; Ljubimov et al., 1998; Uno et al., 2004; Latvala et al., 1996).

SPARC

Epithelial cells must change shape, flattening themselves to migrate. SPARC is secreted to regulate epithelial cell migration and shape during wound healing (Latvala et al., 1996). SPARC was not apparent in the epithelial cells, ECM, and stroma of the control corneas (Fig.11-1, panel A) , but was present at the region of epithelial-stromal separation 24 hours post NM and UVB (Fig.11-1, panels B and C) exposure. On day three after NM exposure the immunoreaction for SPARC was still expressed at the site of the wound bed (Fig.11-1, panel D), but was mostly absent along the BMZ at three days post UVB exposure (Fig.11-1 panel E). The SPARC immunoreaction was discontinuous at the BMZ (yellow and violet arrows) of the 5 day post NM-exposure (Fig.11-1, panel F). No staining was observed in the UVB exposed cornea at 5 days (Fig.11-1, panel G). As soon as corneas were fully covered by an epithelial layer (5-7 days), the SPARC immunoreactivity was gone in both the NM- and UVB-exposed corneas (Fig.11-1, panels G, H, and I).

Western analysis showed that SPARC was present in the protein extraction and also was found in the culture medium (Fig. 11-2, panels A and B). SPARC expression was decreased with time after NM exposure. UVB-exposed corneas contained much less SPARC than those exposed to NM.

Fig. 11-1. Immunofluorescence of SPARC in NM- and UVB-exposed corneas. SPARC (green fluorescence), remained deposited at the BMZ in NM-exposed corneas (B, D, F, and H) longer than in UVB-exposed corneas (C, E, G, and I). (A) Control cornea. (B) 24 hours post NM exposure. (C) 24 hours post UVB exposure. (D) 3 days post NM exposure. (E) 3 days post UVB exposure. (F) 5 days post NM exposure. (G) 5 days post UVB exposure. (H) 7 days post NM exposure. (I) 7 days post UVB exposure. (The numbers in the bottom right corners indicate three different corneas evaluated. Yellow arrows point out the green fluorescence indicating SPARC expression in NM-exposed cornea, while violet arrows point out the matricellular molecule in UVB-exposed corneas.) DAPI stains nuclei blue, and indicates individual cells. (400x magnification)

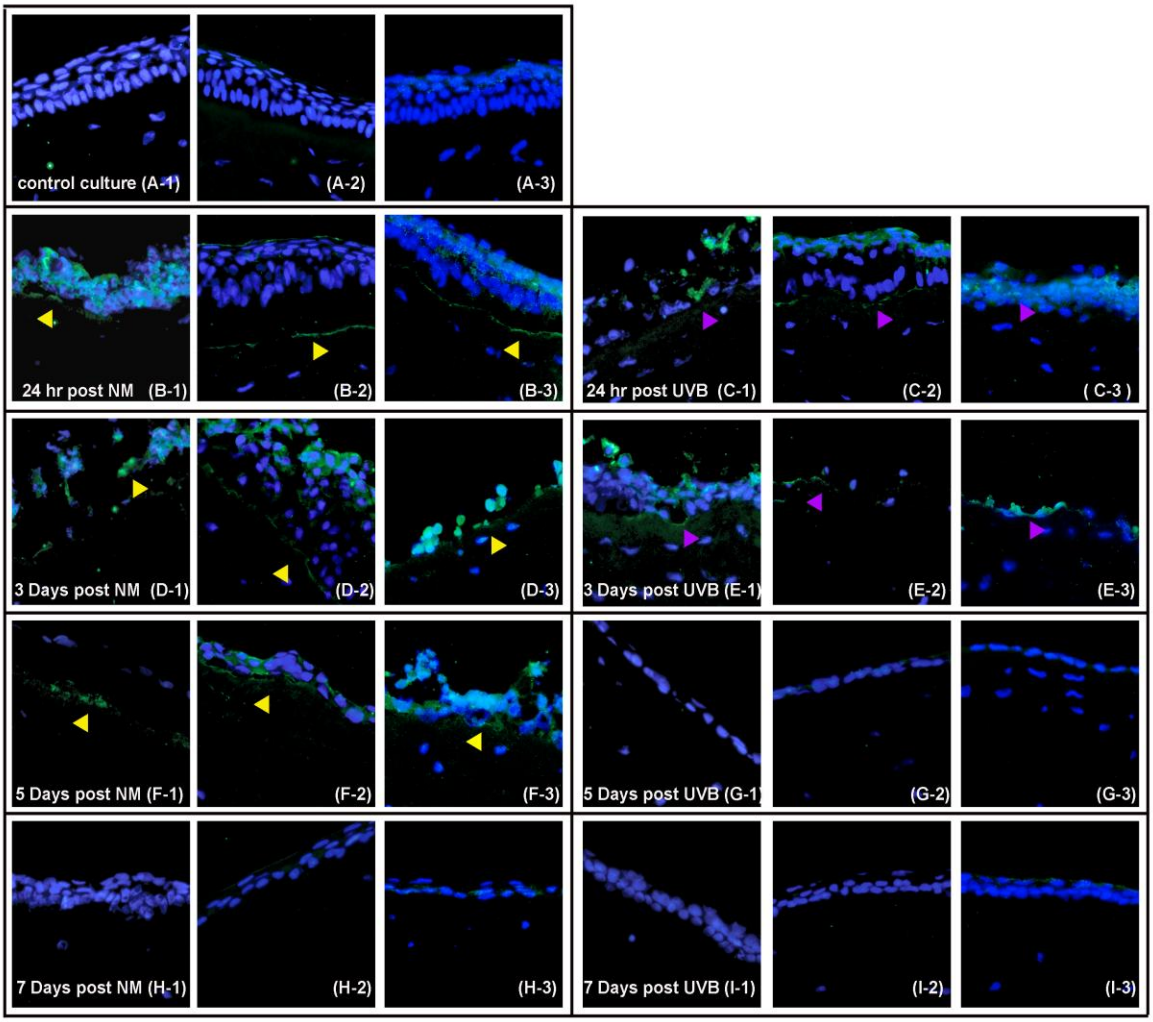

Fig. 11-2. Immunoblot analysis of SPARC expression. (A) Protein extraction and **(B)** culture medium from NM and UVB exposed corneas, 1-7 days post exposure. In both the cell lysates and the culture medium, more SPARC is observed in the NM-exposed corneas than the UVB-exposed corneas.

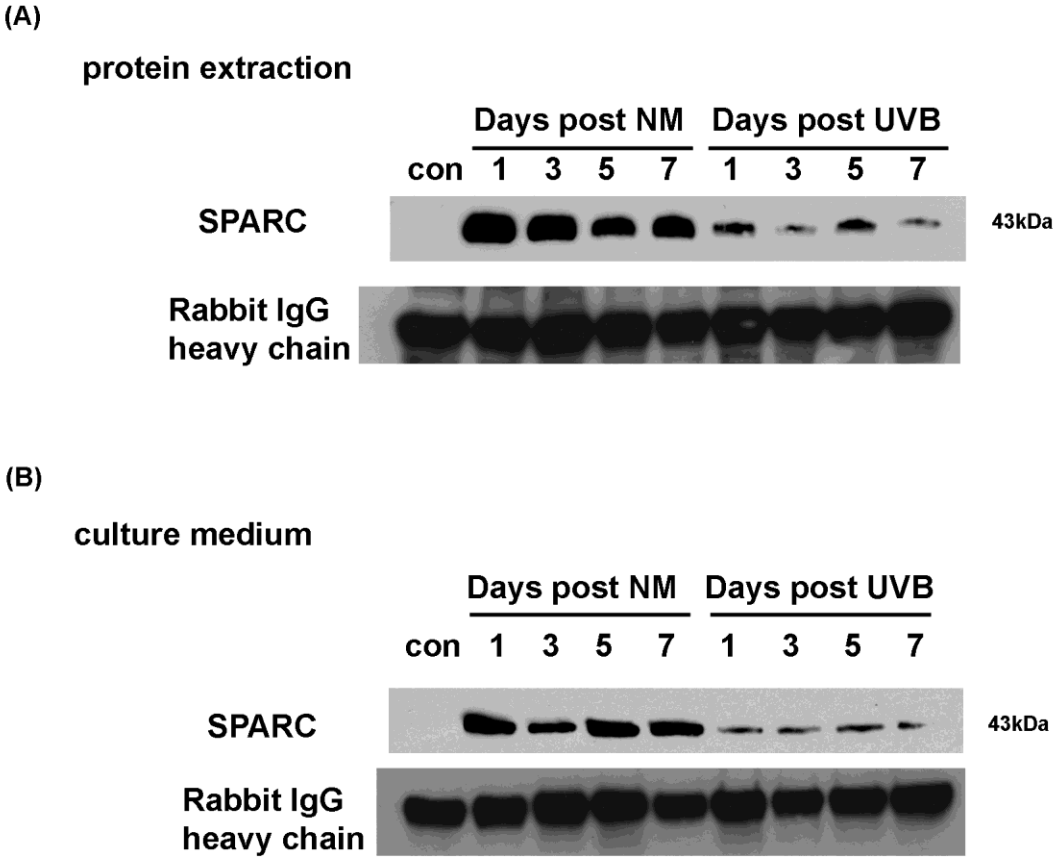

Hevin

Hevin, also called SPARCL1 for SPARC-like 1, is abundantly distributed in the brain, heart, and vasculature. It shares 53 % homology at the amino acid level with SPARC. (Sullivan and Sage, 2004). So far there is no report stating that hevin is expressed in the cornea. Our data is the first. The expression of hevin was determined by staining with monoclonal rat anti-mouse SPARCL1 (hevin) IgG antibody from Lifespan Biosciences. Hevin had no immunoreactivity in the control corneas (Fig.12-1, panel A). Immunoreactivity, however, was strong at the BMZ beneath the basal epithelial cells 24 hours after NM and UVB exposure (Fig.12-1, panels B and C). The hevin distributed continuously beneath the regions of epithelial-stromal separation, and around peeled off epithelial cells 3 days after NM exposure (Fig.12-1, panel D). It also deposited weakly at the BM of the re-formed epithelial layer three days after UVB exposure (Fig.12-1, panel E). NM-exposed corneas took longer to remove hevin from the BMZ (Fig.12-1, panel F) than UVB exposed corneas (Fig.12-1, panel G), which were negative for the molecule at 5 days post exposure. At 7 days post NM exposure hevin was still slightly visible (Fig.12-1, panel H), while no hevin immunoreactivity appeared 7 days after UVB exposure (Fig.12-1, panel I).

Western analysis showed that, mostly, the expected fragments of hevin were present in NM-and UVB-exposed cornea after 24 hours. However, the complicated mature of the full length (130 kDa) and fragmented (80 kDa, 66 kDa, and 48 kDa) hevin made it impossible to correlate these with the Immunofluorescence patterns (Fig. 12-2, panels A and B).

Fig. 12-1. Immunofluorescence of hevin in NM-and UVB-exposed corneas. Immunofluorescence demonstrated that the provisional wound matrix component hevin (green fluorescence), remain deposited in the BMZ and at the basal surface of the basal epithelial cells of the cornea incubated 24 hours in NM-exposed corneas longer than in UVB-exposed corneas. (A) Control culture 24 hours after removal from UVB box (no exposure). (B) 24 hours post NM exposure. (C) 24 hours post UVB exposure. (D) 3 days post NM exposure. (E) 3 days post UVB exposure. (F) 5 days post NM exposure. (G) 5 days post UVB exposure. (H) 7 days post NM exposure. (I) 7 days post UVB exposure. (The numbers in the bottom right corners indicate three different corneas evaluated. Yellow arrows point out hevin expression in NM-exposed cornea, while violet arrows point out the matricellular molecule in UVB-exposed corneas.) DAPI stains nuclei blue, and indicates individual cells. (400x magnification)

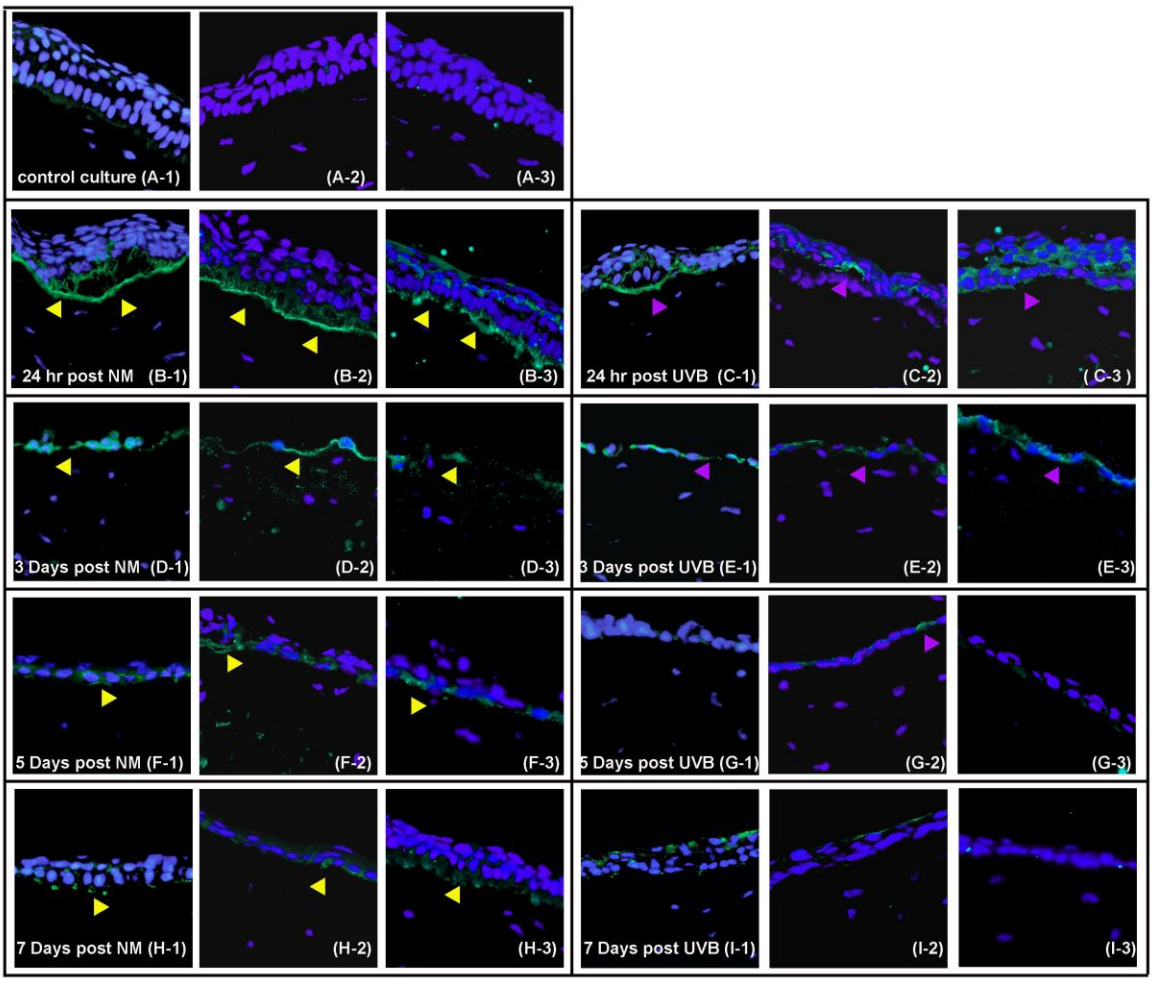

Fig. 12-2. Immunoblot analysis of hevin expression. (A) Protein extraction and **(B)** culture medium from NM-and UVB-exposed corneas, 1-7 days post exposure. In culture medium, full length (130 kDa) hevin is detected in day1 post-NM exposed corneas and decreased with time. More hevin is observed in the NM-exposed corneas than the UVB-exposed corneas. In the culture medium of UVB-exposed corneas, hevin was cleaved to three fragments, 80 kDa, 66 kDa, and 48 kDa. Less hevin cleavage was seen in culture medium of NM-exposed corneas. The pattern of hevin in the cell lysates from both exposures was approximately the same.

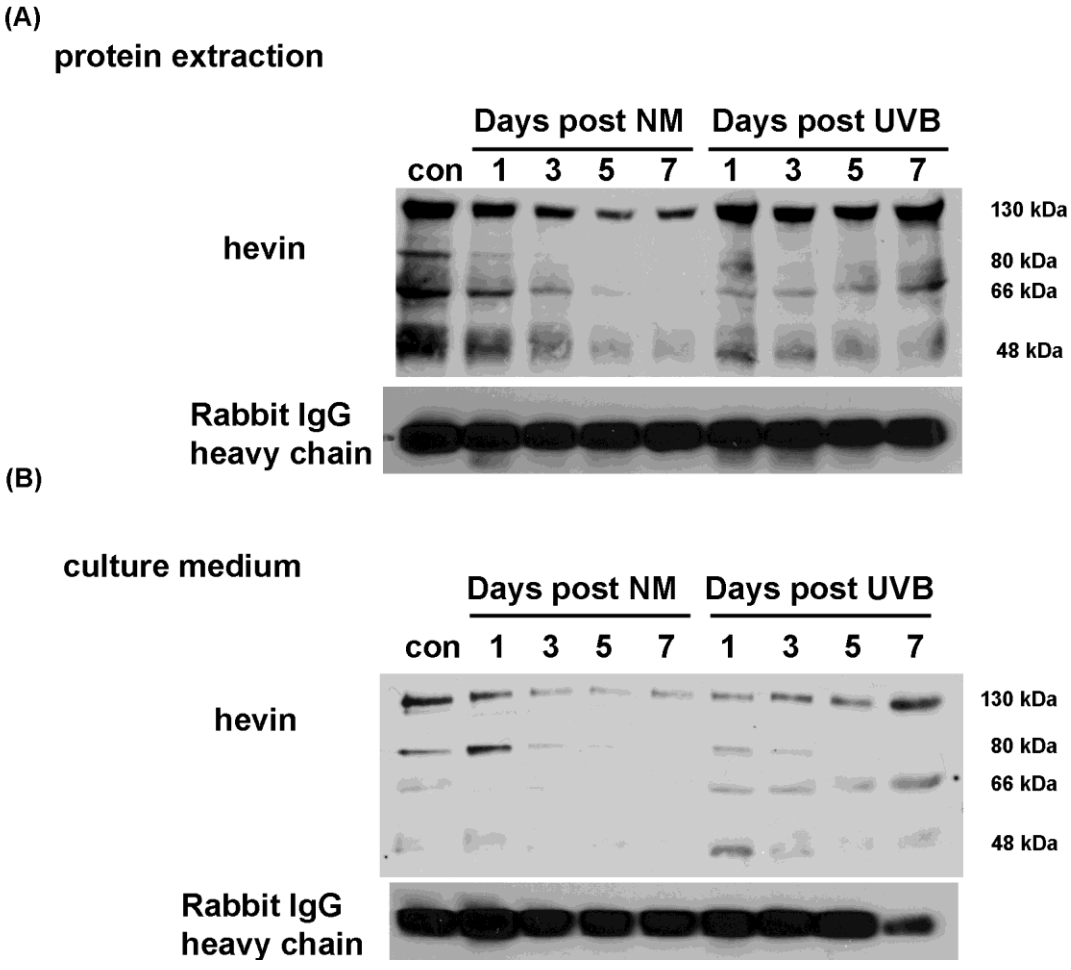

Tenascin-C

Tenascin-C has shown similar anti-adhesive properties as SPARC and TSP-1 during wound healing (Sage and Bornstein, 1991). Tenascin-C is found in regions of inflammation and in active corneal disease, such as pseudophakic and aphakic bullous keratopathy (Maseruka et al., 1997; Ljubimov et al., 1996). Prolonged expression of tenascin-C might also contribute to slower corneal wound healing. Tenascin-C was not present in control corneas (Fig.13, panel A), but was intensely immunofluorescent at the BMZ 24 hr after corneas were injured by NM, and moderately fluorescent after UVB injury (Fig.13, panels B and C).

NM-exposed corneas show tenascin-C at 3 and 5 days after, and barely any at 7 day (Fig. 13, panels D, F, and H). For UVB-exposed corneas, which reformed the epithelial layer around 3 days, had very little expression of tenascin-C at 3 and 5 days, and none at 7 days (Fig. 13, panels E, G, and I). The FBN-1 antibody was not made against the rabbit molecule, and did not work on western blot.

Thrombospondin-1 (TSP-1)

TSP-1 is synthesized by basal corneal epithelial cells and basal conjunctival epithelial cells (Sekiyama et al., 2005) and is up-regulated during corneal wound healing (Uno et al., 2004). Using a mouse anti-human TSP-1 monoclonal IgG antibody, little signal was detected in the control corneas (Fig.14, panel A). Twenty four hrs after the corneas were injured by NM and UVB exposure, TSP-1 was detected (Fig. 14, panels B and C) at the BMZ and in the upper anterior stroma. By 3 days after either cornea injury, TSP-1 was intense in the BMZ (Fig. 14, panels D and E). The TSP-1 persisted at the

Fig. 13. Immunofluorescence of tenascin-C in NM- and UVB-exposed corneas. (A) Control culture 24 hours after removal from UVB box (no exposure). (B) 24 hours post NM exposure. (C) 24 hours post UVB exposure. (D) 3 days post NM exposure. (E) 3 days post UVB exposure. (F) 5 days post NM exposure. (G) 5 days post UVB exposure. (H) 7 days post NM exposure. (I) 7 days post UVB exposure. Tenascin-C (green fluorescence) remained deposited at the BMZ and at the basal surface of the basal epithelia in NM-exposed corneas longer than in UVB-exposed corneas. (The numbers in the bottom right corners indicate three different corneas evaluated. Yellow arrows point out tenascin-C expression in NM-exposed cornea, while violet arrows point out the matricellular molecules in UVB-exposed corneas.) DAPI stains nuclei blue, and indicates individual cells. Green at the corneal surface is auto-fluorescence of the sloughing superficial cells. (400x magnification)

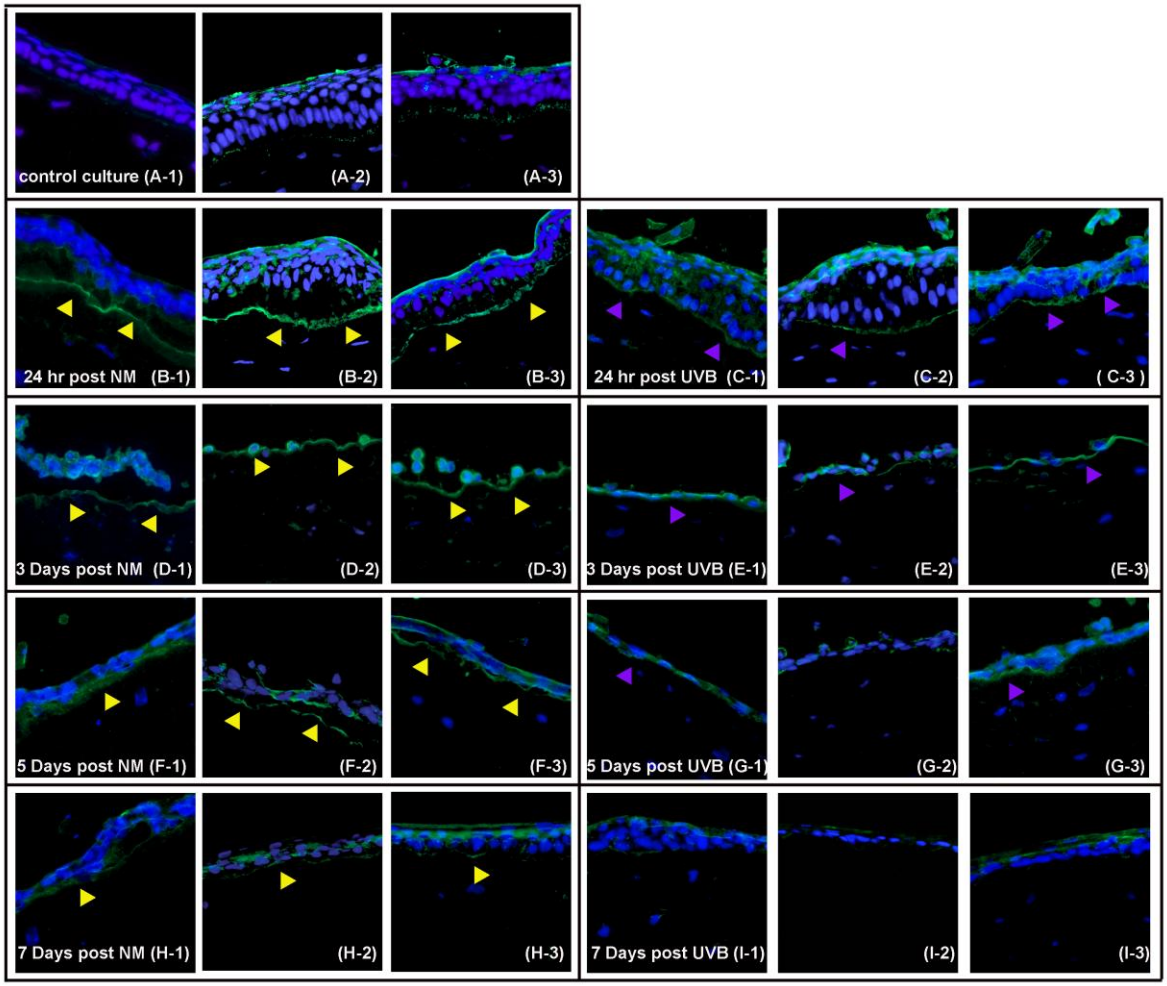

Fig.14. Immunoflorescence of thrombospondin-1 (TSP-1) protein in NM and UVB exposed corneas. TSP-1 (green fluorescence) has a little signal in the control, unexposed corneas. It is expressed in both NM- and UVB-exposed corneas to almost the same degree from day 1 to day 7 after exposure. (A) Control culture. (B) 24 hours post NM exposure. (C) 24 hours post UVB exposure. (D) 3 days post NM exposure. (E) 3 days post UVB exposure. (F) 5 days post NM exposure. (G) 5 days post UVB exposure. (H) 7 days post NM exposure. (I) 7 days post UVB exposure. DAPI stains nuclei blue, and indicates individual cells. The numbers in the bottom right corners indicate three different corneas evaluated. (200x magnification) bar = 100 µm

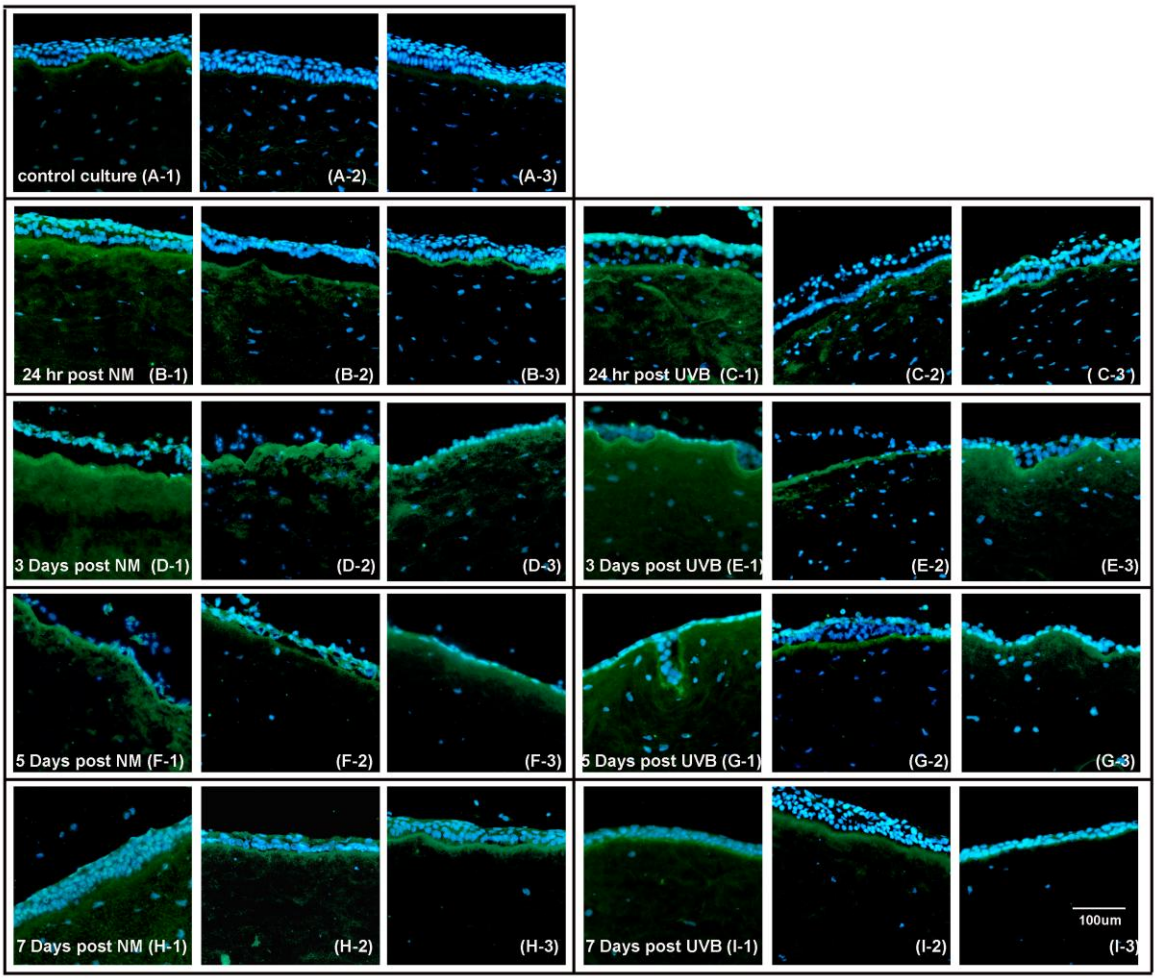

BMZ through 7 days post NM and UVB exposure (Fig. 14, panels F, G, H, I). The TSP-1 antibody was not made against the rabbit molecule, and did not work on western blot.

Fibrillin-1 (FBN-1)

FBN-1 is a matrix molecule with a structural role in elastic tissues. It is also expressed during wound healing in most tissues. For example, FBN-1 is expressed in the cornea afflicted with bullous keratopathy, but not in the normal healthy cornea (Ljubimov et al., 1998). Control corneal sections were reacted with mouse anti-human FBN-1 IgG antibody, and showed a thin, faint band of the molecule at the BMZ (Fig.15, panel A). Twenty four hr after the corneas were exposed to NM and UVB (Fig.15, panels B and C), FBN-1 was also observed in the anterior stroma. On the third day post exposure, the distribution of FBN-1 in the stroma was more abundant in the NM-exposed and UVB-exposed corneal stroma than first day exposure (Fig.15, panels D and E). By 5 days post exposure the intensity had dropped in both. Still the UVB-exposed cornea shows less FBN-1 than the NM-exposed (Fig. 15, panels F and G). Seven days after exposure FBN-1 is still visible in NM-exposed cornea, but is gone from the UVB-exposed cornea (Fig.15, panels H and I). The FBN-1 antibody was not made against the rabbit molecule, and did not work on western blot.

Fig. 15. Immunofluorescence of fibrillin-1 (FBN-1) in NM and UVB exposed corneas. The immunoflorescence analysis demonstrated that the provisional wound matrix components, FBN-1 (green fluorescence) persist in NM-exposed corneas longer than in UVB exposed corneas. (A) Control culture. (B) 24 hours post NM exposure. (C) 24 hours post UVB exposure. (D) 3 days post NM exposure. (E) 3 days post UVB exposure. (F) 5 days post NM exposure. (G) 5 days post UVB exposure. (H) 7 days post NM exposure. (I) 7 days post UVB exposure. FBN-1 shows a faint signal at the BMZ in the control cornea. Twenty four hours to 3 days post exposure, FBN-1 expression increased in both NM and UVB-exposed corneas, especially into the stroma. UVB-exposed corneas had less FBN-1 expression after 5 days compared to NM exposed ones. Seven days after UVB exposure FBN-1 immunofluorescence was nearly absent, but still remained in the NM-exposed corneal stroma. DAPI was used to stain nuclei blue. The numbers in the bottom right corners indicate three different corneas evaluated. (200x magnification) bar = 100 µm

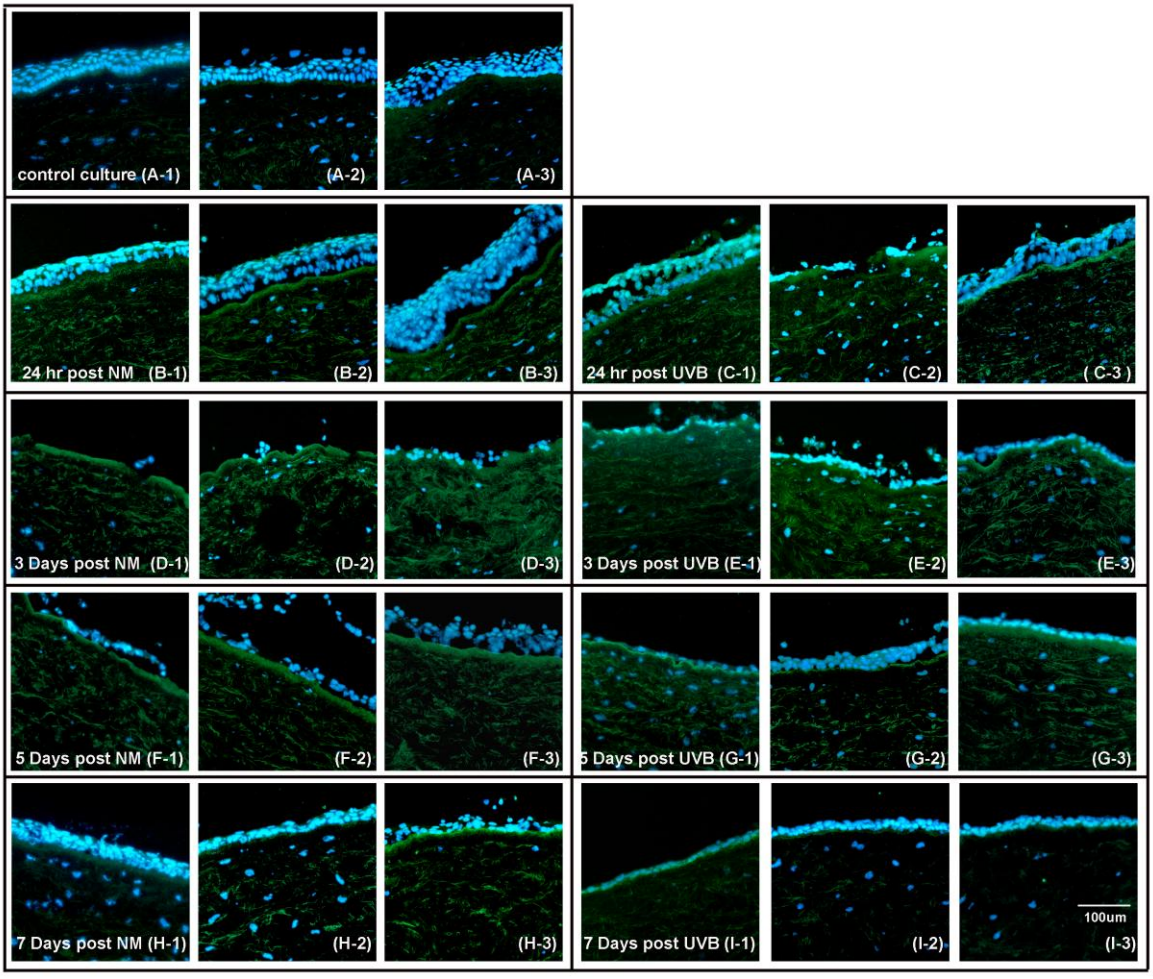

Expression of Fibronectin (FN)

FN is an adhesion glycoprotein that acts as a temporary adhesion surface for cell migration during repair (Fujikawa et al., 1981). In the control corneas, there is faint immunoreactivity of FN at the BMZ (Fig. 16-1, panel A). Interestingly, however, there was no immunoreactivity observed in the corneas 24 hours post NM exposure (Fig. 16-1, panel B), and very faint expression at the BMZ in the UVB-exposed corneas (Fig. 16-1, panel C). At 3 days post UVB irradiation, much more FN was observed in the stroma and BMZ (Fig. 16-1, panel E), but not in the NM-exposed cornea (Fig. 16-1, panel D). At 5 days post UVB-exposure FN is still present, while it is still not in the NM-exposed ones (Fig. 16-1, panels F and G). At 7 days post exposure both the NM- and UVB-exposed corneas contain a considerable amount of FN in their stroma (Fig. 16-1, panels H and I). The immunoreactivity for both is approximately equal.

The immunoblot analysis suggested FN was mainly present in a matrix form (Fig. 16-2, panel A) rather than soluble form in the culture medium (Fig. 16-2, panel B). At 24 hr after UVB and NM exposure, no FN immunoreactivity is present in injured corneas. FN was significantly elevated at three days post UVB exposure, but was weak in the NM-exposed corneas. FN immunoreactivity was intense in the 5 days post UVB-exposed corneas. This did not occur in NM-exposed corneas until 7 days post exposure. This suggests cell migration in UVB-exposed corneas will be favored at earlier days than in NM-exposed corneas.

Fig. 16-1. Immunofluorescence of fibronectin (FN) in NM and UVB exposed corneas. FN appears in the stroma of UVB-exposed corneas earlier than in NM-exposed corneas. (A) Control culture. (B) 24 hours post NM exposure. (C) 24 hours post UVB exposure. (D) 3 days post NM exposure. (E) 3 days post UVB exposure. (F) 5 days post NM exposure. (G) 5 days post UVB exposure. (H) 7 days post NM exposure. (I) 7 days post UVB exposure. Very a little signal is seen at the BMZ of the control cornea. At 24 hours and 3 days post NM exposure, the FN expression was the same as the control. At 5 days post NM exposure a small increased is seen in the stroma. This increases greatly by 7 days post NM exposure. UVB- induction of FN, however, is seen at 3 days post exposure and persists through 5 and 7 days post exposure. The numbers in the bottom right corners indicate three different corneas evaluated. DAPI staining indicates nuclei (blue). (200x magnification) bar = 100 µm

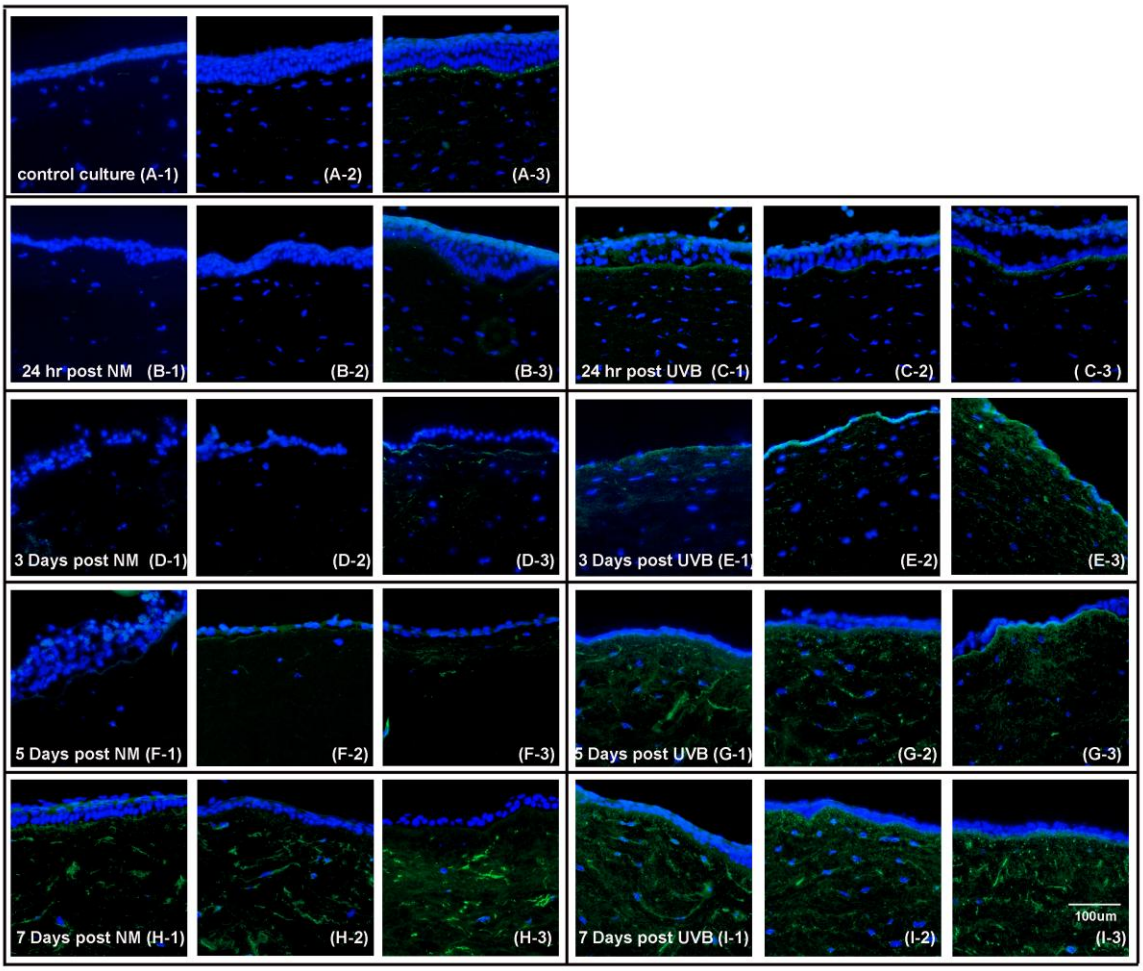

Fig. 16-2. Immunoblot analysis of fibronectin (FN) expression. (A) Protein extraction and **(B)** culture medium from NM and UVB-exposed corneas from day 1 to day 7 post exposure. FN is expressed weakly in the control corneal lysates. FN is elevated at 5 and 7 days post NM exposure. The medium samples demonstrated that FN was predominately present in the matrix form rather than soluble form.

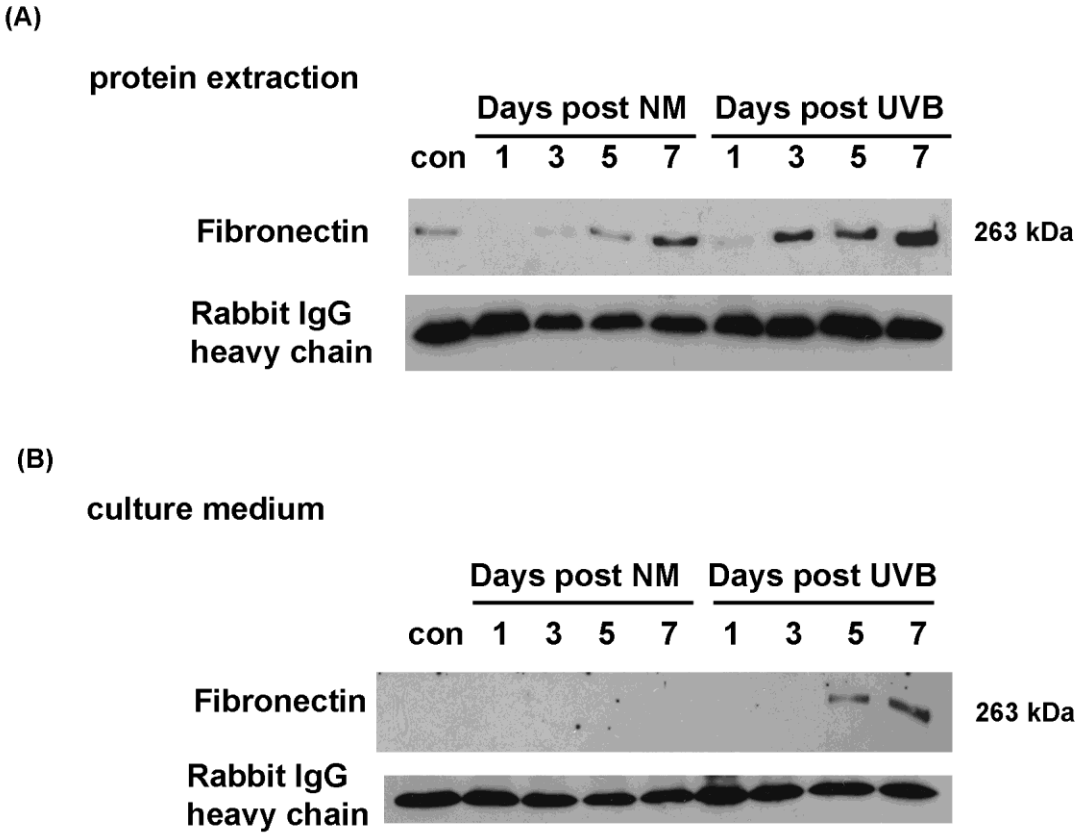

Co-localization of Hevin and ADAMTS4

Hevin distributes in many tissues, and was detected recently co-localized with ADAMTS4 in the brain (Weaver et al., 2010). ADAMTS4 recognizes a cleavage site in hevin at a sequence EA▲ERMHS (residues 358-364). This cleavage generates a fragment similar to SPARC. To determine whether ADAMTS4 interacts with hevin in the NM- and UVB-exposed corneas, we co-stained corneal sections using polycolonal goat anti-human ADAMTS4 (red) and monoclonal rat anti-mouse hevin (green) (Fig. 17). In the control corneas no hevin but slight ADAMTS4 signals were present (Fig. 17, panel A). Twenty four hours and 3 days post UVB and NM exposure co-localization of hevin and ADAMTS4 was seen at the BMZ (Fig. 17, panels B, C, D, and E, yellow stain). More ADAMTS4 immunoreactivity was observed in the stroma during wound healing. In NM-exposed corneas, ADMATS4 and hevin were co-localized at the BMZ, but less ADAMTS4 was present in the stroma at day 5 and day 7 post NM-exposure (Fig. 17, panels Fand H). No hevin immunoreactivity was seen in the UVB-exposed cornea after day 5 and day 7, while a reduced level of ADAMTS4 expression was present in the stroma (Fig. 17, panels G and I).

ADAMTS4 Western Analysis

The blot of the control sample did not show any ADAMTS4 immunoreactivity. However, the full length form of rabbit proADAMTS4 was seen in the samples 5 and 7 days post UVB exposure, demonstrating its size as ~120 kDa (Fig. 18). As true for all MMPs, the molecule has a prodomain that must be removed before enzymatic activity is possible. In rabbit, removal of the prodomain results in an 80 kDa form. For comparison,

in human, the full length form is 125 kDa when directly isolated from tissue, or 100 kDa when isolated from a chondrosarcoma cell line. For both, removal of the prodomain results in a 75 kDa form (Gao et al., 2002). However, Gao, et al. demonstrated that, despite removal of the prodomain, ADAMTS4 was not an active enzyme until the carboxyl end of the molecule was processed, generating a 60 kDa and a 50 kDa peptide containing the catalytic domain. In rabbit we observed two similar bands (50 kDa and 42 kDa) on the ADAMTS4 immunoblot. For the NM exposed corneas, the 50 kDa band remained intense for 1, 3, and 5 days post exposure, while the 42 kDa band was most intense at 1 day post exposure, but less intense at 3 and 5 days post NM. The 7day post NM exposure sample did not show any bands, which suggests the lane may have been misloaded. In the UVB exposed corneas, the 50 kDa and the 42 kDa bands were of equal intensity at each time point, and were most immunoreactive at 1 day post exposure. By 3 days the intensity of the bands was very weak, and by 5 and 7 days after UVB exposure, the bands were undetectable. Only the full length band was observed at these time points, indicating that the processing of ADAMTS4 is extended after NM exposure as compared to UVB exposure. The fact that in the NM exposed samples, the 42kDa band is a much less abundant than the 50kDa band may have functional significance. In fact, at 3 days after exposure, the 42 kDa band is more intense in the UVB exposed cornea than in the NM exposed one. The importance of these potential proteolytic peptides will be explored in future work.

Nuclear Ferritin in the UVB Irradiated Corneas

UV B causes damage to DNA. The corneal epithelium is exposed to UVB each

Fig.17. Hevin and ADAMTS4 co-localization by immunofluorescence. ADAMTS4 distributed among the epithelial cells and the stroma. ADAMTS4 (red) was co-localized (yellow) with the provisional matrix component hevin (green) at the basement membrane and among the epithelium. ADAMTS4 seemed stronger in the NM-exposed cornea than UVB-exposed cornea during corneal wound healing. At day 1 to day 7 post NM exposure, ADAMTS4 co-localized with hevin at the BMZ and among the basal epithelial cells. Hevin was present for 3 days in the UVB-exposed corneas. (400x magnification)

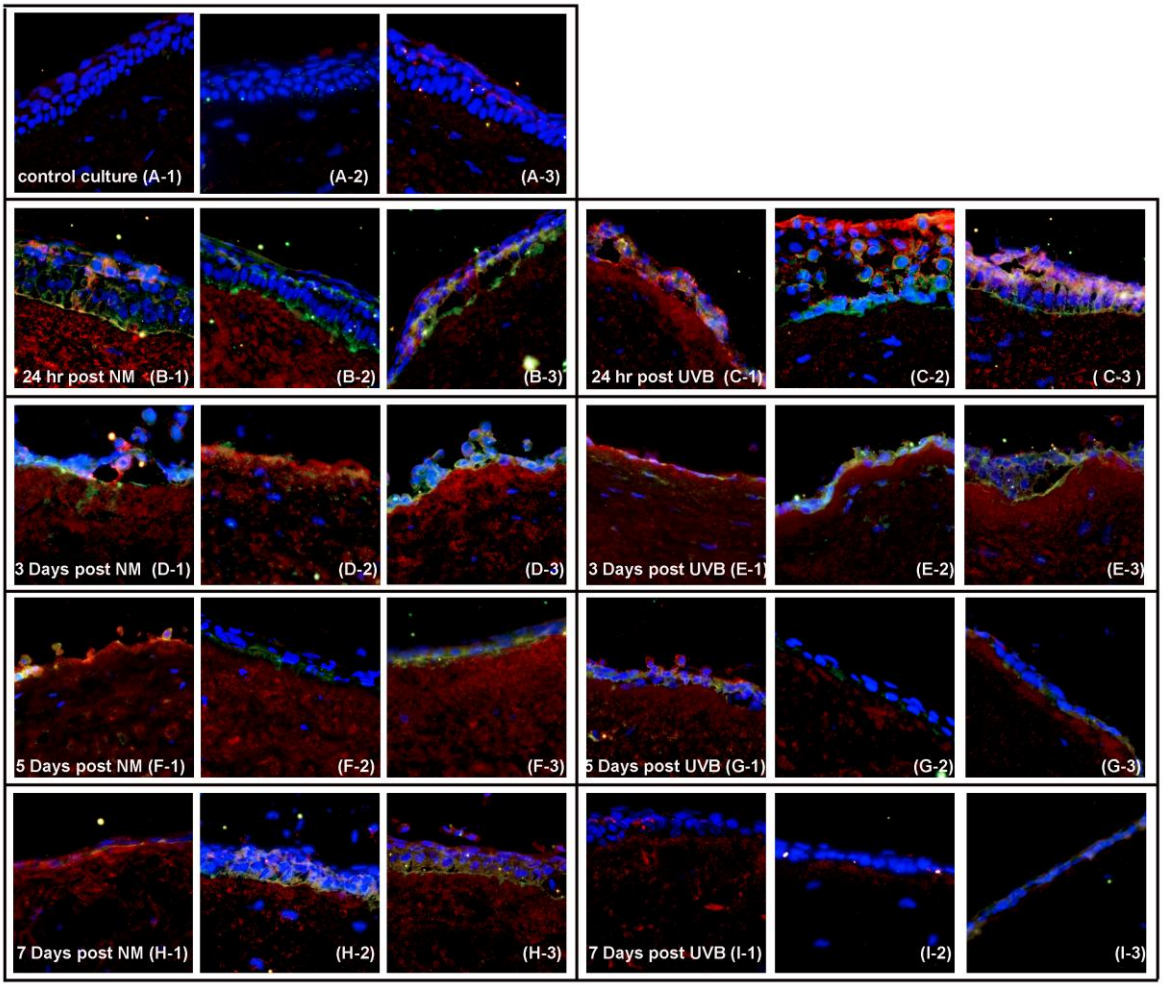

Fig.18. Immunoblot analysis of ADAMTS4 expression. Protein from protein extraction of NM-and UVB-exposed corneas from day 1 to day 7 after exposure were analyzed. The full length form (~120 kDa) of rabbit proADAMTS4 was seen in the samples 5 and 7 days post UVB exposure. The removal of the prodomain results in an 80 kDa form in both NM- and UVB-exposed corneas 24 hrs post exposure. For the NM exposed corneas, the 50 kDa band remained intense for 1, 3, and 5 days post exposure, while the 42 kDa band was most intense at 1 day post exposure, but less intense at 3 and 5 days post NM. The 7day post NM exposure sample did not show any bands. For UVB exposed corneas, the 50 kDa and the 42 kDa bands were of equal intensity at each time point, and were most immunoreactive at 1 day post exposure.

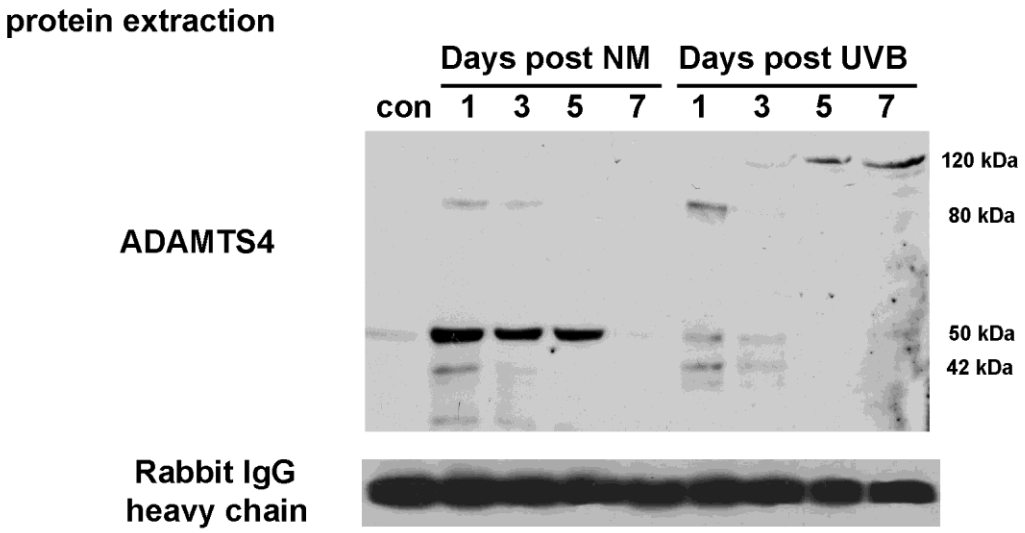

time a person walks out of their house into a sunny environment. Evidence from chicken corneas suggests that ferritin is present in the nuclei of the corneal epithelium to protect the DNA (Cai et al., 2008; Linsenmayer et al., 2005). Nuclear ferritin in corneal epithelial cells was shown to prevent UVB-induced free radicals from causing an oxidative stress-response and may prevent oxidative stress-related eye injuries (Cai et al., 2008). In the nucleus, ferritin scavenges free radicals that are induced by UV irradiation (Linsenmayer et al., 2005). In adult rabbit corneal epithelia, ferritin is localized in the cytoplasm. Whether ferritin could be found in the nucleus after UVB exposure was examined. Short UVB irradiation times (dose-dependent intensities), assessed immediately or 3 hours post exposure, were used to examine the location of ferritin in the rabbit corneal epithelium by immunofluorescence. For controls, some organ cultures were placed under the UVB lamp, but were covered with black vinyl. Ferritin was expressed only in the cytoplasm in controls (Fig.19, panels A and F). It remained in the cytoplasm of the epithelial cells exposed for 2 minutes (40 mJ/cm^2) with UVB (no incubation time) (Fig.19, panel B). Three hours post the 2 minutes (40 mJ/cm^2) UVB exposure, some ferritin was found in nuclei (Fig.19, panel G). More ferritin was detected within the nuclei with immediately after a 15 minute exposure (300 mJ/cm^2) (Fig.19, panel C). However, the nuclear ferritin was not present after 3 hours of this dose of UVB (Fig.19, panel H). In the corneas exposed 30 minutes (600 mJ/cm^2, Fig.19, panel D) or 60 minutes (1200 mJ/cm^2, Fig.19, panel E), with or without a 3 hours post exposure incubation (Fig.19, panel I, J), no nuclear ferritin was observed. Ferritin was entirely in the cytoplasm as it was in controls. The data suggests that ferritin can gain access to the nucleus and might play a role in protecting the corneal epithelium from low intensity

Fig. 19. Nuclear ferritin was detected post UVB irradiation with in short times. (A)(F) The UVB control cornea was covered with black vinyl to prevent UVB irradiation and was placed under the UVB lamps for 60 minutes ((A) collected immediately but (F) analyzed after 3 hours). Rabbit corneas were placed in the UVB box for (B) 2 minutes of UVB exposure (40 mJ/cm^2) and analyzed immediately; (G) 2 minutes of UVB exposure (40 mJ/cm^2) and analyzed after 3 hours; (C) 15 minutes (300 mJ/cm^2) and analyzed immediately; (H) 15 minutes of UVB exposure (300 mJ/cm^2) and analyzed after 3 hours; (D) 30 minutes of UVB exposure (600 mJ/cm^2) and analyzed immediately; (I) 30 minutes of UVB exposure (600 mJ/cm^2) and analyzed after 3 hours; (E) 60 minutes of UVB exposure (1200 mJ/cm^2) and analyzed immediately; (J) 60 minutes of UVB exposure (1200 mJ/cm^2) and analyzed after 3 hours. (Nuclei were stained with DAPI with pseudocolor (red); ferritin heavy chain (green); nuclear ferritin was shown in the merged pictures (yellow). Bar = 25 μm

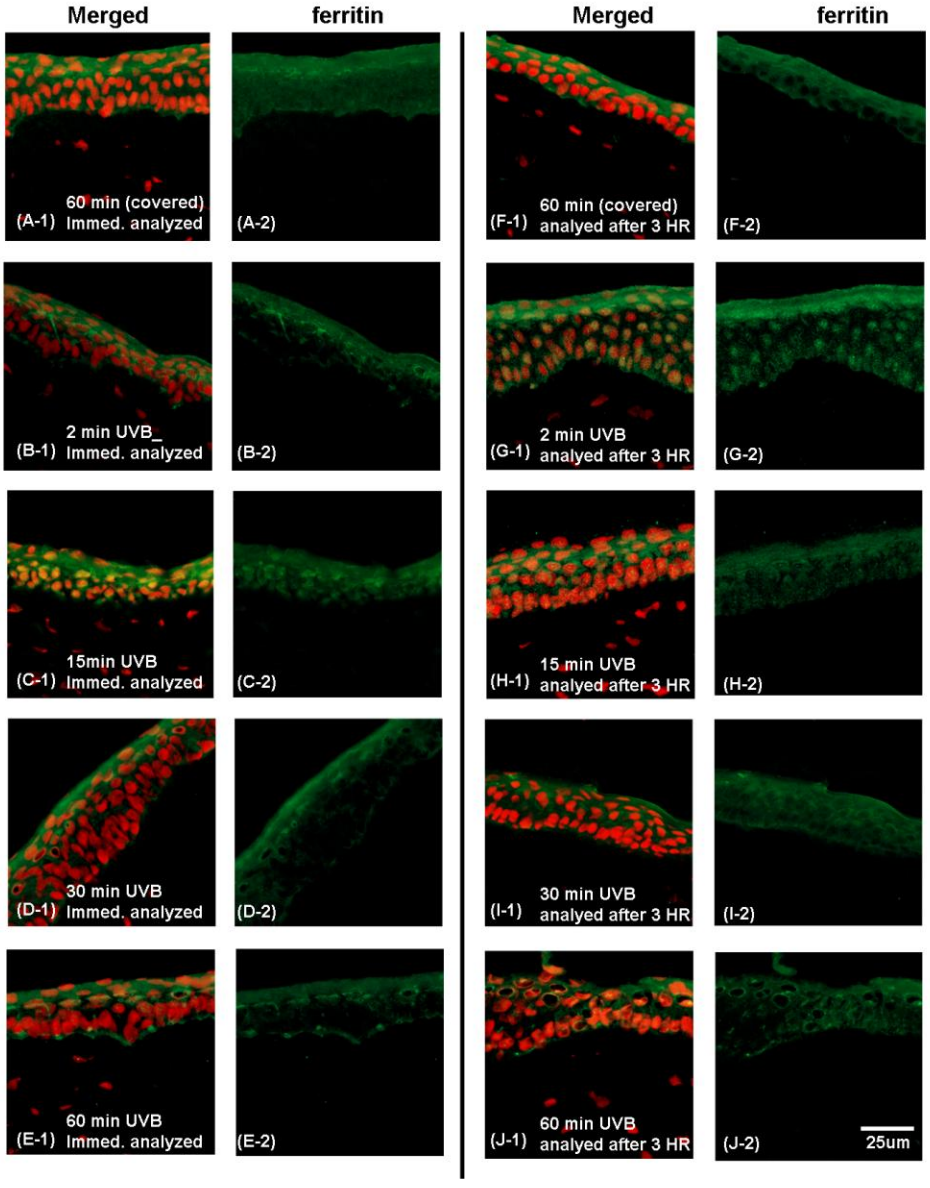

UVB irradiation. Since we could not detect ferritin at higher UVB doses, it is possible that such exposures evoke other processes to attenuate oxidative damage.

Discussion

The bifunctional alkylating agent, sulfur mustard, induces blisters characterized disruption of the epithelial-dermal junction (Monteiro-Riviere et al., 1999; Zhang et al., 1995) or the corneal epithelial-stromal junction (Kadar et al., 2001; Smith and Dunn, 1991; Solberg et al., 1997). Iranian ophthalmologists suggested that mustard-induced corneal injury healed more slowly and resulted, at times, in pathological reoccurrences, sometimes years later (Javadi et al., 2005). No experimental testing on whether the initial mustard injury heals more slowly than other blister injuries has ever been done. Therefore, we tested this with the hypothesis that equivalent nitrogen mustard injury and UVB injury of the cornea would demonstrate UVB injuries heal faster than NM injuries. UVB was the vesicant chosen to compare to mustards because it also has a delay in forming blisters, like nitrogen mustard. This has been seen in those who fall asleep for a couple of hours on the beach. In the eye, the cornea does not form blisters like in the skin. Instead microbullae are formed (Gordon et al., 2010). Human eyes are more often exposed to high intensity of UVB irradiation from welder's flash and snow reflection rather than from the sun (Diffey, 1990).

Corneal organ culture has been used in limited studies of corneal wound healing (Foreman et al., 1996; Gordon et al., 2010; Ljubimov et al., 1996; Tanelian and Bisla, 1992). The advantages of using the rabbit organ culture system: (1) The *in vitro* cultured cornea behaves as the *in vivo* cornea (Tanelian and Bisla, 1992; Crosson et al., 1986; Brazzell et al., 1991); (2) The architecture of cornea is maintained as the *in vivo* (Foreman et al., 1996). A target area can be studied without interfering with other organs,

such as lachrymal glands (Foreman et al., 1996); (3) Rabbit corneas are big and it is easy to apply exogenous chemical on them or perform surgical manipulations on them (Foreman et al., 1996); (4) The cost of rabbit eyes to set up organ culture experiment is much less expensive than purchasing live rabbits; (5) Air-lifted corneal organ cultures mimic the real environment of the eyes and keep the epithelium differentiated (Gordon et al., 2010; Richard et al., 1991). We exposed the central cornea directly to the full intensity of UVB or applied of NM. In our studies the interference of blinking or tears was avoided.

In order to compare wound healing times after NM and UVB exposure of corneas, it was necessary to find equivalent injuries between these two blistering agents at a specific time after exposure. In our previous experiments with 100 nmol NM for 2 hours, healing had been followed for 7 days (Gordon et al., 2010). A 2 hour exposure was done because it simulates the amount of time needed for an exposed person to feel pain and seek medical help. As in the warfare situations, the damage to the cornea 24 hours after this exposure was very severe. However, a 100 and tested a 100 nmol NM exposure for 1 hour, which gave a separation of epithelium and stroma close to 60 % at 24 hours after exposure. We wanted to have some epithelium retained since it allowed a better characterization of the injury than a total loss of the epithelial layer.

Different intensities of UVB were tested to produce epithelial-stromal separation. Our results showed that 5 to 20 minutes of UVB exposure (100 to 400 mJ/cm^2) caused some epithelial downward hyperplasia at 24 hours post exposure, but no obvious separation of cell layers. However, larger regions of separation and loose connections between epithelial cells started to be observed from 40 minutes of UVB exposure (800

mJ/cm^2) at 24 hours post exposure. The 60 minutes (1200 mJ/cm^2), 80 minutes (1600 mJ/cm^2), and 100 minutes (2000 mJ/cm^2) UVB irradiated corneas after 24 hours post exposure were shown more extensive regions of separation and more epithelial cell death following increased UVB intensity. The closest level of corneal epithelial-stromal separation to match equivalent injury induced by 100 nmol NM exposure for an hour after 24 hours is at 100 minutes (2000 mJ/cm^2) UVB irradiated corneas after 24 hours post exposure.

The time of a newly reformed epithelial cell layer to cover the denuded cornea area injured by UVB and NM exposure after 24 hours was evaluated. Similar level of epithelial-stromal separation was induced by 100 nmol NM for an hour and 100 minutes (2000 mJ/cm^2) UVB exposure post 24 hours. Three days post UVB exposure a thin layer of corneal epithelial cells began to migrate and covered the denuded area after 5 days. This took 7 days to heal on NM-exposed corneas. It is an initial data to prove NM-exposed corneas heal slower than UVB-exposed corneas 24 hours post exposure.

As implied by the name of "provisional matrix", members of this family are present "temporarily" during wound healing or development (Berryhill et al., 2003; Bornstein and Sage, 2002; Latvala et al., 1996; Murphy-Ullrich, 2001), secreted as they are needed to lay down a template ECM for tissue remodeling (Bornstein and Sage, 2002; Midwood et al., 2004; Murphy-Ullrich, 2001). Sufficient amount of matricellular proteins and their deposit time on the wound bed are needed for efficient wound healing (Midwood et al., 2004). Excess and prolong deposition of SPARC, tenascin- C, and FBN-1 have been reported in diseased or injured corneas (Maillard et al., 1992; Latvala et al., 1996; Maseruka et al., 1997; Ljubimov et al., 1998; Fujikawa et al., 1981; Mackie et

al., 1988). On the other hand, deficient of SPARC has been reported to cause accelerated wound healing, but form scars (Bradshaw et al., 2002).

Hevin, which is a secreted matricellular protein, shares amino acid homology to SPARC in domains other than the N-terminal domain (56 % identity in the follistatin-like domain and 61 % identity in the Ca^{2+}-binding domain). Expressions of both proteins are increased after tissue injury, and both inhibit adhesion and stimulate cell migration (Bornstein and Sage, 2002). Hevin is also expressed in non-injured tissues. It is found in the central and peripheral nervous system, i.e. brain, spinal cord motoneurons, and peripheral neurons (Johnston et al., 1990), the adrenal gland, eye, heart, lacrimal gland, lung, and pancreas (Weaver et al., 2010). There is no report of hevin localization in the cornea. Our results demonstrate that hevin is not expressed in the normal healthy adult rabbit cornea, but is expressed at the BMZ in the injured cornea. However, once the stroma is allowed to heal and is covered by a thin layer of epithelial cells, the protein is no longer detectable.

SPARC, tenascin-C, and TSP-1 also have counter-adhesive properties (Murphy-Ullrich, 2001). Abnormal secretion or over-expression of these glycoproteins contributes to abnormal ECM remodeling during wound healing. (Yan and Sage, 1999; Muriel et al., 1991). Multiple experiments have shown that over-expression or a deficiency of these provisional matrix components disrupts tissue integrity (Bradshaw et al., 2003; Yan and Sage, 1999; Muriel et al., 1991). SPARC-null mice have inflexible tails and fragile bones (Muriel et al., 1991). The over-expression or under expression of SPARC disrupts eye integrity during development (Bassuk et al., 1999). Excessive deposits of tenascin-C are found in the stroma and the BMZ of central pseudophakic bullous keratopathy (PBK) and

aphakic bullous keratopathy (ABK) (Ljubimov et al., 1996). Comparing the protein expression of these matricellular proteins in the corneas post NM and UVB exposure has shown that SPARC, hevin, tenascin-C and TSP-1 are increased after injury with both, but also that they persist longer in NM-exposed corneas as compared to UVB-exposed corneas. We postulate that the slower clearance of these matricellular proteins may be the cause of delayed corneal epithelial wound healing. Tthe proteases involved in their clearance are still being identified.

After showing the distributions of SPARC, hevin, tenascin-C, TSP-1 during corneal wound healing after NM and UVB exposure, we wished to see if the localization of FN contributes to cell migration. After wounding, a higher level of FN is synthesized by the stromal cells to facilitate rapid migration of the epithelium to cover the wound (Zieske et al., 1987). In our experiments, FN was greater in UVB-exposed corneas compared to NM-exposed corneas from day 3 to day 7. Therefore, a better migration substrate is provided after UVB injury, allowing corneas to heal faster than after NM injury. However, FN has the ability to associate with other matricellular proteins and alter their original functions (Dardic and Lahav, 1999). Tenascin-C has anti-adhesive properties, but in a combination of tenascin-C and FN, the FN overrides the other, allowing epithelial adhesion similar to FN alone (Filenius et al., 2003).

ADAMTS4 degradation of hevin was first identified in the brain tissues, and was found important to maintain normal brain function (Weaver et al., 2010). In our hypothesis, ADAMTS4 cleaves hevin in the injured corneas exposed to NM and UVB as well. The ADAMTS4 recognizes E-(AFVLMY)-X (0, 1)-(RK)-X (2, 3)-(ST) in extracellular matrix proteins (Hills et al., 2007) for cleavage. Hevin was recognized to

have such a consensus sequence at residue 358-364 (EAERMHS). Cleavage of hevin by ADAMTS4 generates a SPARC-like fragment of the C-terminus (Weaver et al., 2010). We confirmed that in cornea, hevin and ADAMTS4 co-localized at the regions of BMZ by immunofluorescence analysis at 24 hours post NM and UVB exposure. The yellow color indicating overlap of the hevin (green) and ADAMTS4 (red) in the merged photos indicate an interaction between the two is possible in the cornea. The human ADAMTS4 bands (60 kDa and 50 kDa) have been demonstrated to cleave hevin, aggrecan and versican. Their analogs in the rabbit cornea are 50 kDa and 42 kDa. Interestingly, the 42 kDa band is generated in lower amounts in the 3 day NM exposed sample compared to the 3 day UVB exposed cornea. This kind of has not previously been reported. What has been published is that freshly dissected synovial membrane and freshly dissected articular cartilage contain the 60 kDa form without the 50 kDa form. When placed in explant culture, only the synovial membrane generates the 50 kDa form (Gao et al., 2002). If the retention of hevin in the provisional matrix is what delays wound healing of the NM-exposed cornea, then perhaps the 42 kDa fragment is a more potent enzyme for hevin cleavage than the 50 kDa fragment. The importance of these two fragments of ADAMTS4 will be explored in future work.

Matricellular proteins bind to many cell-surface receptors, the ECM, growth factors, cytokines and proteases (Bornstein and Sage, 2002). Individual matricellular proteins bind specific receptors to regulate down-stream signaling pathways. Tenascin-C binds to annexin II, calcium binding peripheral membrane protein, at the alternatively spliced TNfnA-D domains (Chung et al., 1996). Calreticulin, is another calcium binding protein which mediates TSP-1 focal adhesion activity via phosphoinositide 3-kinase

activation at hep I (Goicoechea et al., 2000). Hep I is a 19-amino acid sequence from the NH_2-terminal heparin-binding domain (HBD) that regulates the focal reorganizing activity of TSP-1.

Provisional matrix proteins also are reported to bind integrins in a ligand-receptor relationship. The matricellular protein and integrin binding may help or worsen corneal epithelial migration in wound healing (Carter, 2009). Multiple integrin heterodimers are restricted to the basal surface of basal keritinocytes, and are up-regulated after wounding. These include α3β1, α2β1, α5β1, α9β1, αvβ6, αvβ5, and α6β4 (Watt, 2002). Disruption of the function of integrins α6β4, αvβ6, and α9β1 has severely adverse effects on the BMZ, with disassembly of the matrix and detachment of the epithelia. Attenuated α4β6 integrin causes severe skin blistering. In bullous keratopathy, αvβ6 and α9β1 integrins are expressed in subepithelial bullae (Werrlein and Madren-Whalley, 2000; Ljubimov et al., 2001). Even though sulfur mustard decreases production of α6β4 (Werrlein and Madren-Whalley, 2000), the absence of β4 doesn't affect re-epithelialization during cutaneous wound healing (Raymond et al., 2005). Integrin α9β1, especially the β1 cytoplasmic domain, is essential for normal corneal epithelial differentiation, and loss of it causes poor re-epithelization in wound healing (Singh et al., 2008; Grose et al., 2002). Integrin αvβ6 and α9β1are receptors for provisional matrix components tenascin-C and FN (Stepp, 2006; Filenius et al., 2003). Furthermore, integrin αvβ6, α8β1 and α9β1 are related to over-expression of tenascin-C in PBK (Ljubimov et al., 2001). The prolonged expression of matricellular proteins at the wound bed due to binding to integrins receptors may play a large role in poor re-epithelialization.

The eye is often exposed to significant intensities of UVB irradiation in people who work outdoors in the summer. Yet the cornea, unlike the skin, rarely develops cancer. It is possible that nuclear ferritin plays a role in corneal protection. Ferritin in most cells contains heavy and light chains, and is found in the cytoplasm. In developing chick corneas, heavy chain ferritin is present in the cytoplasm, but is transferred into the nucleus during development, remaining there throughout the animal's life. In the nucleus it scavenges free radicals and prevents apoptosis, as demonstrated by the loss of protection from UVB when nuclear ferritin was disabled by deferoxamine (Linsenmayer et al., 2005). In our experiments with adult rabbit cornea, ferritin is in the cytoplasm of the epithelial cells. Ferritin does colocalize with the nuclear stain, however, after short exposures to UVB. Three hours after a 2 minute UVB exposure ($40mJ/cm^2$), ferritin appears in the nucleus. Ferritin was found to be in the nucleus much more quickly after a 15 minute ($300mJ/cm^2$) UVB exposure, but by 3 hours after exposure, the immunoreactivity was all cytoplasmic. Ferritin, however, was not immunodetectible in the nucleus after higher intensity UVB exposures [$600mJ/cm^2$ (30 minutes) to $1200mJ/cm^2$ (60 minutes)]. The UV index used by EPA covers an exposure range of 10 mJ/cm^2 [UVI=1] to $150mJ/cm^2$ [UVI=15] (USEPA, 1994). The range in which ferritin was found in the corneal epithelial nucleus was 40 - 300 mJ/cm^2, i.e., ranges from a UVI=4 to UVI =30. The latter value is two times higher than the top of the index. Thus, if human eyes are similar to rabbit eyes, under normal circumstances, the UVB exposures we encounter may induce the presence of ferritin in the nucleus to protect the corneal epithelial DNA.

Summary and Future work

One primary goal of this work was to verify that mustard injuries of the cornea heal slower than comparable injuries. A second goal was to elucidate a possible reason for why delayed corneal wound healing might occur. We compared equivalent injuries induced by exposure to UVB, a blistering agent, and by nitrogen mustard, to verify whether one allowed faster healing than the other. This was done by examining healing by histology and by each agent's effect on the expression of the provisional matrix that is deposited into the corneal wound bed. Matricellular proteins, which are components of the provisional matrix in the wound bed, are expressed after injury, and are responsible for the regulation of cell migration, adhesion, and proliferation during wound healing. Since a deficiency of a set of matricellular proteins (SPARC, hevin and thrombospondin) induces faster wound closure accompanied by scarring, it seemed possible that the slower healing after NM injury might be the result of retention of the matricellular proteins in the wound. To test our hypothesis, we looked to see whether they were cleared out of the wound bed in a timely manner. To accomplish this, we chose UVB as a blister agent to compare to NM for healing after exposure. Rabbit cornea organ cultures were used to observe corneal epithelial migration during healing over the course of 7 days. Our findings provide support for delayed healing after NM exposure accompanied by abnormal distribution of provisional matrix proteins.

Every matricellular protein likely has a different role in modulating cells for healing. This area requires more study. Persistent expression of SPARC, hevin, and tenascin-C at the wound bed of corneas exposed to NM exposure correlates with slower

wound healing since the components could slow epithelial cell migration. The UVB-irradiated corneas cleared the provisional matrix within the standard time for wound healing of the corneal epithelia. Therefore, we questioned whether ADAMTS4, the enzyme that clears hevin, was activated identically in corneas exposed to NM and UVB, and found it was not. Exactly what occurs is not yet known and requires future investigation.

Future goals will explore the mechanisms of how matricellular proteins regulate corneal wound healing and their downstream signaling pathway. Matricellular proteins act as ligands associated with heterodimers of integrins (receptors) to regulate corneal wound healing. The matricellular proteins regulate extracellular matrix organization through their modulations of integrin linked pathways.

Another avenue for future study is examination of the intracellular calcium concentration changes that occur during wound healing (Vieira et al., 2011). Several provisional matrix components, such as SPARC, hevin, tenascin-C, and TSP-1, contain calcium binding domains. The matricellular proteins may modulate the calcium efflux rate during wound healing. Whether calcium concentration changes interfere with the binding capacity of matricellular proteins could be tested in future experiments.

In conclusion, more experiments need to be performed to explore the role of matricellular proteins in wound healing. The ultimate goal is to understand how to modulate these molecules to facilitate corneal wound healing after mustard exposure. The work presented here was a first step toward understanding how vesicants affect provisional matrix, and to determine whether the matricellular proteins may ultimately

prove to be potential targets for therapy and drug development, to improve corneal healing after sulfur mustard injuries.

References

Alpers, C. E., Hudkins, K. L., Segerer, S., Sage, E. H., Pichler, R., Couser, W. G., Johnson, R. J., Bassuk, J. A. (2002). Localization of SPARC in developing, mature, and chronically injured human allograft kidneys. *Kidney Int.* **62(6):**2073-86.

Bassuk, J.A., Birkebak, T., Rothmier, J.D., Clark, J.M., Bradshaw, A., Muchowski, P.J., Howe, C.C., Clark, J.I., Sage, E.H. (1999). Disruption of the Sparc locus in mice alters the differentiation of lenticular epithelial cells and leads to cataract formation. *Exp Eye Res.* **68(3):**321-31.

Berryhill, B. L., Kane, B., Stramer, B. M., Fini, M. E., Hassell, J. R. (2003). Increased SPARC accumulation during corneal repair. *Exp Eye Res.* **77(1)**:85-92.

Bonanno, J. A. (2003). Identity and regulation of ion transport mechanisms in the corneal endothelium. *Prog Retin Eye Res*. **22(1):**69-94.

Bornstein, P., Sage, E. H. (2002). Matricellular proteins: extracellular modulators of cell function. *Curr Opin Cell Biol*.**14(5)**:608-16.

Bornstein, P. (1992). Thrombospondins: structure and regulation of expression. *FASEB J.* **6(14)**:3290-9.

Bradshaw, A. D., Puolakkainen, P., Dasgupta, J., Davidson, J. M., Wight, T. N., Sage, E. H. (2003). SPARC-null mice display abnormalities in the dermis characterized by decreased collagen fibril diameter and reduced tensile strength. *J Invest Dermatol.* **120(6)**:949-55.

Bradshaw, A. D., Reed, M. J., Sage, E. H. (2002). SPARC-null mice exhibit accelerated cutaneous wound closure. *J Histochem Cytochem.* **50(1)**:1-10.

Brekken, R. A., Sullivan, M. M., Workman, G., Bradshaw, A. D., Carbon, J., Siadak, A., Murri, C., Framson, P. E., Sage, E. H. (2004). Expression and characterization of murine hevin (SC1), a member of the SPARC family of matricellular proteins. *J Histochem Cytochem.* **52(6)**:735-48.

Brekken, R. A., Sage, E. H. (2000). SPARC, a matricellular protein: at the crossroads of cell-matrix communication. *Matrix Biol.***19(8)**:816-27.

Cai, C., Ching, A., Lagace, C., Linsenmayer, T. (2008). Nuclear ferritin-mediated protection of corneal epithelial cells from oxidative damage to DNA. *Dev Dyn.* ***237*(10)**:2676-83.

Calvet, J. H., Planus, E., Rouet, P., Pezet, S., Levame, M., Lafuma, C., Harf, A., D'Ortho, M. P. (1999). Matrix metalloproteinase gelatinases in sulfur mustard-induced acute airway injury in guinea pigs. *Am J Physiol*. **276(5 Pt 1):**L754-62.

Carter, R. T. (2009). The role of integrins in corneal wound healing. *Vet Ophthalmol*. **12 Suppl 1**:2-9.

Chung, C. Y., Murphy-Ullrich, J. E., Erickson, H. P. (1996). Mitogenesis, cell migration, and loss of focal adhesions induced by tenascin-C interacting with its cell surface receptor, annexin II. *Mol Biol Cell.* **7(6):**883-92.

Cowen, R. (1996). Beyound discovery: the path from research to human benefit. *National Academy of Sciences.*

Cullen, A. P. (2011). Ozone depletion and solar ultraviolet radiation: ocular effects, a United nations environment programme perspective. *Eye Contact Lens.* **37(4):**185-90.

Cullen, A. P. (2002). Photokeratitis and other phototoxic effects on the cornea and conjunctiva. *Int J Toxicol.* **21(6):**455-64.

Cox, J. L., Farrell, R. A., Hart, R. W., Langham, M. E.(1970). The transparency of the mammalian cornea. *J Physiol.* **210(3):**601-16.

Delany, A. M, Hankenson, K. D. (2009). Thrombospondin-2 and SPARC/osteonectin are critical regulators of bone remodeling. *J Cell Commun Signal.* **3(3-4):**227-38.

DelMonte, D. W., Kim, T. (2011). Anatomy and physiology of the cornea. *J Cataract Refract Surg.* 37(3):588-98.

Diffey, B. L. (1990). Human exposure to ultraviolet radiation. *Semin Dermatol.* **9**.

Downes, J. E., Swann, P. G., Holmes, R. S. (1994). Differential corneal sensitivity to ultraviolet light among inbred strains of mice. Correlation of ultraviolet B sensitivity with aldehyde dehydrogenase deficiency. *Cornea.***13(1):**67-72.

Farjo, A.A., McDermott, M.L., Soong, H.K. (2009). Corneal anatomy, physiology, and wound healing. *In:* YanoffM, DukerJS, *eds.* Ophthalmology, 3rd *edn. Edinburgh, Mosby Elsevier: Elsevier Inc.,* 203–8.

Filenius, S., Tervo, T., Virtanen, I. (2003). Production of fibronectin and tenascin isoforms and their role in the adhesion of human immortalized corneal epithelial cells. *Invest Ophthalmol Vis Sci.* **44(8):**3317-25.

Foreman, D. M., Pancholi, S., Jarvis-Evans, J., McLeod, D., Boulton, M. E. (1996). A simple organ culture model for assessing the effects of growth factors on corneal re-epithelialization. *Exp Eye Res.* **62(5):**555-64.

Freitag, L., Firusian, N., Stamatis, G., Greschuchna, D. (1991). The role of bronchoscopy in pulmonary complications due to mustard gas inhalation. Chest. **100(5):1436-41**.

Friedenwald, J. S., Scholz, R. O., Snell, A., Moses, S. G. (1948) (1). Primary reaction of mustard with the corneal epithelium. *Bull Johns Hopkins Hosp*. **82(2):**102-20.

Friedenwald, J. S., Buschke, W., Moses, S. G. (1948) (2). Comparison of the effects of mustard, ultraviolet and X-radiation and colchicine on the cornea. *Bull Johns Hopkins Hosp.* **82(2):**312-25.

Fujihara, T., Nagano, T., Endo, K., Nakamura, M., Nakata, K. (2000). Lactoferrin protects against UV-B irradiation-induced corneal epithelial damage in rats. *Cornea. **19*(2):**207-11.

Fujikawa, L. S., Foster, C. S, Harrist, T. J., Lanigan, J. M., Colvin, R. B. (1981). Fibronectin in healing rabbit corneal wounds. *Lab Invest.* **45(2):**120-9.

Gao, G., Westling, J., Thompson, V. P., Howell, T. D., Gottschall, P. E., Sandy, J. D. (2002). Activation of the proteolytic activity of ADAMTS4 (aggrecanase-1) by C-terminal truncation. *J Biol Chem.* **277(13):**11034-41.

Gebhardt, B. M, Shi, W. (2002). Experimental corneal allograft rejection. *Immunol Res*. **25(1):1-26.**

Gipson, I. K., Spurr-Michaud, S. J., Tisdale, A. S. (1987). Anchoring fibrils form a complex network in human and rabbit cornea. *Invest Ophthalmol Vis Sci*. **28(2):**212-20.

Goicoechea, S., Orr, A. W., Pallero, M. A., Eggleton, P., Murphy-Ullrich, J. E. (2000). Thrombospondin mediates focal adhesion disassembly through interactions with cell surface calreticulin. *J Biol Chem.* **275(46):**36358-68.

Gordon, M.K., Desantis, A., Deshmukh, M., Lacey, C.J., Hahn, R.A., Beloni, J., Anumolu, S.S., Schlager, J.J., Gallo, M.A., Gerecke, D.R., Heindel, N.D., Svoboda, K.K., Babin, M.C., Sinko, P.J.(2010). Doxycycline hydrogels as a potential therapy for ocular vesicant injury. *J Ocul Pharmacol Ther*. **26(5):**407-19.

Grose, R., Hutter, C., Bloch, W., Thorey, I., Watt, F. M., Fässler, R., Brakebusch, C., Werner, S. (2002). A crucial role of beta 1 integrins for keratinocyte migration in vitro and during cutaneous wound repair. *Development*. **129(9):**2303-15.

Hall, B. E., Willett, F. M., Feichtmeir, T. V., Reed, E. B., Dowling, W. F. (1956). Current trends in cancer chemotherapy. *Calif Med*. **84(1):**1-9.

Herrmann, H., and Hickman, F. H., (1948). Loosening of the corneal epithelium after exposure to mustard. *Bull Johns Hopkins Hosp.* **82(2):**213-24.

Hills, R., Mazzarella, R., Fok, K., Liu, M., Nemirovski, O., Leone, J,, Zack, M. D., Arner, E. C., Viswanathan, M., Abujoub, A., Muruganandam, A., Sexton, D. J., Bassill, G. J., Sato, A. K., Malfait, A. M., Tortorella, M. D. (2007). Identification of an ADAMTS-4 cleavage motif using phage display leads to the development of fluorogenic peptide substrates and reveals matrilin-3 as a novel substrate. *J Biol Chem*. **282(15):**11101-9.

Hohenester, E., Maurer, P., Timpl, R. (1997). Crystal structure of a pair of follistatin-like and EF-hand calcium-binding domains in BM-40. *EMBO J.* **16(13):**3778-86.

Javadi, M. A., Yazdani, S., Sajjadi, H., Jadidi, K., Karimian, F., Einollahi, B., Ja'farinasab, M. R., Zare, M. (2005). Chronic and delayed-onset mustard gas keratitis: report of 48 patients and review of literature. *Ophthalmology*.**112(4):**617-25.

Javadi, M. A., Jafarinasab, M. R., Feizi, S., Karimian, F., Negahban, K.(2011). Management of mustard gas-induced limbal stem cell deficiency and keratitis. Ophthalmology. **118(7):1272-81.**

Javadi, M.A., Baradaran-Rafii, A.(2009). Living-related conjunctival-limbal allograft for chronic or delayed-onset mustard gas keratopathy. Cornea. **28(1):51-7**.

Jo, M. C. (2005). Ultraviolet (UV) Radiation Safety. Environmental Health and Safety. University of Nevada Reno.

Johnston, I. G., Paladino, T., Gurd, J. W., Brown, I. R. (1990). Molecular cloning of SC1: a putative brain extracellular matrix glycoprotein showing partial similarity to osteonectin/BM40/SPARC. *Neuron.* **4(1):**165-76.

Jose, J. G. (1986). Posterior cataract induction by UV-B radiation in albino mice. *Exp Eye Res.* **42(1):**11-20.

Kadar, T., Turetz, J., Fishbine, E., Sahar, R., Chapman, S., Amir, A. (2001). Characterization of acute and delayed ocular lesions induced by sulfur mustard in rabbits. *Curr Eye Res.* **22(1):**42-53.

Kadar, T., Dachir, S., Cohen, L., Sahar, R., Fishbine, E., Cohen, M., Turetz, J., Gutman, H., Buch, H., Brandeis, R., Horwitz, V., Solomon, A., Amir, A. (2009). Ocular injuries following sulfur mustard exposure--pathological mechanism and potential therapy. *Toxicology.* **63(1):**59-69.

Kantorow, M., Horwitz, J., Carper, D. (1998). Up-regulation of osteonectin/SPARC in age-related cataractous human lens epithelia. *Mol Vis*. **17**;4:17.

Koliopoulos, J. X., Margaritis, L. H. (1979). Response of the cornea to far ultraviolet light: an ultrastructural study. *Ann Ophthalmol.* **11(5):**765-9.

Kuwabara, T., Perkins, D. G., Cogan, D. G. (1976). Sliding of the epithelium in experimental corneal wounds. *Invest Ophthalmol.* **15(1):**4-14.

Lane, T. F., Sage, E. H. (1990). Functional mapping of SPARC: peptides from two distinct Ca+(+)-binding sites modulate cell shape. *J Cell Biol.* **111(6 Pt 2):**3065-76.

Latvala, T., Puolakkainen, P., Vesaluoma, M., Tervo, T. (1996). Distribution of SPARC protein (osteonectin) in normal and wounded feline cornea. *Exp Eye Res*. **63(5):**579-84.

Lawler, J. W., Slayter, H. S., Coligan, J. E. (1978). Isolation and characterization of a high molecular weight glycoprotein from human blood platelets. *J Biol Chem*. **253(23):**8609-16.

Lawler, J. (2000). The functions of thrombospondin-1 and-2. *Curr Opin Cell Biol*.**12(5):**634-40.

Lawler, J., Detmar, M. (2004). Tumor progression: the effects of thrombospondin-1 and -2. *Int J Biochem Cell Biol*. **36(6):**1038-45

Linsenmayer, T. F., Fitch, J. M., Gordon, M. K., Cai, C. X., Igoe, F., Marchant, J. K., Birk, D. E. (1998). Development and roles of collagenous matrices in the embryonic avian cornea. *Prog Retin Eye Res*. **17(2):**231-65.

Linsenmayer, T. F, Cai, C. X, Millholland, J. M., Beazley, K. E., Fitch, J. M. (2005). Nuclear ferritin in corneal epithelial cells: tissue-specific nuclear transport and protection from UV-damage. *Prog Retin Eye Res*. **24(2):**139-59.

Ljubimov, A. V., Burgeson, R. E., Butkowski, R. J., Couchman, J. R., Wu, R. R., Ninomiya, Y., Sado, Y., Maguen, E., Nesburn, A. B., Kenney, M. C. (1996). Extracellular matrix alterations in human corneas with bullous keratopathy. *Invest Ophthalmol Vis Sci*. **37(6):**997-1007.

Ljubimov, A. V., Saghizadeh, M., Spirin, K. S., Mecham, R. P., Sakai, L.Y., Kenney, M. C. (1998). Increased expression of fibrillin-1 in human corneas with bullous keratopathy. *Cornea*. **17(3):**309-14.

Ljubimov, A. V., Saghizadeh, M., Pytela, R., Sheppard, D., Kenney, M. C. (2001) Increased expression of tenascin-C-binding epithelial integrins in human bullous keratopathy. *J Histochem Cytochem*. **49(11):**1341-50.

Mackie, E. J., Halfter, W., Liverani, D. (1988). Induction of tenascin in healing wounds. *J Cell Biol.* **107(6 Pt 2):**2757-67.

Maillard, C., Malaval, L., Delmas, P. D. (1992). Immunological screening of SPARC/Osteonectin in nonmineralized tissues. *Bone.* **13(3):**257-64.

Mann, I., and Pullinger, B. D. (1942). A Study of Mustard Gas Lesions of the Eyes of Rabbits and Men (Section of Ophthalmology). *Proc R Soc Med.* **135(3):** 229–244.7.

Maseruka, H., Bonshek, R. E., Tullo, A. B. (1997). Tenascin-C expression in normal, inflamed, and scarred human corneas. *Br J Ophthalmol.***81(8):**677-82.

Masunaga, T., Shimizu, H., Ishiko, A., Tomita, Y., Aberdam, D., Ortonne, J. P., Nishikawa, T. (1996). Localization of laminin-5 in the epidermal basement membrane. *J Histochem Cytochem.* **44(11):**1223-30.

Matsuda, A., Yoshiki, A., Tagawa, Y., Matsuda, H., Kusakabe, M. (1999) Corneal wound healing in tenascin knockout mouse. *Invest Ophthalmol Vis Sci.* **40(6):**1071-80.

Merindano, M.D., Costa, J., Canals, M., Potau, J.M., Ruano, D. (2002). A comparative study of Bowman's layer in some mammals: Relationships with other constituent corneal structures. *Eur J Anat.* **6 (3):** 133-139

Midwood, K. S., Williams, L. V., Schwarzbauer, J. E. (2004). Tissue repair and the dynamics of the extracellular matrix. *Int J Biochem Cell Biol*. **36(6):**1031-7.

Mishima, H., Hibino, T., Hara, H., Murakami, J., Otori, T. (1998). SPARC from corneal epithelial cells modulates collagen contraction by keratocytes. *Invest Ophthalmol Vis Sci.* **39(13):**2547-53.

Monteiro-Riviere, N. A., Inman, A. O., Babin, M. C., Casillas, R. P.(1999). Immunohistochemical characterization of the basement membrane epitopes in bis(2-chloroethyl) sulfide-induced toxicity in mouse ear skin. *J Appl Toxicol.* **19(5):**313-28.

Muriel, M. P., Bonaventure, J., Stanescu, R., Maroteaux, P., Guénet, J. L., Stanescu, V. (1991). Morphological and biochemical studies of a mouse mutant (fro/fro) with bone fragility. *Bone.* **12(4):**241-8.

Murphy-Ullrich, J. E. (2001). The de-adhesive activity of matricellular proteins: is intermediate cell adhesion an adaptive state? *J Clin Invest.* **107(7):**785-90.

Nishida, T., Tanaka, T. (1996). Extracellular matrix and growth factors in corneal wound healing. *Curr Opin Ophthalmol*. **7(4):**2-11.

Nishida, T. (2010).Translational research in corneal epithelial wound healing. *Eye Contact Lens.* **36(5):**300-4.

Norose, K., Clark, J. I., Syed, N. A., Basu, A., Heber-Katz, E., Sage, E. H., Howe, C. C. (1998). SPARC deficiency leads to early-onset cataractogenesis. *Invest Ophthalmol Vis Sci*. 39(13):2674-80.

Pas, J., Wyszko, E., Rolle, K., Rychlewski, L., Nowak, S., Zukiel, R., Barciszewski, J. (2006). Analysis of structure and function of tenascin-C. *Int J Biochem Cell Biol.* **38(9):**1594-602.

Raymond, K., Kreft, M., Janssen, H., Calafat, J., Sonnenberg, A. (2005). Keratinocytes display normal proliferation, survival and differentiation in conditional beta4-integrin knockout mice. *J Cell Sci.* **118(Pt 5):**1045-60.

Romberg RW, Werness PG, Riggs BL, Mann KG. (1986). Inhibition of hydroxyapatite crystal growth by bone-specific and other calcium-binding proteins. Biochemistry. **25(5):**1176-80.

Sage, E. H., Bornstein, P. (1991). Extracellular proteins that modulate cell-matrix interactions. SPARC, tenascin, and thrombospondin. *J Biol Chem.* **266(23):**14831-4.

Sekiyama, E., Nakamura, T., Cooper, L. J., Kawasaki, S., Hamuro, J., Fullwood, N. J., Kinoshita, S. (2006). Unique distribution of thrombospondin-1 in human ocular surface epithelium. *Invest Ophthalmol Vis Sci.* **47(4):**1352-8.

Shohrati, M., Peyman, M., Peyman, A., Davoudi, M., Ghanei, M.(2007). Cutaneous and ocular late complications of sulfur mustard in Iranian veterans. *Cutan Ocul Toxicol.* **26(2):**73-81**.**

Shtein, R. M., Garcia, D. D., Musch, D. C., Elner, V. M. (2008). HSV keratitis: histopathologic predictors of corneal allograft complications. Trans Am Ophthalmol Soc. **106:**161-68; discussion 168-70.

Shakarjian, M. P., Heck, D. E., Gray, J. P., Sinko, P. J., Gordon, M. K., Casillas, R. P., Heindel, N. D., Gerecke, D. R., Laskin, D. L., Laskin, J. D. (2010). Mechanisms mediating the vesicant actions of sulfur mustard after cutaneous exposure. *Toxicol Sci.* **114(1):**5-19.

Shakarjian, M. P., Bhatt, P., Gordon, M. K., Chang, Y. C., Casbohm, S. L., Rudge, T. L., Kiser, R. C., Sabourin, C. L., Casillas, R. P., Ohman-Strickland, P., Riley, D. J.,

Gerecke, D.R. (2006). Preferential expression of matrix metalloproteinase-9 in mouse skin after sulfur mustard exposure. *J Appl Toxicol*.**26(3):**239-46**.**

Singh, P., Chen, C., Pal-Ghosh, S., Stepp, M. A., Sheppard, D., Van De Water, L. (2008). Loss of integrin alpha9beta1 results in defects in proliferation, causing poor re-epithelialization during cutaneous wound healing. *J Invest Dermatol*. **129(1):**217-28.

Smith, W. J., Dunn, M. A. (1991). Medical defense against blistering chemical warfare agents. *Arch Dermatol.* ***127*****(8):**1207-13.

Solberg, Y., Alcalay, M., Belkin, M. (1997). Ocular injury by mustard gas. *Surv Ophthalmol.* **41(6):**461-6.

Starlinger P, Moll HP, Assinger A, Nemeth C, Hoetzenecker K, Gruenberger B, Gruenberger T, Kuehrer I, Schoppmann SF, Gnant M, Brostjan C. (2010). Thrombospondin-1: a unique marker to identify in vitro platelet activation when monitoring in vivo processes. *J Thromb Haemost.* 2010 Aug;8(8):1809-19.

Stepp, M. A. (2006). Corneal integrins and their functions. *Exp Eye Res.* **83(1):**3-15.

Stepp, M. A., Spurr-Michaud, S., Tisdale, A., Elwell, J., Gipson, I. K. (1990). Alpha 6 beta 4 integrin heterodimer is a component of hemidesmosomes. *Proc Natl Acad Sci U S A*. **87(22):**8970-4.

Sullivan, M. M., Puolakkainen, P. A., Barker, T. H., Funk, S. E., Sage, E. H.(2008). Altered tissue repair in hevin-null mice: inhibition of fibroblast migration by a matricellular SPARC homolog. *Wound Repair Regen*. **16(2):**310-9.

Sullivan, M. M., Sage, E. H. (2004). Hevin/SC1, a matricellular glycoprotein and potential tumor-suppressor of the SPARC/BM-40/Osteonectin family. *Int J Biochem Cell Biol.* **36(6):**991-6.

Sumioka, T., Fujita, N., Kitano, A., Okada, Y., Saika, S. (2011). Impaired angiogenic response in the cornea of mice lacking tenascin C. *Invest Ophthalmol Vis Sci*. **52(5):**2462-7.

Tan, K., Lawler, J. (2009). The interaction of Thrombospondins with extracellular matrix proteins. *J Cell Commun Signal.* **3(3-4):**177-87.

Tanelian, D. L., Bisla, K. (1992). A new In Vitro Corneal Preparation to Study Epithelial Wound Healing. *Invest Ophthalmol Vis Sci.* **33**:11.

Tang, B. L. (2001). ADAMTS: a novel family of extracellular matrix proteases. *Int J Biochem Cell Biol.* **33(1):**33-44.

Termine, J. D., Belcourt, A. B., Conn, K. M., Kleinman, H. K. (1981). Mineral and collagen-binding proteins of fetal calf bone. J Biol Chem. **256(20):**10403-8.

Tortorella, M. D., Burn, T. C., Pratta, M. A., Abbaszade, I., Hollis, J. M., Liu, R., Rosenfeld, S. A., Copeland, R. A., Decicco, C. P., Wynn, R., Rockwell, A., Yang, F., Duke, J. L., Solomon, K., George, H., Bruckner, R., Nagase, H., Itoh, Y., Ellis, D. M., Ross, H., Wiswall, B. H., Murphy, K., Hillman, M. C. Jr., Hollis, G, F,, Newton, R. C., Magolda, R. L., Trzaskos, J. M., Arner, E. C. (1999). Purification and cloning of aggrecanase-1: a member of the ADAMTS family of proteins. *Science.* **284(5420):**1664-6.

Tremble, P.M., Lane, T.F., Sage, E.H., Werb, Z. (1993). SPARC, a secreted protein associated with morphogenesis and tissue remodeling, induces expression of metalloproteinases in fibroblasts through a novel extracellular matrix-dependent pathway. *J Cell Biol*. **121(6):**1433-44.

United State Environmental Protection Agency. (1994). The Federal experimental ultraviolet index : what you need to know. *EPA* **430-F-94-019**

United States. Environmental Protection Agency. (updated on 06, May, 2010). UV Index scale. Retrieved from http://www.epa.gov/sunwise/uviscale.html.

Uno, K., Hayashi, H., Kuroki, M., Uchida, H., Yamauchi, Y., Kuroki, M., Oshima, K. (2004). Thrombospondin-1 accelerates wound healing of corneal epithelia. *Biochem Biophys Res Commun*. **315(4):**928-34.

Vieira, A. C., Reid, B., Cao, L., Mannis, M. J., Schwab, I. R., Zhao, M. (2011). Ionic components of electric current at rat corneal wounds. *PLoS One.* **6(2):**e17411.

Watanabe, K., Nakagawa, S., Nishida, T. (1987). Stimulatory effects of fibronectin and EGF on migration of corneal epithelial cells. *Invest Ophthalmol Vis Sci.* **28(2):**205-11.

Watt, F. M. (2002). Role of integrins in regulating epidermal adhesion, growth and differentiation. *EMBO J*. **21(15):**3919-26.

Weaver, M. S., Workman, G., Cardo-Vila, M., Arap, W., Pasqualini, R., Sage, E. H. (2010). Processing of the matricellular protein hevin in mouse brain is dependent on ADAMTS4. *J Biol Chem.* **285(8):**5868-77.

Werrlein, R. J., Madren-Whalley, J. S. (2000). Effects of sulfur mustard on the basal cell adhesion complex. *J Appl Toxicol.* **20 Suppl 1**:S115-23.

Yan, Q., Sage, E. H. (1999). SPARC, a matricellular glycoprotein with important biological functions. *J Histochem Cytochem.* **47(12):**1495-506.

Yan, Q, Sage, E.H., Hendrickson, A.E. (1998). SPARC is expressed by ganglion cells and astrocytes in bovine retina. *J Histochem Cytochem*. **46(1):**3-10.

Young, A. R. (2006). Acute effects of UVR on human eyes and skin. *Prog Biophys Mol Biol*. **92(1):**80-5.

Zhang, Z., Peters, B. P., Monteiro-Riviere, N. A. (1995). Assessment of sulfur mustard interaction with basement membrane components. *Cell Biol Toxicol*. **11(2):**89-101.

Zieske, J. D., Higashijima, S. C., Spurr-Michaud, S. J., Gipson, I. K. (1987). Biosynthetic responses of the rabbit cornea to a keratectomy wound. *Invest Ophthalmol Vis Sci.* ***28*(10):**1668-77.